Sede Amministrativa: Università degli Studi di Padova
Dipartimento di Biologia

SCUOLA DI DOTTORATO DI RICERCA IN BIOSCIENZE E BIOTECNOLOGIE
INDIRIZZO BIOTECNOLOGIE
CICLO XXIV

MICRO-ENGINEERED SKELETAL AND CARDIAC MUSCLE FOR DUCHENNE MUSCULAR DYSTROPHY *IN VITRO* MODELS

Direttore della Scuola: Ch.mo Prof. Giuseppe Zanotti

Coordinatore d'indirizzo: Ch.mo Prof. Giorgio Valle

Supervisore: Dr. Nicola Elvassore

Dottorando: Susi Zatti

TABLE OF CONTENTS

SOMMARIO

La distrofia muscolare di Duchenne è una delle più frequenti e severe patologie genetiche neuromuscolari che affliggono la funzionalità del muscolo scheletrico e cardiaco. Il gene codificante la distrofina, proteina la cui mutazione è alla base della patologia, è stato scoperto più di vent'anni fa. Da allora, notevoli progressi sono stati compiuti nella comprensione della patogenesi di questa malattia e diverse strategie sperimentali volte al suo trattamento sono state testate, sia *in vitro* su convenzionali colture cellulari che *in vivo* su diversi animali modello. Tuttavia, eccezione fatta per alcuni promettenti risultati recentemente ottenuti in trials clinici, ad oggi non vi è ancora una cura efficace e definitiva in grado di alterare o rallentare la progressione di questa patologia, il cui tasso di mortalità è pari al 100%. In tale contesto, lo scopo di questa tesi di dottorato è quello di sviluppare dei modelli *in vitro* micro-ingegnerizzati di muscolo scheletrico e cardiaco umano, che siano rappresentativi dei tessuti distrofici e dunque utili per testare approcci terapeutici volti al ripristino dell'espressione di distrofina. La strategia applicata per l'ottenimento di tali modelli si basa sull'applicazione di tecnologie su microscala per riprodurre *in vitro* i principali stimoli che guidano il differenziamento e consentono la funzionalità del muscolo scheletrico e cardiaco *in vivo*. In particolare, le proprietà meccaniche del micro-ambiente e l'organizzazione topologica della coltura cellulare sono stati ottimizzati sia per il muscolo scheletrico che cardiaco. Tali tecnologie su micro-scala sono state accoppiate con un'appropriata fonte cellulare umana. Per l'ingegnerizzazione del muscolo scheletrico sono stati utilizzati mioblasti umani primari derivanti da biopsie di pazienti DMD mentre, per la modellazione del muscolo cardiaco, cellule umane pluripotenti indotte (iPS) sono state differenziate in cardiomiociti paziente-specifici. Entrambi i modelli *in vitro* di muscolo distrofico ottenuti sono stati validati testando l'abilità di diversi approcci terapeutici nel ripristinarne l'espressione di distrofina. In particolare, tre diversi tipi cellulari miogenici sono stati testati nel muscolo scheletrico distrofico ingegnerizzato. Inoltre, nei cardiomiociti distrofici derivanti da cellule iPS è stato testato il ripristino dell'espressione di distrofina per mezzo di un cromosoma artificiale portante la sua completa sequenza genomica. Da tali risultati emerge come i modelli umani *in vitro* sviluppati in questo lavoro possano rappresentare un'utile piattaforma su cui effettuare test pre-clinici preliminari di diverse strategie terapeutiche. Inoltre, essi posso potenzialmente essere utilizzati come strumento complementare durante i trials clinici, per testare, ad esempio, diverse preparazioni di cellule destinate al paziente.

SUMMARY

Duchenne muscular dystrophy (DMD) is the most common and severe genetic neuromuscular disorder affecting both skeletal and cardiac muscle functionality. More than twenty years have passed since the identification of the dystrophin gene, which mutations cause the disease. Many progresses have been made in understanding the pathogenesis and different experimental strategies has been tested both *in vitro*, on bench-top cell cultures, and *in vivo*, on different animal models. So far, despite some promising outcomes coming from recent clinical trials, this has not resulted in an effective and definitive cure significantly altering the relentless progression of this disease, which has still a 100% mortality rate. In this context, the aim of this PhD thesis is the development of micro-engineered human skeletal and cardiac muscles representing *in vitro* models of DMD patient tissues useful for testing therapeutic approaches aimed at restoring a proper dystrophin expression. The strategy applied for the obtainment of such human *in vitro* models rely on the application of micro-scale technologies for reproducing *in vitro* the main physiological cues that guide differentiation and allow functionality of skeletal and cardiac muscles *in vivo*. In particular, the mechanical properties of the cell micro-environment and the topologic organization over the cell culture were optimized for both skeletal and cardiac muscle. Such micro-scale technologies were coupled with an appropriate human cell source. Human primary myoblasts from biopsies of DMD patient were used for skeletal muscle engineering, while DMD patient-specific cardiomyocytes were differentiated from human pluripotent stem (hiPS) cells for modeling the cardiac muscle. Both the obtained DMD *in vitro* models were validated for testing the ability of different therapeutic approaches in restoring dystrophin expression. In particular, three different myogenic cell types were tested on the engineered DMD skeletal muscle, while dystrophin expression restoration by a human artificial chromosome carrying the full-length genomic dystrophin sequence was tested on hiPS cells-derived cardiomyocytes. In these perspectives, the developed human *in vitro* models can represent a useful platform for performing preliminary or pre-clinical tests of different therapeutic strategy for DMD. In addition, they can be used as complementary tool in a clinical trial, for test different batches of cells before using them on patients.

INTRODUCTION

DMD is considered the most common and severe genetic neuromuscular disorder. This lethal disease leads to a progressive skeletal muscle degeneration and a series of cardiac complications remarkably affecting quality of life and finally resulting in patients premature death, usually in their early twenties[1]. DMD is caused by mutations in the dystrophin gene, encoding a key structural protein of the dystrophin glycoprotein complex (DGPC), which connects the contracting cytoskeletal apparatus of skeletal and cardiac muscle fibers to the extracellular matrix scaffold.

The human DMD gene, located in Xp21, is the largest gene described in the human genome. It measures 2.4 Mb, which correspond to about 0.1% of the total human genome and about 1.5% of the entire X chromosome. Transcription from different promoters and a series of exon skipping and exon scrambling events, generate a great number of isoforms functioning in skeletal and cardiac muscles but also in many other tissues of the body such as brain[2]. The full restoration of these finely-regulated gene expression machinery in DMD patient is a challenging issue. In addition, an effective therapeutic strategy need to be coupled with efficient delivery system to target all different muscles in the body, including respiratory and cardiac muscles[3].

For all these reasons DMD is among the most difficult diseases to treat[4]. Several promising experimental approaches are currently under investigation, including stem cell-based therapies focusing on the delivery of different healthy or genetically-corrected myogenic stem cells; gene replacement therapy aimed at reintroducing a functional version of the DMD gene; exon-skipping approaches that redirect dystrophin gene. Some of these are entering or are ready to enter clinical trials. However, at present, there is no effective therapy to stop its lethal progression.

The process of new therapies development for a genetic disease, such as DMD, starts from the *in vitro* testing of hypothesis on conventional bench-top cell culture and progress towards the assessment of the response of an entire organism through the *in vivo* experimentation in different animal models, identified as genetic homologues of the human pathology. After many years of research and the obtainment of promising results, the study enters the phase of clinical trial on human patients. However, therapies that looked promising in pre-clinical studies have repeatedly yielded disappointing results in clinical trial on patients[5].

In this scenario, the aim of this PhD thesis is the development of micro-engineered human skeletal and cardiac muscles representing *in vitro* models of DMD patient tissues useful for testing therapeutic strategies aimed at restoring a proper dystrophin expression.

These human *in vitro* models want to represent a complementary tool in the process of new therapy development, bridging the existing gaps between Petri-dish cultures, animal models and clinical trials on patients. To this purpose, they should (a) maintain the simplicity and rapidity of *in vitro* testing conventional cell cultures; (b) correctly reproduce human tissue functionality, giving a prediction of the effects on patient tissues; (c) provide robust and reproducible biological and physiological functional data; (d) offer a standard background with defined variables, allowing the comparison of different strategies and testing combined approaches; (e) be easily transferable to research laboratory for facilitating the therapy development process in reduced time and at lower cost.

To meet these requirement, such *in vitro* models should be obtained from a human cell source and applying micro-scale technologies, reproducing *in vitro* the main physiological cues that guide differentiation and allow functionality of skeletal and cardiac muscles *in vivo*. A multidisciplinary approach, coupling biological principles with chemical engineering and material sciences, has been applied.

For the development of DMD skeletal muscle *in vitro* model, the cell source is represented by human primary myoblasts obtained from DMD patient biopsies. Specific aims of this research work are (i) correctly reproduce *in vitro* the process of myogenesis guiding skeletal muscle differentiation *in vivo* and the main environmental cues directing its key phases; (ii) obtaining an engineered skeletal muscle tissue characterized by a functional differentiation and carrying the genetic defect of the patient from which it is derived; (iii) validating the use of the engineered *in vitro* model for testing different therapeutic approaches.

Despite the primary target of each therapeutic strategy aimed at the treatment of DMD should be skeletal muscle, therapies restricted to skeletal muscles alone have been shown to accelerate heart disease in DMD patients. Moreover, the increased lifespan of DMD patient due to the recent improvements in the treatment of respiratory muscle disease, has allowed cardiac disease to emerge as a major cause of patient morbidity and mortality. Cardiomyopathy is now a leading cause of death in DMD patients2[6]. The development of a therapeutic strategy must be then performed with the foresight that cardiac and skeletal muscle should be treated equally and its effects have to be carefully evaluated also on cardiac muscle function. In this context, the realization of a DMD cardiac muscle *in vitro* model is of paramount importance.

In this case, due to the impossibility to directly isolate and maintain *in vitro* human cardiac cells, the first critical step became the obtainment of an adequate cell source. Human induced pluripotent stem (hiPS) cells, obtained for the first time in 2007 by Yamanaka and colleagues, offer the unique possibility to derive patient- and disease-specific stem cell lines. More recently, hiPS cells were derived from a DMD patient and then genetically corrected by a human artificial chromosome (HAC) carrying a full-length genomic dystrophin sequence (DYS-HAC). HAC is an highly promising gene delivery tool, presenting several advantages over conventional vectors, such as the stably maintenance at episomal level, without integration into the host genome and the capacity to carry large genomic loci with all their regulatory elements.

Specific aim of this part of the work are then (i) the obtainment of DMD patient-specific cardiomyocytes from these hiPS cells, that can be used for the *in vitro* modeling of DMD cardiac muscle; (ii) testing dystrophin expression restoration on DMD cardiomyocytes genetically corrected with the DYS-HAC. At the same time, in this case, the application of micro-scale technologies, is aimed at: (iii) realizing an *ad-hoc* microenvironment for contracting cells, optimizing their long-term stability in culture; (iv) maximizing the number of output information per single experiment also reducing the high variability usually observed when working with a primary human cell source.

The progression of the work is represented in figure 1. In this figure, the results obtained are marked in black, while light grey indicates the identified future perspectives.

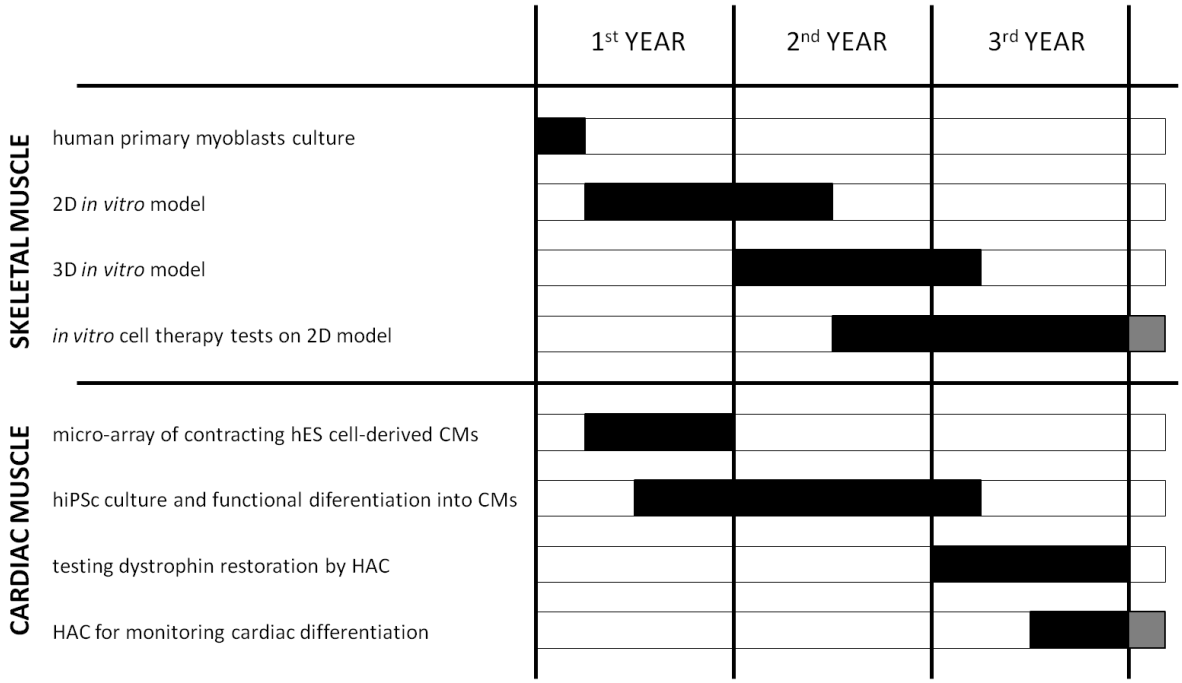

Figure 1. Schematic representation of the main phases of this PhD research, for the development of a human *in vitro* model of skeletal and cardiac muscle. Black bars show the results obtained in this work, while the light grey gives the future perspectives.

Concerning the skeletal muscle *in vitro* modeling, the main phases are: (i) human primary myoblasts culturing; (ii) development of a 2D *in vitro* model; (iii) development of a 3D *in vitro* model; (iv) validation of the *in vitro* model testing different cell therapy approaches (preformed on the 2D *in vitro* model).

Concerning the skeletal muscle *in vitro* modeling, the main phases are: (i) development of a micro-array of contracting cardiomyocytes (using embryonic stem cells-derived cardiomyocytes); (ii) hiPS cells culturing and functional differentiation into cardiomyocytes; (iii) testing dystrophin expression restoration by the DYS-HAC, (iv) development of an HAC for monitoring cardiac differentiation.

The thesis is organized as follows:

Chapter 1, after a brief overview on Duchenne muscular dystrophy (DMD), reviews the most promising therapeutic strategies for its treatment and the tools currently available in the process of new therapy development, highlighting the main limitations and thus contextualizing motivation of

this work. The aim of this PhD thesis is illustrated and the concept of micro-engineered human *in vitro* models is introduced.

Chapter 2 reports the micro-scale technologies, used to realize the engineered human *in vitro* models of skeletal and cardiac muscles, aimed at reproducing *in vitro* some of the main physiological cues driving cell differentiation and tissue function *in vivo*. State of the art and main methodologies are here reported. Complete and detailed protocols are reported in Appendix 1-5.

Chapter 3 describes the development of human *in vitro* models of skeletal muscles through the application of the micro-scale technologies reported in chapter 2. In particular, two different *in vitro* models are described: (i) a two-dimensional (2D) *in vitro* model consisting of an array of parallel aligned, functionally differentiated myotubes obtained on micro-patterned hydrogel substrates; (ii) a three-dimensional (3D) *in vitro* model consisting of a series of myotubes bundles embedded in the micrometric channels of an elastic and compliant hydrogel scaffold. Finally, the possibility to exploit the realized 2D *in vitro* model of skeletal muscle, for studying the capability of different myogenic cells in restoring dystrophin expression, is reported.

Chapter 4 describes the obtained results concerning the development of a human *in vitro* model of cardiac muscle. In particular, the first part focuses on human embryonic stem cells-derived cardiomyocytes and their organization into an array of contracting dots through the micro-scale technologies reported in chapter 2. The second part move on human induced pluripotent stem cells that were used to obtain DMD patient-specific cardiomyocytes and report the study of dystrophin expression restoration on DMD cardiomyocytes genetically corrected by a human artificial chromosome carrying a full-length genomic dystrophin sequence. Finally, as future perspective, preliminary results about the possibility to improve cardiac differentiation from pluripotent stem cells through HAC technology are reported.

Chapter 5 presents the conclusions of the thesis project and discusses the future perspective of the work.

References

1. Blake, D.J., Weir, A., Newey, S.E. & Davies, K.E. Function and genetics of dystrophin and dystrophin-related proteins in muscle. Physiol. Rev. 82, 291-329 (2002).

2. Muntoni, F., Torelli, S. & Ferlini, A. Dystrophin and mutations: one gene, several proteins, multiple phenotypes. Lancet Neurol 2, 731-740 (2003).

3. Goyenvalle, A., Seto, J.T., Davies, K.E. & Chamberlain, J. Therapeutic approaches to muscular dystrophy. Hum. Mol. Genet. 20, R69-78 (2011).

4. Cossu, G. & Sampaolesi, M. New therapies for Duchenne muscular dystrophy: challenges, prospects and clinical trials. Trends Mol Med 13, 520-526 (2007).

5. Collins, C.A. & Morgan, J.E. Duchenne's muscular dystrophy: animal models used to investigate pathogenesis and develop therapeutic strategies. Int J Exp Pathol 84, 165-172 (2003).

6. Spurney, C.F. Cardiomyopathy of Duchenne muscular dystrophy: current understanding and future directions. Muscle Nerve 44, 8-19 (2011).

Chapter 1

DEVELOPMENT OF NEW THERAPIES FOR DMD: STATE OF THE ART, CURRENT LIMITATIONS AND NEED FOR NEW MODELS

After a brief overview on Duchenne muscular dystrophy (DMD), this chapter reviews the most promising therapeutic strategies for its treatment, focusing in particular on the approaches that will be part of the following chapters discussion. The tools currently available in the process of new therapies development are also presented highlighting the main limitations and thus contextualizing motivation of this work. The aim of this PhD thesis is illustrated and the concept of micro-engineered human *in vitro* models is introduced.

1.1. DMD in skeletal and cardiac muscle

DMD is one of the most common and severe inherited neuromuscular disorder, affecting 1 in 3500 newborn males. DMD is caused by mutations in the dystrophin gene, encoding a key structural protein of the dystrophin glycoprotein complex (DGPC), which connects the contracting cytoskeletal machinery of skeletal and cardiac muscle fibers to the extracellular matrix scaffold.

Due to the absence of dystrophin, and the consequent DGPC disassembly, DMD patients skeletal muscles are characterized by an increased fragility of the sarcolemma during lengthening–contraction induced stress. Disruption of the membrane integrity involves an increase in intracellular calcium content that, in turn, promotes calcium-activated proteolysis that degrades the contractile proteins and other intracellular structures. This finally results in a progressive myofibers weakness, wasting and degeneration. Damaged or dead fibers can be repaired or replaced by satellite cells, resident 'stem-like' cells located between the basal lamina and the sarcolemma, responsible for muscle growth, repair and regeneration in postnatal life. However, dystrophic satellite cells share the same molecular defect and produce fibers that are also prone to degeneration. With time, the population of satellite cells is exhausted and the muscle tissue is progressively replaced by connective and adipose tissue[1].

In the heart, along with membrane integrity, the loss of dystrophin affects L-type calcium channels and mechanical stretch-activated receptors; abnormalities that contribute to an increased intracellular calcium content and proteases activation. As with skeletal muscle, this leads to the same pathological cycle resulting in myocardial cell death and fibrosis. However, cardiac muscle is a non-regenerating tissue. The loss of viable myocardium leads to increased wall stress, increased vulnerability to pressure overload, increased myocardial oxygen demand within the remaining viable

myocardium, continued cardiomyocyte death and further fibrosis[2,3]. Cardiac complications associated with DMD include dilated cardiomyopathy with reduced systolic function and cardiac arrhythmias that may consist of both bradycardic and tachycardic rhythm disturbances. Although these cardiac complications frequently display a later age of onset than skeletal muscle symptoms, they represent a significant source of morbidity and mortality in DMD patients[4].

Overall, the absence of dystrophin in DMD patients leads to a broad spectrum of physical consequences. The decreased muscle strength and joint contractures finally result in wheelchair dependence, usually by the age of 12. Most patients die in their early twenties for respiratory complications due to intercostal muscle weakness and respiratory infection. Approximately 20% of deaths are the result of cardiomyopathy and/or cardiac conduction abnormalities[5].

1.2. Dystrophin: gene and protein

The human dystrophin gene (also known as DMD) is located in Xp21 and is the largest gene described in the human genome (Figure 1.1 A). It measures 2.4 Mb, which correspond to about 0.1% of the total human genome and about 1.5% of the entire X chromosome. 99% of the gene for dystrophin is made of introns; and the coding sequence is made by 86 exons. The full-length 14.000 bp mRNA transcribed from the DMD gene is predominantly expressed in skeletal and cardiac muscle with small amounts in brain. However, transcription from different promoters and a series of exon skipping and exon scrambling events, generate a great protein diversity and account for the complex expression regulation of the tissue-specific dystrophin functions[5,6].

Three independently regulated tissue-specific promoters, situated within a large genomic interval of 400 kb at the 5' end of the gene, drive the expression of three full-length dystrophin isoforms: Dp427B, Dp427M, Dp427P. The brain (B), muscle (M), and Purkinje (P) promoters consist of unique first exon spliced to a common set of 78 exons. The names in each case refer to the major but not exclusive sites of expression (Table 1.1). An additional full-length isoform has also been described (initiating isoform Dp427I) in lymphoblastoid cells from a DMD patient with a deletion including all the above mentioned promoters, suggesting the existence of a more 5' promoter[7].

The full-length dystrophin is a large cytoskeletal protein with a molecular weight of 427 kDa that is a member of the β-spectrin/α-actinin protein family. The dystrophin protein comprises four domains: (i) the NH_2 terminus (232 and 240 residues, depending on the isoform); (ii) the central rod domain (about 3000 residues), a succession of 25 triple-helical repeats that are thought to give the molecule a flexible rod-like structure; (iii) the cysteine-rich domain (280 residues); (iv) the COOH-terminal domain (420 residues) (Figure 1.1 B). The NH_2 terminus and a region in the rod domain of dystrophin bind directly to cytoskeletal actin while, through its COOH-terminal region, dystrophin interacts at the sarcolemma with integral membrane proteins (sarcoglycan, dystroglycans, syntrophin, and dystrobrevin complexes) that are assembled in the dystrophin glycoprotein complex (DGPC)[6] (Figure 1.1 C). It has been recently demonstrated that dystrophin is also a microtubules-associated protein that stabilizes costameric MTs and functions as a costameric cytolinker in skeletal muscle[8].

In addition to the main 427 kDa protein, there are at least four shorter dystrophin isoforms that lack the actin-binding terminus but retain the cysteine rich and carboxy-terminus domains. Expression of these isoforms, again tissue-specific (Table 1.1), is driven by internal promoters of the DMD gene. Each promoter uses a unique first exon that splices into exons 30, 45, 56, and 63 to generate protein

products of 260 kDa (Dp260), 140 kDa (Dp140), 116 kDa (Dp116), and 71 kDa (Dp71)[5,6] (Figure 1.1 A,B).

Alternative splicing at the 3'end of the DMD gene generates an even greater number of isoforms[9] that can be differentially expressed also during skeletal muscle, heart, and brain development[10,11].

Table 1.1. Position of the transcription start site and expression pattern of the different dystrophin isoforms.

Isoform	Promoter first exon localization	Pattern of protein expression
Dp427B	5' of the muscle promoter	Cortical neurons and the hippocampus of the brain, retina, skeletal and cardiac muscle.
Dp427M	between B promoter and intron 1	Skeletal and cardiac muscle, retina, glial cells.
Dp427P	between intron 1 and intron 2	Purkinje cerebellar neurons (skeletal muscle).
Dp260	intron 29	Expressed at high level in retina; (at low level in brain and heart).
Dp140	intron 44	Brain, retina, and kidney.
Dp116	intron 55	Schwann cells (adult peripheral nerves).
Dp71	intron 62	Brain, liver, skeletal and cardiac muscle; (ubiquitously expressed also in other non-muscle tissues including retina, kidney and lung).

Expression is low in tissues in brackets. *(Adapted from Muntoni et al, 2003[6])*.

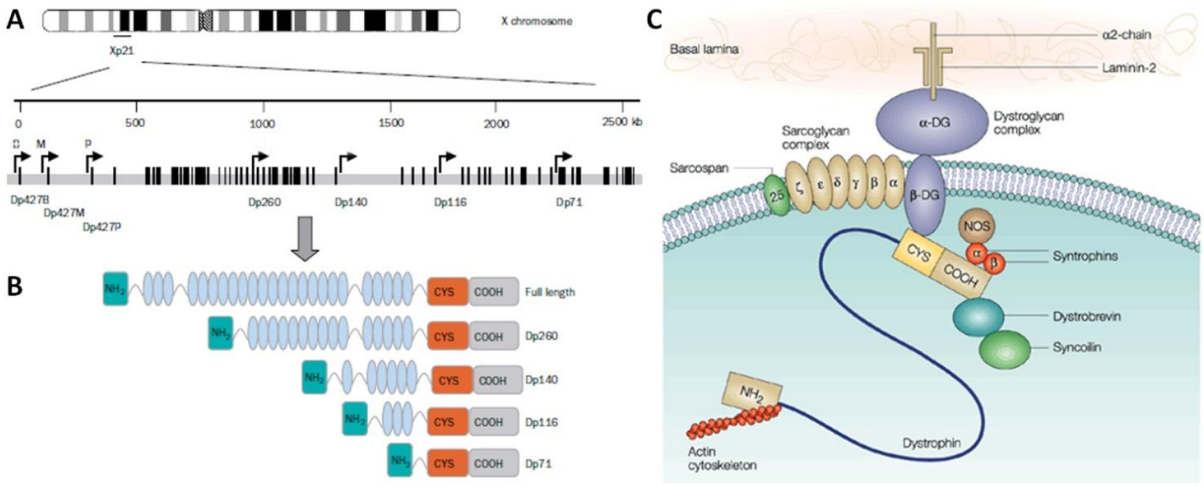

Figure 1.1. (A) Genomic organization of the dystrophin gene, located in Xp21. Black vertical lines represent exons. Arrows indicate promoters driving expression of the different isoforms. (B) Domain composition of the various dystrophin isoforms. *(Adapted from Muntoni et al, 2003[6])*. (C) Schematic representation of the organization of the DGPC showing dystrophin interactions. *(Adapted from Khurana at al, 2003[12])*.

1.3. Therapeutic strategies for DMD

DMD is among the most difficult diseases to treat[1]. Nowadays, conventional DMD therapy is based on symptomatic treatment and supportive care, mainly with steroids that can improve strength and prolong ambulation. At present, there is no effective therapy to stop its lethal progression. However, several promising experimental strategies are currently under investigation, some of which are entering or are ready to enter clinical trials. These include cell-based therapies focused on the delivery of different healthy or genetically-corrected myogenic stem cells; gene replacement therapy aimed at reintroducing a functional version of the DMD gene; exon-skipping approaches that redirect dystrophin gene processing and by-pass protein truncating mutations; read-through strategies for non-sense mutations; up-regulation of the dystrophin-homologous utrophin and pharmacological approaches. All these therapeutic strategies must face major challenges imposed by the nature of the disease, as the need to target all different muscles in the body, including respiratory and cardiac muscles, the need for long-term effect and the potential immune response[13].

1.3.1. Stem cell-based therapies

The potential use of myogenic stem cells to repair damaged DMD muscles is possible because skeletal muscle, although a largely post-mitotic tissue, is capable of growth, repair and regeneration. This is mediated mainly by **satellite cells**, quiescent stem cells located between the basal lamina and the sarcolemma, that can be activated to give a pool of progeny muscle precursor cells, or **myoblasts**.

Myoblasts can be easily isolated and expanded *in vitro* but, after some encouraging studies in mice, phase I clinical trials showed that they contribute only to limited muscle regeneration following direct intra-muscular transplantation. This is mainly due to a strong immune response, the exhaustion of their proliferative capacity *in vivo*, the restricted region of influence around the graft site for their limited migration capacity and an ineffective delivery in all the muscles of the body. On the other hand, the transplantation of freshly isolated satellite cells was demonstrated to contribute to muscle regeneration efficiently but the *in vitro* expansion significantly reduces their *in vivo* myogenic potential, so that it would be very difficult to obtain a sufficient quantity of this kind of cells[14]. Despite these limitations, hampering the possibility to directly use them for clinical treatment, the easiness of satellite cells isolation and myoblasts culture *in vitro* make them good candidates for preliminary investigations and broad range of experiments.

The discovery of other myogenic stem cells that are able to proliferate and could be delivered through the vasculature, raised the possibility to overcome satellite cells and myoblasts limitations. These stem cell populations (reviewed by Farini et al, 2009[14]) were found to derive both from the skeletal muscle itself, such as muscle-derived stem cells, muscle side-population cells and muscle-derived CD133+ stem cells; and from other non-muscular tissues of the body, such as bone marrow-derived mesenchymal stem cells, mesoangioblasts (identified in the dorsal aorta of avian and mammalian species), pericytes (founded in the basement membrane of the vessels) and blood-derived CD133+ stem cells (Figure 1.2).

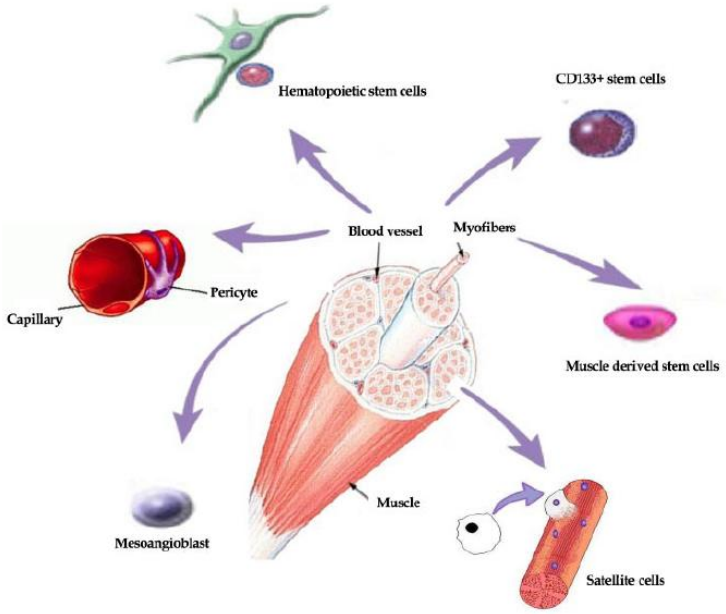

Figure 1.2. Different myogenic stem cell populations derived from skeletal muscle and blood. *(From Farini et al, 2009[14]).*

Among these, **mesoangioblasts (MABs)** are one of the most promising cell type. MABs are multipotent progenitors of mesodermal tissues physically associated with the embryonic dorsal aorta in avian and mammalian species[15]. Intra-arterial MAB transplantation was demonstrated to significantly ameliorate muscular dystrophy in α-sarcoglycan-null mice[16] and GRMD dogs[17]. More recently, genetically-corrected MABs from *mdx* mouse were shown restoring dystrophin expression and led to a significant, long-term morphological and functional amelioration of the dystrophic phenotype[18]. Based on these studies, donor-derived MABs have been expanded under clinical-grade conditions and are being transplanted into DMD patients for a Phase I/II clinical trial.

Beside the adult stem cells populations above described, **human embryonic stem cells (hESc)**, since their tremendous self-renewal and multilineage differentiation potential, possess undoubtedly unique advantages for cell therapies against genetic disorders such as DMD[19].

Furthermore, the efficient reprogramming of differentiated human somatic cells into a pluripotent state by Yamanaka and colleagues in 2007[20], that was heralded as one of the most important scientific findings of the last decade, opens the perspective of deriving patient- and disease-specific stem cells without any ethical implications.

The technology of **human induced pluripotent stem cells (hiPSc)**, if coupled with efficient methodologies for lineage-specific reprogramming and genetic correction, would be an ideal, autologous cell source for the treatment of neuromuscular disorders such as DMD. However, the development of similar approaches is still in their infancy days and milestones have to be overcome, in particular the possibility to obtain pure population of the desired cell type avoiding any tumorigenic risk, that is correlated to the ability of these cells to proliferate indefinitely in their undifferentiated state.

1.3.2. Exon skipping and gene replacement therapies

Numerous strategies of gene therapy have been developed for the treatment of DMD, mainly aimed at (i) modifying dystrophin pre-mRNA splicing (exon skipping approaches) or (ii) introducing of a functional, recombinant copy of the dystrophin gene (gene replacement approaches).

A promising treatment for DMD is the manipulation of dystrophin pre-mRNA using **antisense oligonucleotides (AOs)**. Skipping specific exons allows restoration of the reading frame and results in the production of internally deleted, but essentially functional dystrophin, as observed in the milder Becker muscular dystrophies (BMD), thus providing significant functional improvement of DMD muscles. AOs target one or more of the donor splice sites, acceptor splice sites or exonic sequences essential for pre-mRNA splicing of specific exons. Upon binding of these molecules, the target exon will be spliced out with its flanking introns and the disrupted open reading frame will be restored. AOs chemistry has evolved considerably and is still being refined to reduce its toxicity while improving its affinity, stability and delivery. Many effort focus on defining AOs that can correct the maximum number of genetic mutations. Single exon skipping could theoretically be applied to the 64% of all DMD patients. In particular, exon 51 has been chosen as target of a current clinical trial since its skipping could be applicable for 13% of dystrophin deletions[21]. However, exon skipping will not be applicable to all patients, such as those who have mutations in promoter regions or essential functional domains. Moreover, readministration of AOs will also be necessary as these compounds have a limited half-life[22].

An alternative treatment, that is not dependent on the particular mutation of the patient's gene, is the gene replacement therapy. However, identifying safe and efficient methods to deliver a dystrophin or dystrophin-like gene to all muscles of the body and allow its long-term expression is a daunting challenge. In addition, results from recent studies in larger animal models and in early human trials highlight immunological complications associated with viral vector-mediated gene transfer as the major barrier to clinical success[13]. Three types of viral vectors have been used for this type of approach: lentiviral, adenoviral and adeno-associated viral vectors. All three vectors have shown some success in transduction and stable expression of striated muscles; however, only adeno-associated virus vectors have progressed into clinical trials. **Lentiviral vectors**, as retroviral vectors, possess an intrinsic limitation due to their ability to integrate transgenes into the host genome, that can cause insertional mutagenesis and potential activation of oncogenes, although this occurs at a low frequency. In contrast to lentiviruses, **adenoviral vectors** do not integrate into the host genome allowing transgene existance as non-integrated episomal DNA. However, adenoviral gene transfer is more efficient in immature or regenerating muscle than in mature muscle and this vectors seem to cause a severe immune response. **Adeno-associated virus (AAVs)**, in particular their recombinant form (rAAV), efficiently infect both dividing and non-dividing cells. Stable, long-term gene expression following intramuscular rAAV injection has been reported in mice, dogs and monkeys. Unlike adenovirus, AAVs appeared to exhibit low immunogenicity and the ability to be efficiently extravasated from capillaries, allowing a systemic delivery. The main disadvntage of these vectors is their limited cloning capacity (~4.7 kb), in particular if compared with the 2.4 Mb of the DMD gene. Elegant structure–function studies have led to the development of highly functional truncated dystrophins that are small enough to be packaged within the AAV capsid. The construction of these **"mini"- or "micro"-dystrophins** derive from the study of Becker Muscular Dystrophy (BMD) patients that present a milder phenotype than DMD ones, despite carrying large genomic deletions of dystrophin. In particular, two large regions of dystrophin (most of the rod domain, triple-helical

repeats, and the COOH-terminal domain), can be truncated with minimal functional impact. The rAAV-mediated delivery of “mini”- or “micro”-dystrophins expression cassettes is actually one of the most promising gene therapy approaches for the treatment of DMD[13]. However, these smaller, internal truncated molecules may not be expected to fully replace dystrophin’s function[4].

An highly promising gene delivery tool that possesses several advantages over conventional, above described, gene delivery systems is represented by **human artificial chromosomes (HACs)**. A HAC is an exogenous mini-chromosome that can be artificially created using either a “top-down approach” (engineered chromosome), or a “bottom-up” approach (*de novo* artificial chromosome) and which possess several characteristics required for gene therapy vectors[23]. Like native chromosomes, HAC vectors have the capacity to replicate and segregate autonomously and are stably maintained at episomal level, without integration into the host genome. In addition, HACs have the capacity to carry large genomic loci with all their regulatory elements.

Oshimura laboratory developed an HAC vector carrying, for the first time, the whole dystrophin genomic locus including also the associated regulatory elements (DYS-HAC). In addition, a gene encoding green fluorescent protein was inserted into the vector to allow the presence of the latter to be monitored within cells, and a suicide gene encoding thymidine kinase was also introduced into the vector so as to allow negative selection against the transduced cells if necessary[24].

In a recent work by Oshimura and Yamanaka groups, the DYS-HAC was used for a complete correction of the genetic deficiency in hiPSc derived from a DMD patient[25]. DYS-HAC enabled different dystrophin isoforms expression in various tissues of chimeric mice produced from *mdx*-derived iPS cells genetically corrected with this vector. The combination of patient-derived hiPSc with an HAC vector containing the normal version of a defective dystrophin gene have pioneered an innovative and promising therapeutic approach to the treatment of DMD[26].

1.3.3. Treatment of DMD-associated cardiac dysfunctions

Improvements in the treatment of respiratory muscle disease, including assist devices and mechanical ventilation, allow DMD patients to live longer with improved respiratory function. However, this increased lifespan has allowed cardiac disease to emerge as a major cause of patient morbidity and mortality. Cardiomyopathy is now a leading cause of death in DMD patients[2].

Currently, the treatment of DMD cardiac disfunction relies on the same drugs used in non-genetic forms of cardiomyopathy standard therapy, in particular angiotensin-converting enzyme (ACE) inhibitors, β-adrenergic blockers and diuretics[3,4].

Unfortunately, many experimental therapies have mainly focused on skeletal muscle, in order to restore dystrophin expression in myofibers, and have failed to improve cardiac function. For instance, it appears that AOs-induced exon skipping, one of the most promising therapies already entered in clinical trials, may not be efficacious for the heart, although more detailed studies are needed[4]. Moreover, therapies restricted to skeletal muscles alone, have been shown to accelerate heart disease in DMD patients. Improvements in skeletal and not cardiac muscle could thus become a limiting factor in relation to stem cell, gene or exon-skipping therapy[2,3].

From this scenario, it clearly emerges that the development of a therapeutic strategy must be done with the foresight that cardiac and skeletal muscle could be treated equally and its effects have to be carefully evaluated also on cardiac muscle function.

1.4. Tools for DMD therapies development

More than twenty years have passed since the identification of the molecular defect underling DMD[27]. Many progresses have been made in understanding the genetics and pathogenesis of the disease and several studies has been conducted both *in vitro*, on bench-top cell cultures, and *in vivo*, on different animal models identified as genetic homologues of the human pathology. Despite some promising outcomes coming from recent clinical trials, this has not, so far, resulted in an effective and definitive cure significantly altering the relentless progression of this disease, which has still a 100% mortality rate.

In understanding the reasons of this delay, it should be considered that the process of new therapies development for a genetic disease, such as DMD, requires high costs and long time before the researchers' efforts could effectively be translated into benefits for patients. This could be at least partly attributed to the fact that the majority of research is carried out in systems which do not adequately model the human physiology and pathology[28].

Conventional, Petri-dish-like ***in vitro* cell cultures** are certainly a major tool in basic research. Thanks to the simplicity in handling, they allow fast and low-cost hypothesis investigation, testing of different conditions and screening of compounds, also in an high-throughput fashion. However, they are far from being representative of a functional tissue and results coming from this system should be evaluated carefully and confirmed by analyses in models more closely related to the human *in vivo* condition.

Beside using *in vitro* cell culture for preliminary and validation experiments, the most commonly used laboratory model of DMD is the ***mdx* mouse**. Being a genetic and biochemical homologue of the disease and thanks to their genetic tractability and convenient size, this mouse model has been undoubtedly a pivotal and indispensable tool in understanding DMD pathogenic mechanism and for development of therapeutic approaches. However, dystrophin deficiency does not fully recapitulate the human DMD and its progression in *mdx* mice, which display a much milder phenotype. Muscle pathology is comparatively moderate and mechanical function is less seriously compromised, resulting in an almost normal lifespan[28,29]. These problems has been only partially solved with the obtainment of murine models reproducing more closely the human disease. Examples are mice which are null for both dystrophin and the dystrophin homologue utrophin (***mdx/utrn*$^{-/-}$**), presenting a much more severe phenotype than *mdx* mice[30], and the more recently generated *mdx* mice lacking telomerase activity (***mdx/mTR***), having shortened telomeres in muscle cells and severe muscular dystrophy that progressively worsens with age[31].

Another key model is the **Golden Retriever Muscular Dystrophy (GRMD)**. These dogs exhibit muscle changes which model human pathogenesis far more faithfully than the murine models does and adult individuals also have a body mass comparable to the DMD patients one. However, dogs are not ideal laboratory animals; colonies are expensive to maintain, the species is not genetically manipulable and is highly sentient and emotive. Obviously, they are not suitable for high-throughput studies[28,29].

Both murine models and GRMD dogs are tools of paramount importance in the development of new therapies for DMD but they all remain animal models, fairly representative of an entire organism, but quite far from the human phato−physiology. This implies that findings of studies conducted in these models should not be extrapolated to the human disease without caution. Historically, therapies that

looked promising in animal models (such as myoblast transfer) have repeatedly yielded disappointing results in clinical trial[28].

It should be considered that a definitive therapy for DMD patients, effective both at skeletal and cardiac muscle level, will be probably based on a combined approach, integrating different of the previously described strategies. Testing similar combined approaches in a single pre-clinical trial, based on the currently available tools and technologies, can become extremely challenging.

In this sight, one of the most promising strategy, that can be coupled with conventional tools for lowering time and costs required in the process of new therapies development, is the *in vitro* testing on engineered systems able to give a prediction of the therapy effects on human tissue and their functionality.

Vandenburgh and colleagues already applied this strategy realizing engineered contractile muscle tissues from *mdx* murine myoblasts for semiautomated drug screening of compounds that may improve muscle strength in DMD patients[32]. Many groups explored a similar approach in the field of cardiac drugs. In particular, Mummery's lab described the use of hESc-derived cardiomyocytes coupled with a microelectrode arrays as a renewable, scalable, and reproducible system on which to base cardiac safety pharmacology assays. They propose that assays based on hESc-derived cardiomyocytes could complement or potentially replace some of the preclinical cardiac toxicity screening tests currently used for lead optimization and further development of new drugs[33]. Gepstein's lab proposes the use of a similar system as a novel model for screening cardiac electrophysiological studies, drug screening, and target validation[34].

1.5. Aim of the thesis

The aim of this PhD thesis is the development of micro-engineered human skeletal and cardiac muscles representing *in vitro* models of DMD patient tissues useful for testing therapeutic strategies aimed at restoring a proper dystrophin expression.

These human *in vitro* models wants to couple the simplicity and rapidity of conventional cell cultures with a correct representation of human tissues and their functionality. Beside pre-clinical trials on animal models, testing therapies on these human *in vitro* models could mean obtaining a prediction of the effects on patient tissues directly on bench top, before moving to clinical trials. In these perspectives, they could potentially represent a complementary tool in the process of new therapies development bridging the existing gaps between Petri-dish cultures, animal models and clinical trials on patients (Figure 1.3).

To these purposes, such *in vitro* models should be obtained (i) from a human cell source, in order to obtain significant data representative of DMD patient tissues biology, and (ii) applying microscale technologies, to engineer the cell culture microenvironment, reproducing *in vitro* the main physiological cues that guide differentiation and allow functionality of skeletal and cardiac muscles *in vivo*. A multidisciplinary approach, integrating engineering and biotechnology techniques and methodologies, should be applied.

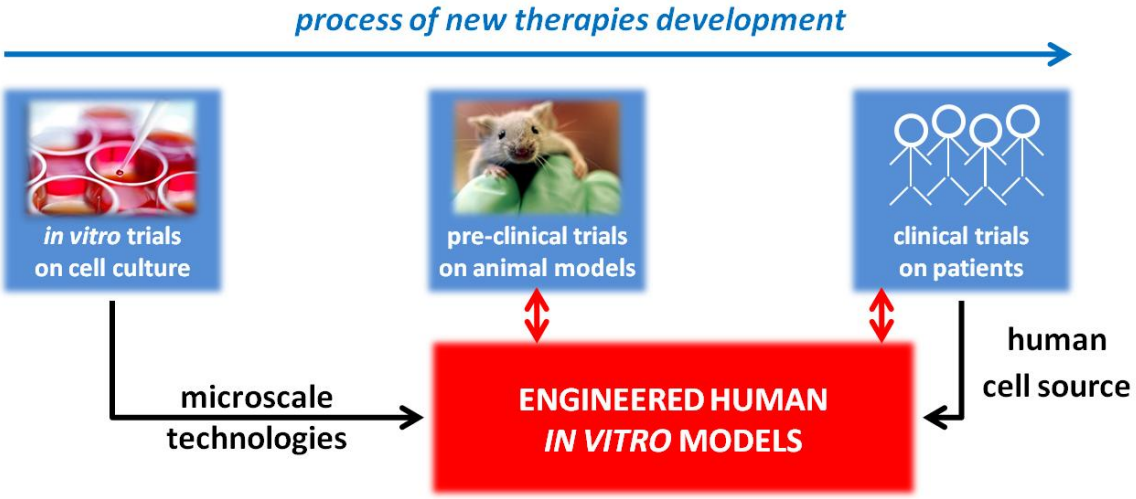

Figure 1.3. The engineered human *in vitro* models, representing the final goal of this work (red inset), could potentially represent a complementary tool in the process of new therapies development. They should be obtained applying microscale technologies, to engineer the cell culture microenvironment, and from a human cell source, to obtain significant data representative of patient tissues biology.

1.6. References

1. Cossu, G. & Sampaolesi, M. New therapies for Duchenne muscular dystrophy: challenges, prospects and clinical trials. Trends Mol Med 13, 520-526 (2007).

2. Spurney, C.F. Cardiomyopathy of Duchenne muscular dystrophy: current understanding and future directions. Muscle Nerve 44, 8-19 (2011).

3. Fayssoil, A., Nardi, O., Orlikowski, D. & Annane, D. Cardiomyopathy in Duchenne muscular dystrophy: pathogenesis and therapeutics. Heart Fail Rev 15, 103-107 (2010).

4. McNally, E.M. New approaches in the therapy of cardiomyopathy in muscular dystrophy. Annu. Rev. Med. 58, 75-88 (2007).

5. Blake, D.J., Weir, A., Newey, S.E. & Davies, K.E. Function and genetics of dystrophin and dystrophin-related proteins in muscle. Physiol. Rev. 82, 291-329 (2002).

6. Muntoni, F., Torelli, S. & Ferlini, A. Dystrophin and mutations: one gene, several proteins, multiple phenotypes. Lancet Neurol 2, 731-740 (2003).

7. Nishio, H. et al. Identification of a novel first exon in the human dystrophin gene and of a new promoter located more than 500 kb upstream of the nearest known promoter. J. Clin. Invest. 94, 1037-1042 (1994).

8. Prins, K.W. et al. Dystrophin is a microtubule-associated protein. J. Cell Biol. 186, 363-369 (2009).

9. Feener, C.A., Koenig, M. & Kunkel, L.M. Alternative splicing of human dystrophin mRNA generates isoforms at the carboxy terminus. Nature 338, 509-511 (1989).

10. Bies, R.D. et al. Human and murine dystrophin mRNA transcripts are differentially expressed during skeletal muscle, heart, and brain development. Nucleic Acids Res. 20, 1725-1731 (1992).

11. Lai, D., Lan, C.-C., Leong, I.U.S. & Love, D.R. Zebrafish dystrophin and utrophin genes: Dissecting transcriptional expression during embryonic development. Int. J. Mol. Med. 29, 338-348 (2012).

12. Khurana, T.S. & Davies, K.E. Pharmacological strategies for muscular dystrophy. Nat Rev Drug Discov 2, 379-390 (2003).

13. Goyenvalle, A., Seto, J.T., Davies, K.E. & Chamberlain, J. Therapeutic approaches to muscular dystrophy. Hum. Mol. Genet. 20, R69-78 (2011).

14. Farini, A., Razini, P., Erratico, S., Torrente, Y. & Meregalli, M. Cell based therapy for Duchenne muscular dystrophy. J. Cell. Physiol. 221, 526-534 (2009).

15. Cossu, G. & Bianco, P. Mesoangioblasts--vascular progenitors for extravascular mesodermal tissues. Curr. Opin. Genet. Dev. 13, 537-542 (2003).

16. Sampaolesi, M. et al. Cell therapy of alpha-sarcoglycan null dystrophic mice through intra-arterial delivery of mesoangioblasts. Science 301, 487-492 (2003).

17. Sampaolesi, M. et al. Mesoangioblast stem cells ameliorate muscle function in dystrophic dogs. Nature 444, 574-579 (2006).

18. Tedesco, F.S. et al. Stem cell-mediated transfer of a human artificial chromosome ameliorates muscular dystrophy. Sci Transl Med 3, 96ra78 (2011).

19. Darabi, R., Santos, F.N.C. & Perlingeiro, R.C.R. The therapeutic potential of embryonic and adult stem cells for skeletal muscle regeneration. Stem Cell Rev 4, 217-225 (2008).

20. Takahashi, K. et al. Induction of pluripotent stem cells from adult human fibroblasts by defined factors. Cell 131, 861-872 (2007).

21. Aartsma-Rus, A. et al. Theoretic applicability of antisense-mediated exon skipping for Duchenne muscular dystrophy mutations. Hum. Mutat. 30, 293-299 (2009).

22. Foster, K., Foster, H. & Dickson, J.G. Gene therapy progress and prospects: Duchenne muscular dystrophy. Gene Ther. 13, 1677-1685 (2006).

23. Kazuki, Y. et al. Refined human artificial chromosome vectors for gene therapy and animal transgenesis. Gene Ther. 18, 384-393 (2011).

24. Hoshiya, H. et al. A highly stable and nonintegrated human artificial chromosome (HAC) containing the 2.4 Mb entire human dystrophin gene. Mol. Ther. 17, 309-317 (2009).

25. Kazuki, Y. et al. Complete genetic correction of ips cells from Duchenne muscular dystrophy. Mol. Ther. 18, 386-393 (2010).

26. Park, I.-H. DYS-HAC-iPS cells: the combination of gene and cell therapy to treat duchenne muscular dystrophy. Mol. Ther. 18, 238-240 (2010).

27. Hoffman, E.P., Brown, R.H., Jr & Kunkel, L.M. Dystrophin: the protein product of the Duchenne muscular dystrophy locus. Cell 51, 919-928 (1987).

28. Collins, C.A. & Morgan, J.E. Duchenne's muscular dystrophy: animal models used to investigate pathogenesis and develop therapeutic strategies. Int J Exp Pathol 84, 165-172 (2003).

29. Nakamura, A. & Takeda, S. Mammalian models of Duchenne Muscular Dystrophy: pathological characteristics and therapeutic applications. J. Biomed. Biotechnol. 2011, 184393 (2011).

30. Deconinck, A.E. et al. Utrophin-dystrophin-deficient mice as a model for Duchenne muscular dystrophy. Cell 90, 717-727 (1997).

31. Sacco, A. et al. Short telomeres and stem cell exhaustion model Duchenne muscular dystrophy in mdx/mTR mice. Cell 143, 1059-1071 (2010).

32. Vandenburgh, H. et al. Automated drug screening with contractile muscle tissue engineered from dystrophic myoblasts. FASEB J. 23, 3325-3334 (2009).

33. Braam, S.R. et al. Prediction of drug-induced cardiotoxicity using human embryonic stem cell-derived cardiomyocytes. Stem Cell Res 4, 107-116 (2010).

34. Caspi, O. et al. *In vitro* electrophysiological drug testing using human embryonic stem cell derived cardiomyocytes. Stem Cells Dev. 18, 161-172 (2009).

Chapter 2

MICROSCALE TECHNOLOGIES FOR SKELETAL AND CARDIAC MUSCLES *IN VITRO* ENGINEERING

This chapter reports the microscale technologies used to realize the engineered human *in vitro* models of skeletal and cardiac muscles that will be discussed in the following chapters. The described micro-technologies are aimed at reproducing *in vitro* some of the main physiological cues driving cell differentiation and tissue function *in vivo*. In particular, (i) an elastic hydrogel substrate is used to simulate the physiological mechanical properties; (ii) micro-contact printing of adhesion proteins is employed to impose a topologic control over the cell culture; (iii) an hydrogel scaffold containing micrometric channels is produced to obtain three-dimensional cultures.

2.1. Cell culture microenvironment engineering

Cells *in vivo*, within organs or tissues, are organized within a complex and highly structured microenvironment (Figure 2.1). This microenvironment, defined by the molecular framework of extracellular matrix (ECM) and the neighboring cells, imposes specific boundary conditions that influence cell mechanics and architecture[1].

The biochemical composition and stiffness of the microenvironment affect intracellular integrin-mediated signaling pathways that, in turn, dictate the assembly and dynamics of cytoskeleton networks. In addition to have a role in the configuration of intra-cellular organization, the cell microenvironment also influences gene expression and cell behavior, including self-renewal and differentiation. Size and shape of the microenvironment limits cell volume and spreading. Its structure, given by the positioning of adjacent cells and the location and orientation of ECM fibers, dictates the spatial distributions of cell adhesion sites and that of unattached cell surfaces. Therefore, the properties of the microenvironment are crucial for the regulation of cellular functions[1,2].

However, these important properties of the cell microenvironment are completely lost on the traditional cell culture systems. In a Petri dish, cells encounter a homogeneous adhesion substrate that is unstructured and rigid and thus is completely forced and unnatural for cells[1,3].

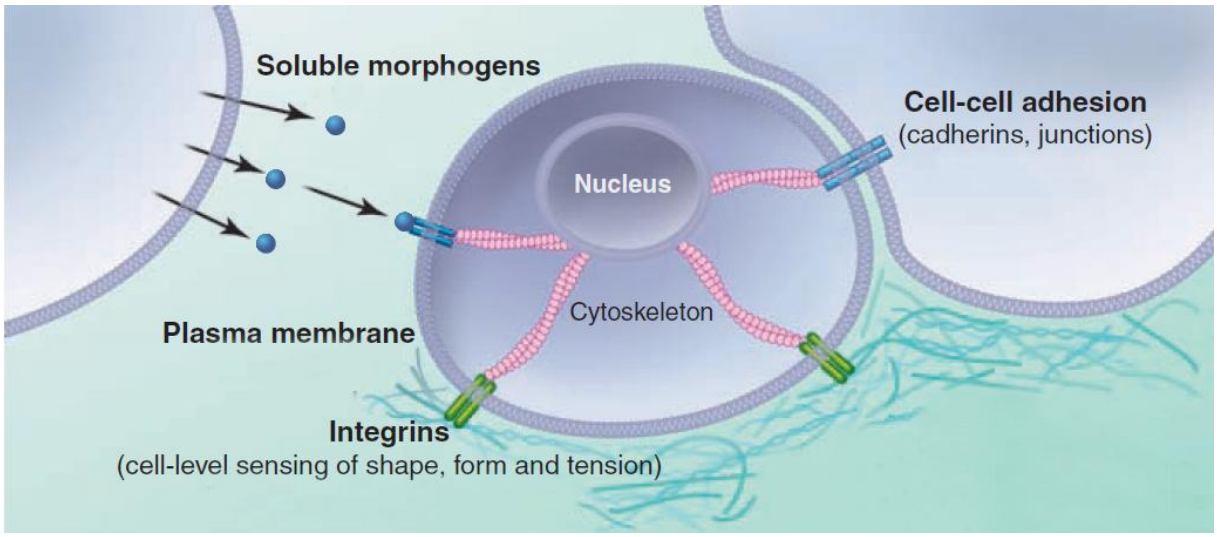

Figure 2.1. Schematic representation of cell microenvironment *in vivo*. One cell is connected to its neighbor by receptors such as cadherins. Other connectors, such as integrins, mechanically link cells to the molecular framework of ECM. Cytokine stimulation can also affecting cell behavior. *(Adapted from Engler et al, 2009)*.

In this work, in order to correctly direct cell differentiation towards the obtainment of functional skeletal or cardiac muscle tissues, the cell culture system has been engineered simulating some of the main physiological cues of the *in vivo* microenvironment, in particular:

1) the **physiological stiffness** of skeletal and cardiac muscle *in vivo* has been reproduced *in vitro* using an hydrogel with tunable elastic proprieties as substrate for cell culture **(§ 2.2)**;

2) the **optimal tissue architecture**, directing skeletal myoblasts alignment and fusion or minimizing the contractile stress of cardiac cells, has been achieved through a topologic control of the cell culture, achieved by micro-patterning of adhesion proteins **(§ 2.3)**;

3) the **third dimension**, combining both physiological mechanical properties and appropriate topological cues, has been introduced realizing a three-dimensional hydrogel scaffold containing a series of parallel-aligned micrometric channels **(§ 2.4)**.

2.2. Substrate stiffness control by *ad-hoc* hydrogel design

Physical properties of the extracellular matrix (ECM) and mechanical forces consequently generated by living cells have recently emerged to be crucial in defining tissue architecture and driving specific cell differentiation programs during embryonic development[4], as well as in maintenance of adult tissue homeostasis and functionality[5].

Cells sense their physical surroundings through mechanotransduction signaling processes[6] as well as they fell different concentration gradients of soluble factors and cytokines. Elegant studies have shown how stem cells can be guided towards specific differentiation fates based on geometry and stiffness of the culture substrate[7]. Cells from many differentiated tissue have been shown not only to adhere to but also to pull on their microenvironment, thereby responding to its stiffness in ways that relate to tissue elasticity. Variation in matrix stiffness for these cells is known to influence focal-adhesion structure and dynamics, the cytoskeleton assembly and cell spreading[8].

In particular, it has been demonstrated that substrate elasticity plays a crucial role in the cytoskeletal organization of skeletal muscle cells and in their acquisition of a striated functional phenotype[9]; in muscle stem cell self-renewal and fate[10]; as well as for the maintenance of a correct beating rate in cardiomyocytes[11]. Furthermore, in these tissues, changes in substrate stiffness are peculiar of pathological conditions. Dystrophic muscles are characterized by a chronic inflammation that is associated with biosynthesis of ECM molecules, most notably collagens type I and type III, accumulating in the interstitial space where they act as mere passive space-filling material[12]. In the resulting stiff fibrotic tissue the original elasticity of a functional muscle is lost. Similarly, the fibrotic scar tissue replacing contracting cardiomyocytes in a damaged heart, is responsible for an increased, non-physiological stiffness affecting cardiac functionality. In this context, for the design and realization of skeletal and cardiac muscles *in vitro* models, it is of paramount importance to correctly reproduce a physiological mechanical microenvironment, in particular in terms of substrate stiffness.

In this work, in order to reproduce *in vitro* a physiological stiffness, a poly-acrylamide hydrogel (PA HY) has been chosen as substrate for the realization of micro-engineered skeletal and cardiac muscle tissues.

Hydrogels are physically or chemically cross-linked polymer networks that are able to absorb and retain large amounts of water. Because of their soft consistence, elastic properties and high water content they closely resemble living tissues ECM and possess an excellent biocompatibility[13]. They can be prepared with several polymers, both naturally derived (such as hyaluronic acid, collagen, gelatin, fibrin, alginate, agarose, chitosan) or synthetically derived, such as (such as poly(acrylic acid), poly(ethylene oxide), poly(vinyl alcohol), polyphosphazene, polypeptides), offering a broad spectrum of mechanical and chemical properties[14,15].

Remarkably, the mechanical properties of PA HYs used in this work can be easily controlled by tuning the pre-polymer chemical composition. In particular, changing the concentration of acrylamide/bis-acrylamide in the liquid pre-polymer solution, stiff or soft PA HYs, characterized by different elastic modulus (or Young's modulus), can be obtained once polymerization is completed (§ 2.2.2).

In addition, PA HYs, typically used in molecular biology as an analytical tool for separating proteins and oligonucleotides, are easy to fabricate, inexpensive and posses a series of features that make them ideal biomaterials for the realization of micro-engineered tissues. Thanks to a rapid chemical or photo-polymerization process they can be produced as bi-dimensional (2D) thin layers or three-dimensional (3D) scaffolds, easily modulable in shape and thickness. This allow an *ad-hoc* design for different experiments. Having an high water content, PA HYs are permeable to small molecules and do not hinder mass transport of metabolites and nutrients required for cells survival and growth. Both 2D and 3D PA HYs are completely transparent and can be covalently bounded to conventional microscope slides, by an easy chemical treatment of the glass surface. The resulting systems are compatible with any image analyses and possess a long term stability in culture. PA HYs have a non fouling surface, with a minimal tendency to adsorb proteins from fluids because of their low interfacial tension, which allow to perform micro-patterning of adhesion proteins on the 2D layers surface.

2.2.1. Micro-fabrication of 2D PA HYs

2D PA HYs with a circular shape, 16 mm in diameter and about 50 µm thick, are prepared on glass slides or coverslips, chemically modified by (3-aminopropyl)triethoxy-silane and glutaraldehyde (Figure 2.2). Briefly, 20 µl of the liquid prepolymer solution, composed of acrylamide/bis-acrylamide 29:1 mixture diluted in phosphate-buffer saline (PBS) to the final desired concentration and supplemented with 20 mg/ml photoinitiator (Irgacure 2959), are polymerized by UV light exposure for 3 min in an high-pressure mercury vapor lamp emitting at 365 nm. A selective photo-polymerization is achieved by interposing a photomask with the desired geometry between the light source and the glass slide. Glass slides with covalently bounded PA HYs are then immersed in sterile PBS for 48 h to ensure complete removal of the un-reacted monomeric units or photoinitiator. After rinsing with PBS, PA HYs are allowed to dry completely for 1 h and then sterilized by exposure to UV light for 20 minutes under a sterile hood.

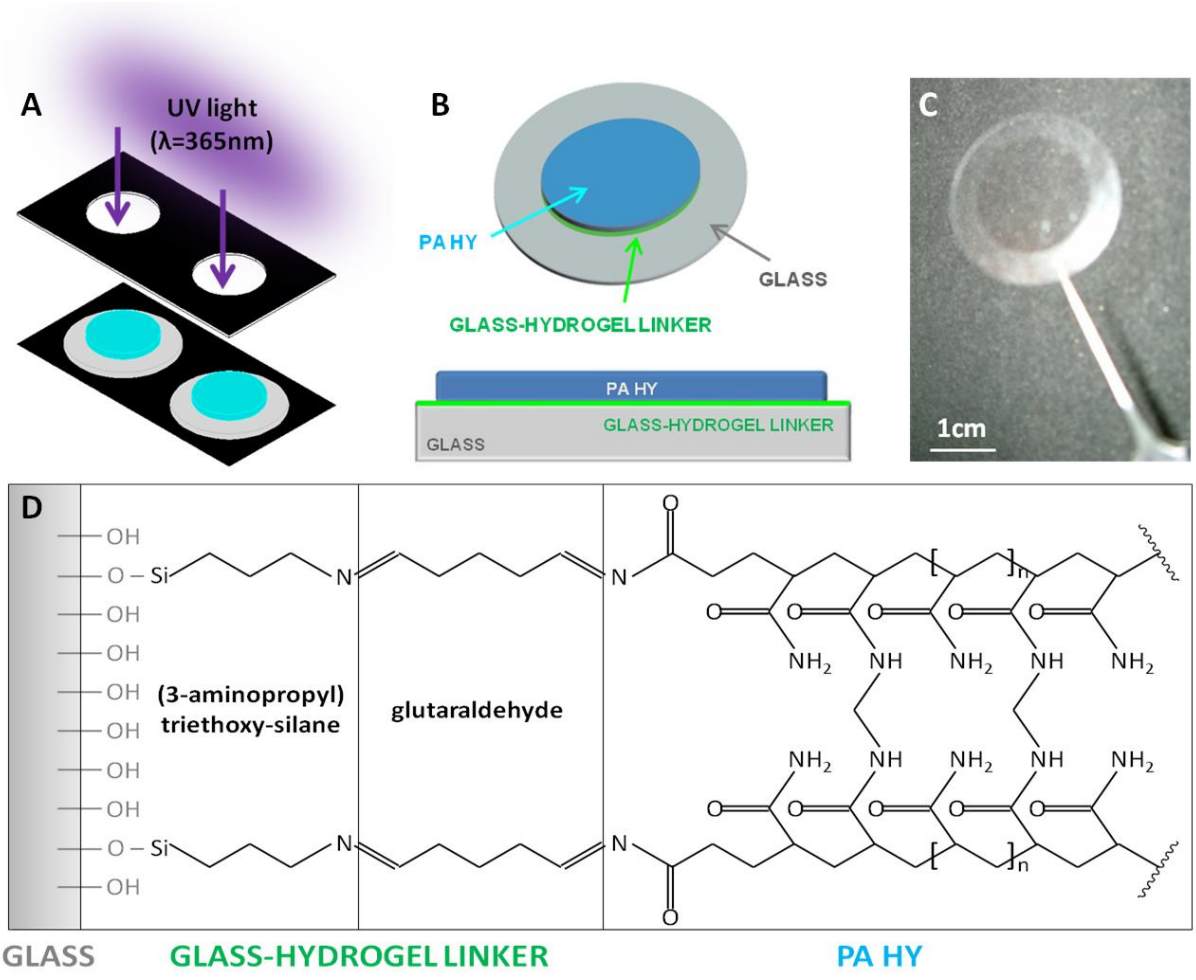

Figure 2.2. (A) PA HY *(blue)* are polymerized by UV light exposure (365nm), interposing a photomask *(black)* with circular holes between the light source and the glass slide *(grey)*. (B) Schematic representation (top and side view) of a PA HY polymerized on the supportive glass slide. (C) Picture of a ready-to-use PA HY. (D) Schematic representation of the PA HY chemistry. The acrylamide/bis-acrylamide polymer is covalently bound to the glass surface through a linker made by glutaraldehyde and 3-aminopropyltriethoxysilane.

2.2.2. Tuning stiffness of PA HYs

In order to study the effect of an increased stiffness on skeletal muscle functional differentiation (see § 3.1.2. and appendix B), four different PA HY substrates with different mechanical properties, in terms of elastic modulus, have been realized tuning the pre-polymer chemical composition, as reported in figure 2.3.

A

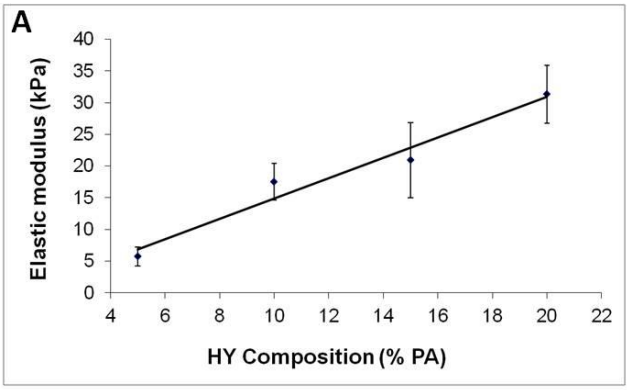

B

PA HY COMPOSITION

HY composition (% PA)	Elastic modulus (kPa)
8	12
10	15
12	18
14	21

Figure 2.3. (A) Graph representing the linear correlation between HY composition and elastic modulus. Reported values of elastic modulus were obtained by standard compression tests previously performed by Ing. Cimetta and the chemical engineers team of the laboratory (as reported in "Cimetta et al, 2009"[16]). Linear interpolation of these data was used to determine HY compositions reported in B. (B) Table reporting HY composition (in terms of concentration of acrylamide/bis-acrylamide29:1 mixture in the pre-polymer solution (% v/v)) and the corresponding elastic modulus, for the four PA HY substrates realized and used in this work (§ 3.2.1 and appendix B).

According to literature data, the elastic modulus of 10% PA HYs is consistent with the stiffness of a native skeletal muscle (E≈12±4 kPa)[9] and the substrate elasticity that maximizes cardiomyocytes work (E≈11-17 kPa)[11]. The selected range (8÷14% PA HYs) was chosen because pre-polymer solutions with acrylamide/bis-acrylamide concentriation lower than 5% resulted in PA HY too soft and not homogeneously polymerized; on the contrary, solutions with acrylamide/bis-acrylamide concentriation higher than 20% resulted in PA HYs with a tight network hindering an optimal proteins adsorption on their surface and thus compromising cell adhesion.

2.3. Cell topology control by micro-patterning of adhesion proteins

In vivo skeletal muscle is composed by highly organized, parallel aligned myofibers bundles formed by the fusion of myoblasts into multi-nucleated myotubes. Each myofibers is, in turn, organized in a series of densely packed actin and myosin filaments running parallel to each other on the long axis of the fiber. Sarcomeres, the functional unit of skeletal muscle, are perfectly aligned, giving the typical striated aspect of muscles. This alignment is crucial for skeletal muscle function because allow sarcomeric structures of different myofibers to cooperate in the same direction during contraction, generating force. However, when cultured *in vitro* on conventional systems such as Petri-dishes or glass slides, the anatomical structure is lost such that myoblasts grow in a randomly oriented fashion, resulting in a disorganized, branched network of myotubes which do not resemble physiological muscle architecture. Myoblasts adhesion and growth *in vitro* can be guided into defined geometries, simulating the *in vivo* muscle structure and promoting their alignment and fusion. In this way myotubes can be fostered to assume a more physiological orientation.

Concerning cardiac muscle, despite is not such a crucial parameter for differentiation, the topologic control play a key role in ensuring the maintenance in culture of beating cardiomyocytes. The most stable geometrical conformation for contracting cardiomyocytes is the circular one. If confined into round-shaped spots, the mechanical stress of beating cells is minimized and equally distributed in all the directions, reducing the detachment risk.

Cell topologic control into defined geometries can be achieved in different ways. Through *ad-hoc* micro-patterning of adhesion proteins[16–18]; through fabrication of substrates characterized by of micro-structured surface topology[19–21]; through polymer microfibers that form parallel arrays upon which cells are cultured[22–25].

In this work, a micro-patterning technique has been used to obtain a precise topologic control (with a resolution of ~1 μm) of both skeletal myoblasts and cardiomyocytes cultures. With this technique adhesion proteins are printed with a defined geometry onto a cell repellent surface, in this case a PA HY layer.

2.3.1. Obtainment of micro-patterned PA HY substrates

Protein micro-patterning is performed by micro-contact printing (μCP) (Figure 2.3 A), using an elastomeric stamp presenting, as bas relief, the desired geometry to be produced. For skeletal myoblasts, a geometry of parallel lanes had been chosen (Figure 2.3 B,C). Five configuration differing in lane width (from 100 to 500 μm) and inter-spacing length (from 50 to 200 μm) have been realized (see also appendix A). For cardiomyocytes a geometry of circular dots 300 μm in diameter and 700 μm center to center spaced have been used (Figure 2.3 D,E) (see also appendix C).

The elastomeric stamps are obtained by replica molding, casting a poly(dimethyl)-siloxane (PDMS) over a micro-structured master. Once solidify, stamps are removed from the master and can be used several times (by washing with PBS and sterilizing them after use). The micro-structured master is produced by soft-lithography techniques optimized by the chemical engineer team of the laboratory[16].

The PDMS stamp is then “loaded” by inking it in the protein solution for few seconds or dropping over it, with a micropipette, 50 μL of the protein solution. The exceeding solution is removed with the vacuum pump. A conformal contact between the dry hydrogel surface and the PDMS stamp is obtained by applying a gentle pressure, thus transferring the desired protein micro-pattern onto the substrate surface. Adhesion proteins are thus immobilized on the hydrogel surface through physical adsorption (Figue 2.4 B,D). The high water content of the hydrogel allow proteins to maintain their native structure.

Different adhesion proteins have been tested: laminin, fibronectin and matrigel®. Laminin and fibronectin are used at a concentration of 100 μg/ml in PBS, while matrigel® is diluted at 2.5% v/v in DMEM. Such concentration has been empirically determined by the analysis of transfer efficiency and homogeneity of the obtained pattern, as extensively described in my master degree thesis[26]. Collagen or gelatin can not be used for micro-patterning because of their gelatinous nature, which prevent absorption inside the PA HY network, causing the formation of a gel layer over the PA HY surface that easily detach from the substrate.

Cells can be then seeded and let attach to the micro-patterned hydrogel layer (Figure 2.4 C,E). 300 μl of cell suspension are dropped over the hydrogel, forming a bubble-like structure. Skeletal myoblasts

are seeded at a density of 200 cell/mm^2 or 400 cell/mm^2, cardiomyocytes are seeded at a density of 600 cell/mm^2.

The obtained protein micro-pattern and the consequent cell adhesion topology is highly precise and reproduces exactly the stamp geometry. Such engineered cell culture system have been stably maintained in culture for up to 12 days.

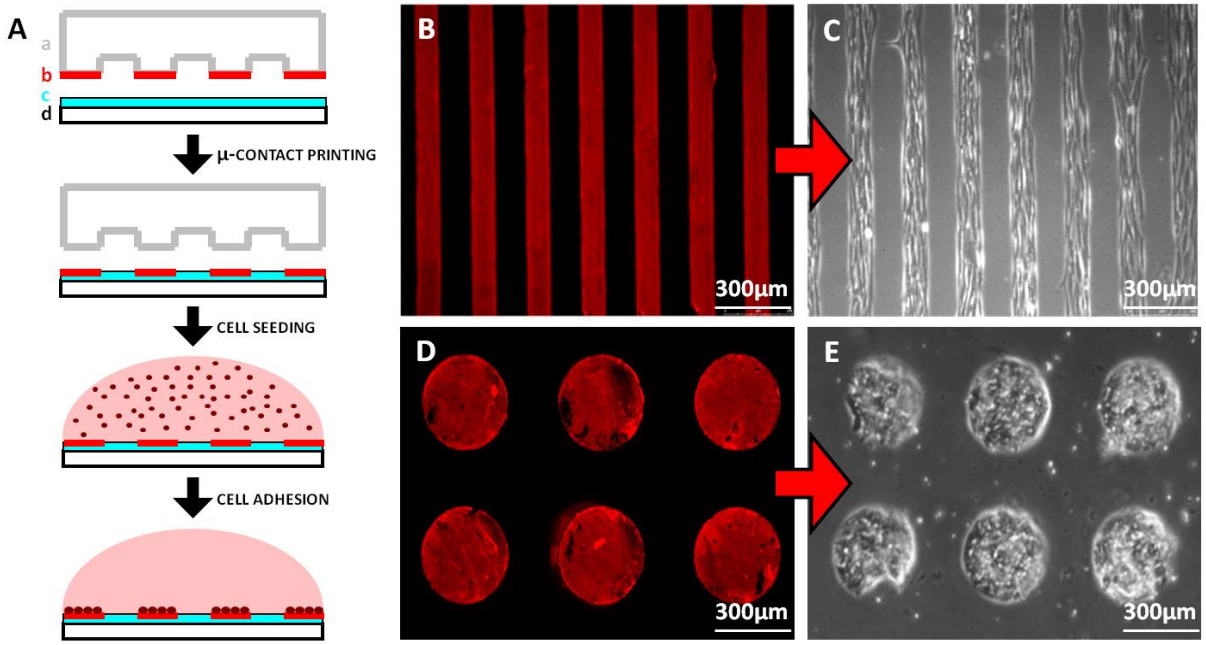

Figure 2.4. (A) Through µCP technique, ECM adhesion proteins (b) are printed with a PDMS mold (a) onto the PA HY (c), polymerized over a glass slide (d). Cells are seeded on the printed PA HY and adhere only to the to the protein pattern with micrometric precision. (B,C) Topologic control of skeletal myoblasts culture: (B) laminin immunofluorescence on adhesion proteins micro-patterned in parallel lanes 100 µm wide and 100 µm spaced; (C) human primary myoblasts 24h after seeding on the micro-patterned PA HY substrate. (D,E) Topologic control of cardiomyocytes culture: (D) laminin immunofluorescence on adhesion proteins micro-patterned in circular dots 300 µm in diameter and 700 µm center to center spaced; (E) hESc-derived cardiomyocytes 24h after seeding on the micro-patterned PA HY substrate.

2.4. Modeling skeletal muscle in 3D

For a further improvement of the skeletal muscle *in vitro* model, in order to obtain a more physiological morphology and cellular architecture of the engineered myotubes, a new generation of three-dimensional (3D) cell culture systems have been designed and developed.

To this purpose, 3D PA HY scaffolds have been realized. These 3D PA HYs (2mm high, 14mm width, 6mm dept) are characterized by the same chemical composition and elastic modulus allowing an optimal differentiation of skeletal myotubes on the 2D micro-patterned substrates (§ 3.1.2. and appendix B). They have been design to contain a series of parallel aligned micrometric channels having a diameter comparable to the middle section of a single human muscle fiber (Figure 2.5).

In this way, physiological mechanical stimuli, recreated using the PA HY, are combined with topologic constrains, given by the aligned micrometric channels, in a 3D context.

3D PA HYs are realized by chemical polymerization upon a glass slide (previously treated with (3-aminopropyl)triethoxy-silane and glutaraldehyde), confining the pre-polymer solution inside a PDMS holder that define shape, dimension and thickness. Briefly, 500 µl of the liquid prepolymer solution, composed of acrylamide/bis-acrylamide 29:1 mixture diluted at 10% (v/v) in PBS and supplemented with the initiator ammonium peroxydi-sulfate (APS) (0,001% v/v), are poured inside the PDMS holder and polymerized in about 5 minutes after the addition of the catalyzer N,N,N',N'-tetramethylethylenediamine (TEMED) (0,001% v/v).

Micrometric channels are obtained using removable polymeric cylindrical fillers which can be easily removed from the PDMS holder or dissolved by immersion in a 1,1,1,3,3,3-hexafluoro-2-propanol 50% aqueous solution, once the polymerization is complete (Figure 2.5 A).

Similarly to micro-patterning lanes, that have been realized with different widths, also micrometric channels of different diameters have been produced. To this purpose, polymeric cylindrical fillers of different size have been used: 80, 120, 140, 160 µm. Dimension of the obtained channels closely reproduce the one of the cylindrical filler used and are highly reproducible.

Once obtained, 3D PA HYs (Figure 2.5 B) are partially dried for 20 minutes, then micrometric channels are injected with laminin 100 µg/ml and partially dried for additional 10 minutes. In this way laminin is efficiently absorbed and immobilized on the inner walls, obtaining a functionalized surface for cells adhesion.

3D scaffolds are then purified by immersion in sterile PBS for 72 h to ensure complete removal of the un-reacted monomeric units or initiators. After rinsing with PBS, they are partially dried for 20 minutes and then sterilized by exposure to UV light for 20 minutes under a sterile hood. Before their use for myoblasts culture, PA HYs are equilibrated overnight in sterile medium at 37°C, 5% CO_2.

A cells suspension with a density of 1×10^6 cells/µl in matrigel® 50% (v/v in DMEM) is injected inside the micrometric channels, using a siringe with a 21G needle. Matrigel® solution rapidly solidify at 37°C, trapping cells into the channels. The high cell density is required for the obtainment an initial homogeneous cell distribution into the whole volume of the channel. However, since the micrometric dimensions of the channels, small amount of cells can be used for the injection of different channels. For instance, 1×10^6 cells are enough to seed 3 channels, 80 µm in diameter. 3D PA HYs injection and manipulation is carried out using a stereomicroscope, under a sterile hood (Figure 2.5 C).

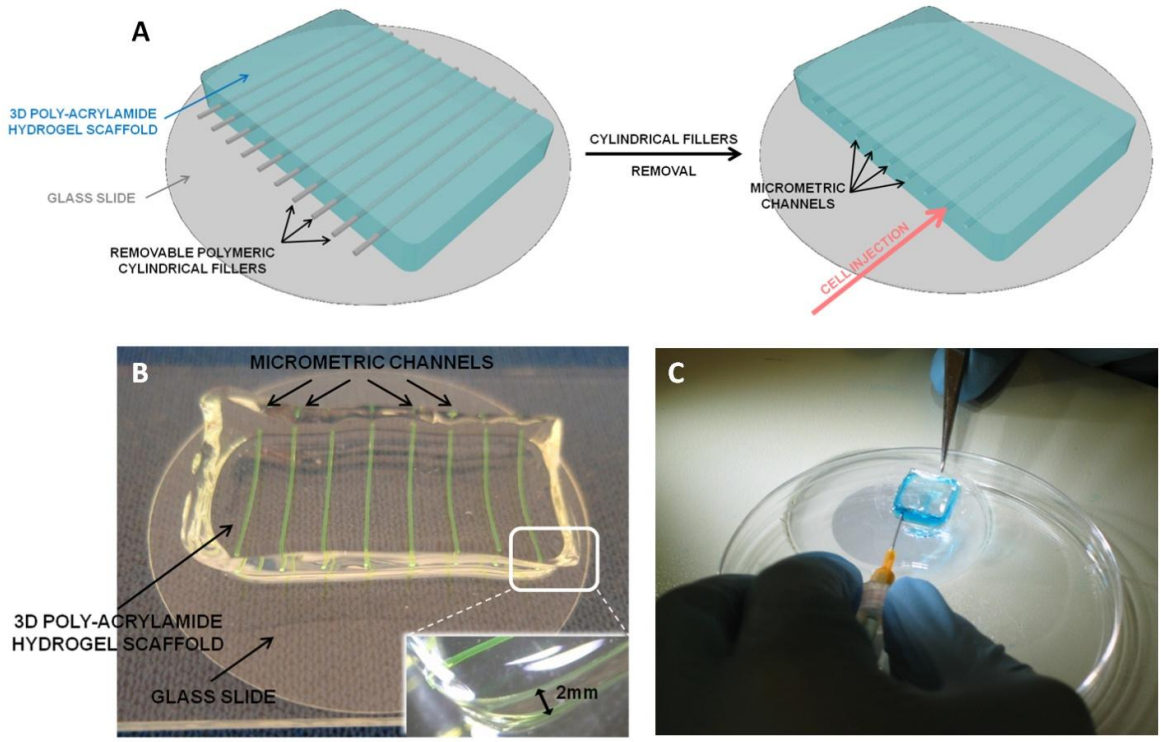

Figure 2.5. (A) Obtainment of micrometric channels inside a 3D PA HY scaffold using polymeric cylindrical fillers easily removable. (B) Picture of a 3D PA HY where micrometric channels, 160 µm in diameter, are emphasize with a green filler. (C) Micro-manipulation of a 3D PA HY (treated with a blue dye) under the stereomicroscope.

Myotubes obtained in this system can be analyzed by frozen and cryosectioning the 3D scaffold. To this purpose, the 3D PA HY can be mechanically detached from the glass slide, fixed in paraformaldehyde (PFA), dehydrated overnight in sucrose (30% solution in PBS) and embedded in OCT. 20µm cryosections can be used for immunofluorescence analyses. The 3D engineered system realized is then compatible with conventional procedures used for tissue analyses.

In addition, the system was designed in order to be completely transparent and then compatible with in-line optical analyses.

2.5. References

1. Théry, M. Micropatterning as a tool to decipher cell morphogenesis and functions. J. Cell. Sci. 123, 4201-4213 (2010).

2. Dickinson, L.E., Kusuma, S. & Gerecht, S. Reconstructing the differentiation niche of embryonic stem cells using biomaterials. Macromol Biosci 11, 36-49 (2011).

3. Fu, R.-H. et al. Differentiation of stem cells: strategies for modifying surface biomaterials. Cell Transplant 20, 37-47 (2011).

4. Mammoto, T. & Ingber, D.E. Mechanical control of tissue and organ development. Development 137, 1407-1420 (2010).

5. Jaalouk, D.E. & Lammerding, J. Mechanotransduction gone awry. Nat. Rev. Mol. Cell Biol. 10, 63-73 (2009).

6. Dupont, S. et al. Role of YAP/TAZ in mechanotransduction. Nature 474, 179-183 (2011).

7. Engler, A.J., Sen, S., Sweeney, H.L. & Discher, D.E. Matrix elasticity directs stem cell lineage specification. Cell 126, 677-689 (2006).

8. Discher, D.E., Janmey, P. & Wang, Y.-L. Tissue cells feel and respond to the stiffness of their substrate. Science 310, 1139-1143 (2005).

9. Engler, A.J. et al. Myotubes differentiate optimally on substrates with tissue-like stiffness: pathological implications for soft or stiff microenvironments. J. Cell Biol. 166, 877-887 (2004).

10. Gilbert, P.M. et al. Substrate elasticity regulates skeletal muscle stem cell self-renewal in culture. Science 329, 1078-1081 (2010).

11. Berry, M.F. et al. Mesenchymal stem cell injection after myocardial infarction improves myocardial compliance. Am. J. Physiol. Heart Circ. Physiol. 290, H2196-2203 (2006).

12. Alexakis, C., Partridge, T. & Bou-Gharios, G. Implication of the satellite cell in dystrophic muscle fibrosis: a self-perpetuating mechanism of collagen overproduction. Am. J. Physiol., Cell Physiol. 293, C661-669 (2007).

13. Van Vlierberghe, S., Dubruel, P. & Schacht, E. Biopolymer-based hydrogels as scaffolds for tissue engineering applications: a review. Biomacromolecules 12, 1387-1408 (2011).

14. Tibbitt, M.W. & Anseth, K.S. Hydrogels as Extracellular Matrix Mimics for 3D Cell Culture. Biotechnol Bioeng 103, 655-663 (2009).

15. Lee, K.Y. & Mooney, D.J. Hydrogels for tissue engineering. Chem. Rev. 101, 1869-1879 (2001).

16. Cimetta, E. et al. Production of arrays of cardiac and skeletal muscle myofibers by micropatterning techniques on a soft substrate. Biomed Microdevices 11, 389-400 (2009).

17. Tourovskaia, A., Figueroa-Masot, X. & Folch, A. Long-term microfluidic cultures of myotube microarrays for high-throughput focal stimulation. Nat Protoc 1, 1092-1104 (2006).

18. Ahmed, W.W. et al. Myoblast morphology and organization on biochemically micro-patterned hydrogel coatings under cyclic mechanical strain. Biomaterials 31, 250-258 (2010).

19. Truckenmüller, R. et al. Fabrication of cell container arrays with overlaid surface topographies. Biomed Microdevices (2011).doi:10.1007/s10544-011-9588-5

20. Sun, M., McGowan, M., Kingham, P.J., Terenghi, G. & Downes, S. Novel thin-walled nerve conduit with microgrooved surface patterns for enhanced peripheral nerve repair. J Mater Sci Mater Med 21, 2765-2774 (2010).

21. Shimizu, K., Fujita, H. & Nagamori, E. Alignment of skeletal muscle myoblasts and myotubes using linear micropatterned surfaces ground with abrasives. Biotechnol. Bioeng. 103, 631-638 (2009).

22. Surrao, D.C., Hayami, J.W.S., Waldman, S.D. & Amsden, B.G. Self-crimping, biodegradable, electrospun polymer microfibers. Biomacromolecules 11, 3624-3629 (2010).

23. Vaquette, C. et al. Aligned poly(L-lactic-co-e-caprolactone) electrospun microfibers and knitted structure: a novel composite scaffold for ligament tissue engineering. J Biomed Mater Res A 94, 1270-1282 (2010).

24. Hwang, C.M. et al. Controlled cellular orientation on PLGA microfibers with defined diameters. Biomed Microdevices 11, 739-746 (2009).

25. Neumann, T., Hauschka, S.D. & Sanders, J.E. Tissue engineering of skeletal muscle using polymer fiber arrays. Tissue Eng. 9, 995-1003 (2003).

26. Zatti, S. Ingegneria tessutale su microscala: ottimizzazione di substrati microstrutturati per il differenziamento funzionale di miotubi umani. Master Degree Thesis 2008

Chapter 3

MICRO-ENGINEERED SKELETAL MUSCLES FOR DMD *IN VITRO* MODELS

This chapter describes the development of skeletal muscles human *in vitro* models through the application of the microscale technologies reported in chapter 2. In particular, two different *in vitro* models are described: (i) a two-dimensional (2D) *in vitro* model consisting of an array of parallel aligned, functionally differentiated myotubes obtained on micro-patterned hydrogel substrates; (ii) a three-dimensional (3D) *in vitro* model consisting of a series of myotubes bundles embedded in the micrometric channels of an elastic and compliant hydrogel scaffold. Finally, as proof of concept, § 3.3 reports a study on the possibility to exploit the realized 2D *in vitro* model of skeletal muscle for studying the capability of different myogenic cells in restoring dystrophin expression. Results described in § 3.1.1 and § 3.1.2 have been already published as "*Zatti et al, Langmuir, 2011*" (appendix A) and "*Serena et al, Integrative Biology, 2010*" (appendix B). Results described in § 3.3. are main part of a third work now in preparation.

The cell source used for skeletal muscle *in vitro* modeling is represented by primary human myoblasts, provided by Telethon Biobank ("Carlo Besta" Neurological Institute, Milan, Italy). They were derived from biopsies of both healthy (wild type) and DMD affected donors. The culture had a high myogenic potential within early passages *in vitro*: >84% desmin positive cells, >90% MyoD positive cells. The fusion index was highly related to the biopsy, however it ranged from an average of (50 ± 4.8) % for healthy myoblasts to (20 ± 3.2) % for DMD myoblasts. Detailed protocols are reported in appendix A and B.

3.1. Two-dimensional (2D) *in vitro* model of human skeletal muscle

The main goal of the work reported in this chapter is the obtainment of human skeletal muscle *in vitro* models useful for testing therapeutic strategies aimed at restoring a proper dystrophin expression. To this purpose, such *in vitro* models should be representative of DMD patient skeletal muscles biology and functionality. In this perspective it is of paramount importance to correctly reproduce *in vitro* the process of myogenesis guiding skeletal muscle differentiation *in vivo* and the main environmental cues directing its key phases.

In vivo skeletal muscle development is a process characterized by a defined series of events that includes myoblast proliferation, alignment and fusion into multinucleated myotubes[1], and their further differentiation into functional myofibers[2,3]. This process, termed myogenesis, is deeply influenced by the surrounding microenvironment, given by extracellular matrix (ECM), neighboring cells and soluble molecules[4].

ECM is a dynamic structure that provides support and anchorage for cells, further to initiate signal transduction pathways[5]. Mechanical properties (stiffness) and molecular composition of the ECM are important regulators of cell functions and are crucial for cells survival and differentiation[6,7]. Cells continually secrete complex mixtures of ECM proteins and soluble regulators of cell behavior. An important general function of the extracellular matrix is to serve as a reservoir for growth factors and cytokines produced by cells[8]. Gradients of such secreted soluble factors also control tissue patterning by activating genetic programs, thereby inducing and maintaining cellular identity and directing higher-order tissue architecture[9]. Myokines, specific cytokines secreted by skeletal muscle, are known to maintain a balance between growth and differentiation of myoblasts[1] and are emerging as key regulator of myogenesis, extensively expressed also *in vitro* by muscle cells[10].

In order to correctly simulate myogenesis *in vitro*, the main properties of the *in vivo* microenvironment should be reproduced. In particular biochemical, mechanical and topological stimuli are crucial for the obtainment, *in vitro*, of functional skeletal muscle tissue. Furthermore, in the design of *in vitro* engineered tissues, it should be taken into account the ability of gels or matrix to retain soluble factors produced by cells, establishing local concentration gradients of these compounds which may remarkably affect cell behavior.

In this work, for the obtainment of a human skeletal muscle *in vitro* model, micro-scale technologies have been used to reproduce some of the main physiological stimuli directing myogenesis *in vivo*. Such, micro-scale technologies have been *ad-hoc* designed to direct specific phases of the *in vitro* myogenesis:

1) a topologic control over the cell culture, achieved by micro-patterning of adhesion proteins, has been used to direct myoblast alignment and fusion in the early stages of myogenesis (§ 3.1.1);

2) a physiological stiffness of the substrate, achieved by using an hydrogel with tunable elastic proprieties, has been used to allow a functional differentiation of myotubes in the late phases of myogenesis (§ 3.1.2).

3.1.1. Micro-patterning topology direct myoblast behavior in early myogenesis

A key requirement for the *in vitro* engineering of skeletal muscle is the topologic control over the cell culture. Through an imposed geometry of adhesion proteins, myoblasts can be forced to assume a physiological morphology and induced to differentiate. In addition, limiting the size of cell cluster in which cells are organized can influence local concentration of soluble secreted factors, which accumulate into the polymeric biomaterials used as substrate. This can remarkably affect myoblast behavior, with consequences on myoblast differentiation process.

3.1.1.1. Micro-patterned parallel lanes guide myoblasts alignment

In the perspective of reproducing *in vitro* the main cues of the physiological microenvironment, the topologic control on the cultured cells give the possibility to simulate the highly aligned architecture of *in vivo* myofibers. As described in § 2.3, such topologic control can be obtained through micro-patterning of adhesion proteins into defined geometries of parallel lanes on the surface of a PA HY substrate.

Human primary myoblasts seeded onto these engineered substrates adhere with micrometric precision to the protein pattern since the first hours after seeding, showing the typical elongated morphology. Myoblasts grow in an aligned direction and, after 72 h, result fully confluent within the patterned lanes. At the same time, they start to form multinucleated myotubes. About 4 days after seeding an array of parallel aligned myotubes is obtained (Figure 3.1 A). On the opposite, myoblasts cultured onto conventional cell culture surfaces such as Petri-dishes or glass slides, started to align in random directions only 48 h after seeding, when cells density is sufficiently high. This cultures finally result in a complex, disorganized and branched network of myotubes, frequently overlapping each other (Figure 3.1 B).

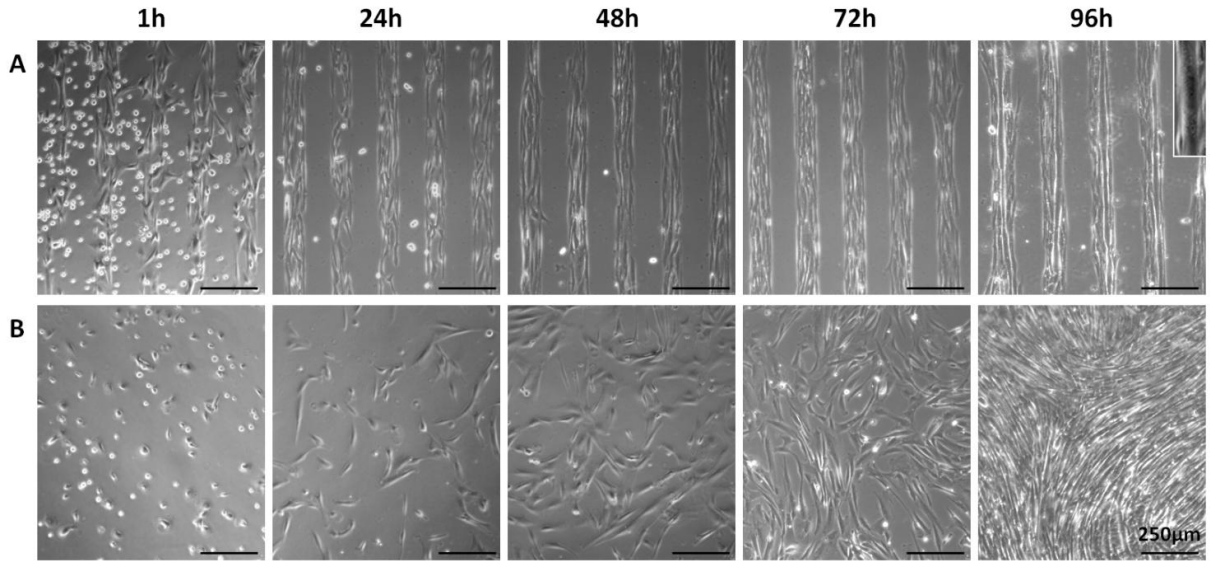

Figure 3.1. Time course of human primary myoblasts seeded on (A) a PA HY substrate micro-patterned with laminin 100 µg/ml in 100 µm wide parallel lanes; (B) a conventional glass slide.

From these results it clearly emerges that micro-patterned PA HY substrates: (i) guide a rapid myoblast alignment and their consequent fusion into myotubes during the early stages of myogenesis; (ii) ensure the obtainment of a single layer of cells thus increasing the uniformity of conditions; (iii) keep cells separated and well defined, allowing an accurate optical definition of myoblasts/myotubes in arrayed and independent lanes.

3.1.1.2. Micro-patterning geometries affect myoblast proliferation and fusion index

In order to rationally study how the realized engineered substrates affect myoblast behavior in the early stages of *in vitro* myogenesis, different micro-patterning geometries were designed. A total of five configurations were produced patterning 100 µg/ml laminin on 15 kPa PA HYs. In three of them, lane and inter-spacing widths are the same (100, 300, and 500 µm). In the other two configurations, lane width is maintained fixed (100 µm), while the inter-spacing varies (50 and 200 µm). Proliferation and differentiation into multinucleated myotubes were evaluated for C2C12 and human primary myoblasts seeded on substrates micro-patterned with these different configurations.

First of all, C2C12 proliferation was investigated by BrdU pulse and chase analyses 48 after seeding in the three geometries with equal lane and inter-spacing widths (Figure 3.2 A). Two different seeding densities were used (200 and 400 cell/mm^2). The percentage of proliferating cells reaches the maximum when C2C12 are cultured in 100 µm wide lanes geometry ((52 ± 1) % for the higher seeding density and (69 ± 8) % for the lower seeding density), then significantly decreased using the

300 and 500 µm wide lane geometries ((31 ± 2) % and (27 ± 4) % respectively for the higher seeding density; (58 ± 3) % and (39 ± 7) % respectively for the lower seeding density) (Figure 3.2 C). On the other hand, the percentage of proliferating cells remained unchanged on the three geometries differing in inter-spacing width. Differentiation was evaluated by myosin heavy chain immunofluorescence analyses 6 days after seeding (Figure 3.2 B). C2C12 fusion index increased with patterning lane width, from a minimum of (46 ± 8) % for 100 µm wide lanes to a maximum of (66 ± 7) % for 500 µm wide lanes (Figure 3.2 D). Myoblasts differentiation showed then an opposite trend compared to proliferation rate. The wider the micro-patterning lanes are, the more the effect on myoblast withdrawal from cell cycle and consequent fusion into myotubes is relevant.

The experiments were replicated culturing human primary myoblasts on the three different micro-patterned surfaces (100, 300 and 500 µm lanes) using a seeding density of 400 cells/mm^2. Human myoblast proliferation was the same in all micro-patterning width (about 40 %). Such discrepancy relies on the different proliferation medium used for cell cultures, containing high serum and growth factors which have a predominant effect of human primary myoblast proliferation. Concerning differentiation, the positive trend obtained for C2C12 was confirmed. A more relevant increase of fusion index was observed in wider patterning lanes, from a minimum of (15 ± 4) % for the 100 µm lanes geometry to a maximum of (36 ± 2) % for the 500 µm lanes geometry (complete data are reported in appendix A).

These results can be explained taking into account the key role of myokines in promoting myoblasts differentiation. These soluble secreted factors can act in an auto/paracrine manner mediating the interaction between fusion partner cells, as well as the direct contact of neighboring cell membrane proteins.

The accumulation, at local level, of soluble myokines secreted by cells may be highly influenced by the presence of the PA HY substrate, having a low diffusion coefficient and then acting as a reservoir. The extent of this accumulation increase with the width of the lanes where cells attach. This hypothesis was confirmed by computational modeling data performed by Ing. Luni and conditioned medium experiments (both reported in appendix A). In particular, myoblasts cultured using medium pre-conditioned by a confluent C2C12 culture showed a remarkable decreases in proliferation rate if compared to cells cultured in conventional conditions using fresh medium. This findings strengthen the hypothesis that an increase in myokines concentration, which is likely to happen in wider patterning, negatively affects cell proliferation and enhances cell differentiation, regardless of the cell density and, consequently, from cell-cell interaction through adhesion molecules.

These data highlight the role of micro-patterning in shaping the cellular niche through secreted factor accumulation and are of paramount importance in rationally understanding myogenesis *in vitro* for the correct design of *in vitro* skeletal muscle models.

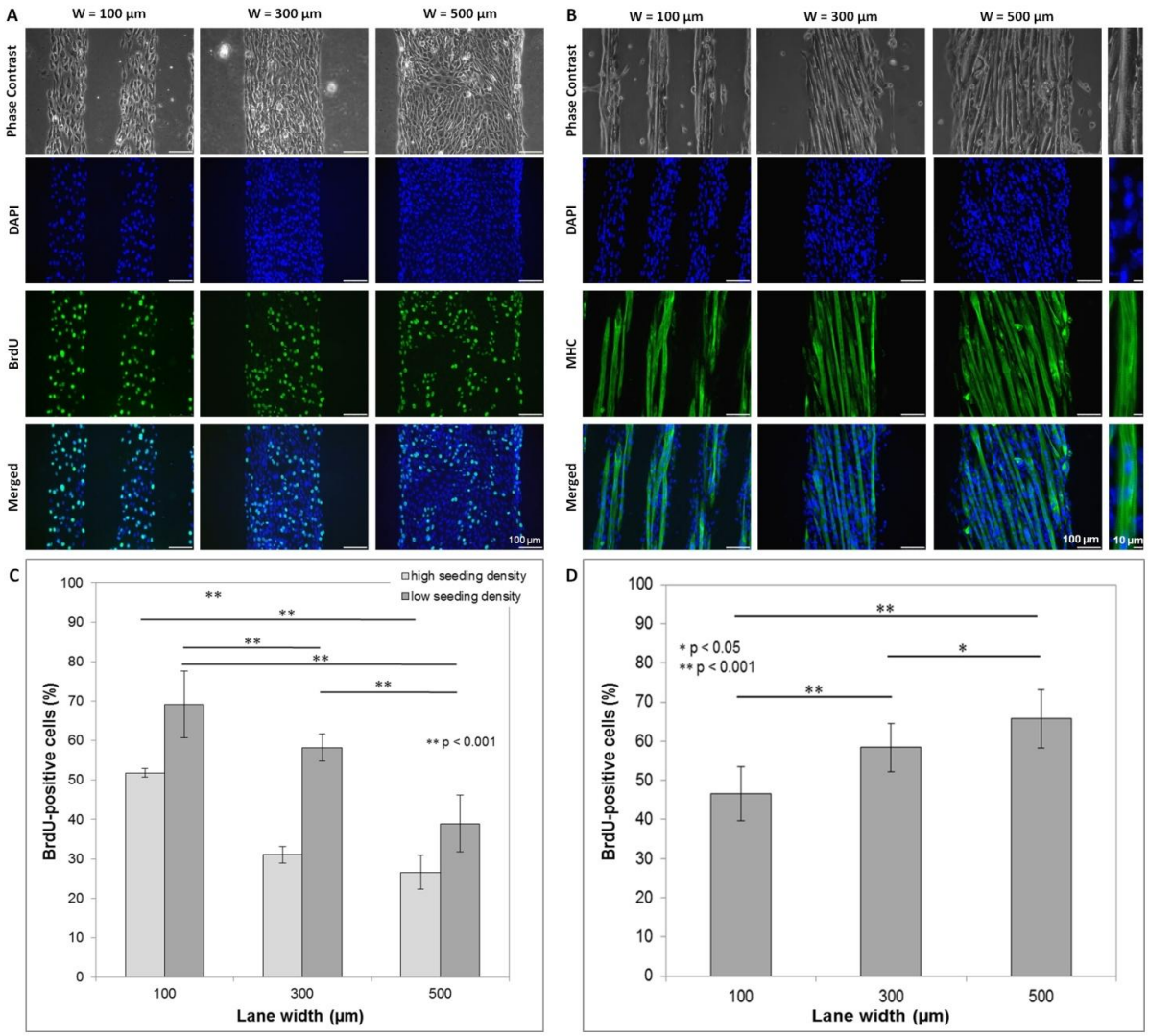

Figure 3.2. Immunofluorescence of BrdU (A) and myosin heavy chain (B) on C2C12 cultures on micro-patterning lanes with 100, 300 and 500 µm width, 48 h (A) and 6 days (B) after seeding. (C) Histogram reporting the percentage of BrdU-positive C2C12 cells for each micro-patterning lanes width and for two different seeding densities. (D) Histogram reporting C2C12 fusion index for each micro-patterning lanes width. Reported p-values were obtained by one-way ANOVA analyses of 5 (C) and 8 (D) independent images. Error bars represent standard deviations.

3.1.2. Elastic substrates drive optimal myotubes differentiation in late myogenesis

As above described, in the myogenesis process, single myoblasts align and fuse into multinucleated syncytia called myotubes. After this early phase, myotubes progressively differentiate towards myofibers, by the development of a contractile apparatus, the maturation of a functional calcium-handling machinery, the expression of acetylcholine receptors and nuclear margination.

It has been reported that the substrate mechanical properties have a key role in myotubes functional differentiation *in vitro* highlighting that sarcomere formation in culture depends on optimal outside-in signaling of matrix elasticity. Engler and colleagues proved that murine myotubes cultured *in vitro* require a substrate with muscle-like stiffness to optimally differentiate (E = 12±4 kPa)[11].

Similarly, myotubes obtained from human primary myoblasts cultured for 7 days on our micro-patterned PA HYs showed a remarkable sarcomeric organization of myosin heavy chain and α-actinin. On the contrary, myotubes obtained in the same culture conditions but cultured on conventional glass substrates did not develop the characteristic sarcomeric cytoskeletal architecture and only an un-structured cytoplasmic staining were observed for both proteins (Figure 3.3 A).

On micro-patterned PA HYs, the obtained human myotubes ranged from 500 mm to 1 mm in length and the sarcomeric striations, observed on their entire length, were characterized by physiological dimensions: contiguous Z-disks were 2.5 mm spaced.

Consequently to these results, the effects of the substrate stiffness in the functional differentiation of human myoblasts, in terms of sarcomere formation, were investigated. To this purpose human primary myoblasts were cultured on micro-patterned PA HYs with increasing elastic modulus: E ≈ 12 kPa, 15 kPa, 18 kPa and 21 kPa (realized as described in § 2.3). In addition, several adhesion proteins were used (100 mg/ml fibronectin, 100 mg/ml laminin and 2.5% v/v matrigel®).

The highest percentage of striated myotubes was always reached using a 10% PA HY with an elastic modulus of 15 kPa, resembling the stiffness of a physiological skeletal muscle tissue, regardless of the adhesion protein used (Figure 3.3 B).

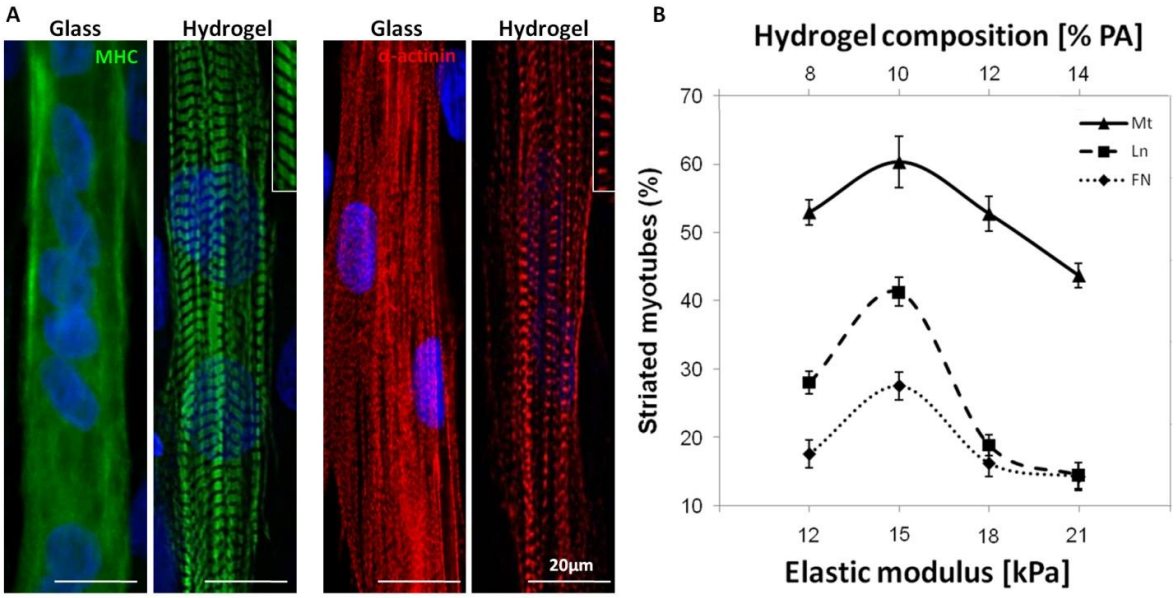

Figure 3.3. (A) Immunostaining of myosin heavy chain II (green) and a-actinin (red) on dystrophic myotubes formed after 7 days of culture on PA HY (15 kPa elastic modulus) micro-patterned with laminin 100 µg/ml. Nuclei are counterstained with DAPI. (B) Graph reporting the percentage of striated myotubes as a function of the PA HY stiffness micro-patterned with fibronectin (FN), laminin (LN) and matrigel® (Mt) after 7 days of culture. The average fusion indexes were 23%, 23%, 13% and 14% onto hydrogel with elastic modulus respectively 12 kPa, 15 kPa, 18 kPa and 21 kPa.

These results show that the percentage of human striated myotubes is strongly dependent on substrate stiffness. At these conditions, electrically induced contractions were observed for both DMD and healthy myotubes.

In the interpretation of these results, it should be considered that myofibrillogenesis, the process resulting in the definition of a functional sarcomeric cytoskeletal architecture, begins at the membrane and proceed in generating a mature myofibrils in a contractile force-dependent

manner[2,3]. In particular, myofibrils assembly is dependent from β1 integrin membrane proteins that in turn bind to RGD (arginine-glycine-aspartate) motifs, present in many ECM proteins, such as laminin and fibronectin[12].

The tissue-like elastic properties and high water content (90% v/v) of the PA HY could allow a certain degree of lateral and rotational mobility to the ECM proteins adsorbed on its surface. These hydrogel properties could strongly affect β1 integrin-ECM proteins interaction and the consequent β1 integrin mobility and arrangement on cell membrane. On substrate with physiological elasticity, β1 integrin could be then easily reorganized in the periodic and ordered structure required for a proper sarcomere assembly.

In contrast, ECM proteins permanently adsorbed on rigid substrates, such as glass, do not have any dynamic conformational change, limiting integrin mobility and the consequent myofibrillar proteins reorganization into striations. On the other hand, cell adhesion on extremely soft substrate, can not efficiently develop contractile forces, that play a key role in miofibrillogenesis.

3.1.3. Dystrophin expression on functionally-differentiated myotubes

The combination of: (i) the topologic control of the cell culture, inducing efficient myoblast alignment and fusion into myotubes during the early stages of myogenesis, and (ii) the elastic hydrogel substrate, reproducing physiological stiffness, allowed the obtainment of an array of parallel aligned myotubes presenting a well-defined sarcomeric cytoskeletal architecture. As expected, the same results were obtained using human primary myoblasts from both DMD patients and healthy donors, since sarcomere formation is not directly correlated to the absence or presence of dystrophin.

In order to be exploited as valuable *in vitro* model of DMD skeletal muscle, the differentiation level of the obtained myotubes array must reach a stage where the target of DMD pathology could be properly expressed. The readout to asses this point is a remarkable and correct dystrophin expression.

Dystrophin expression restoration in myofibers is the primary target of most experimental strategies addressed the treatment of DMD[13]. Thus, having functionally-differentiated human myotubes expressing dystrophin is the first and fundamental prerequisite to set up a human *in vitro* model-based assay aimed at testing the feasibility and efficacy of different approaches.

Myotubes obtained from healthy donors' myoblasts on 15 kPa PA HYs, micro-patterned with 2,5% v/v matrigel®, remarkably expressed dystrophin after 10 days of culture (Figure 3.4). The analysis with a confocal microscope revealed that dystrophin was specifically expressed at membrane level.

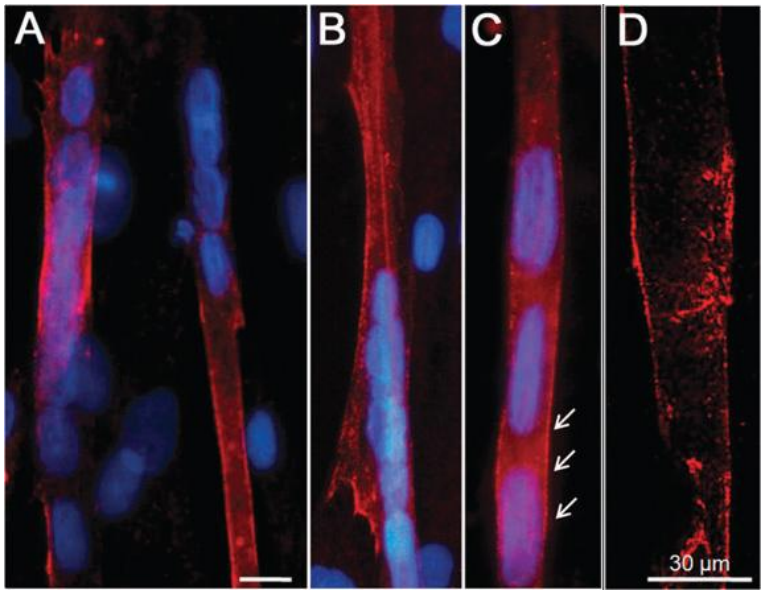

Figure 3.4. Dystrophin expression on myotubes derived from healthy donors cultured for 11 days on PA HY (15 kPa elastic modulus) micro-patterned with laminin 100 µg/ml. Nuclei are counterstained with DAPI. Dystrophin expression occurs partially (A) or along the entire myotube (B). Higher magnification (C, arrows) and confocal microscope image (D) show that dystrophin is expressed on the myotube membrane.

3.2. Three-dimensional (3D) *in vitro* model of human skeletal muscle

In vitro, cells classically grown on flat two-dimensional (2D) substrates can differ considerably in their morphology, cell-cell, cell-matrix interactions and differentiation from those growing in a physiological 3D environment[8]. In particular, skeletal muscle *in vivo* is composed of myofiber bundles, tightly held together by a 3D extracellular matrix scaffold to form a highly organized tissue with a high cell density and a precise orientation that generates the longitudinal contraction. Myofibers are multinucleated cells (up to several hundred for each fiber) derived from alignment and fusion of individual myoblasts within the 3D muscle architecture. The size of a myofibers can range from millimiters to centimeters in length and from 10 to 100 µm in width. Myofiber diameter is thinner near the myotendinous junctions and reach the maximum in the muscle middle section. Neo-formed and regenerating myofibers are centro-nucleated and, proceeding with the miofibrillogensis process that originate the functional sarcomeric architecture, nuclei are marginated at the sarcolemma, the plasma membrane enclosing each myofibers[14]. All these morphological and functional features are at least partially lost in conventional 2D culture, where myoblasts and myotubes adopt a flat, spread shape and differentiation usually can not reach a physiological level.

A 3D tissue culture environment allow individual cells to assume a shape and exhibit a phenotype that are more *in vivo*-like than those formed in a 2D environment[15]. Furthermore, compared with conventional 2D cultures in a large Petri dish, dense 3D cultures with confined extracellular space can amplify local autocrine and paracrine actions of cells[16]. From this context clearly emerges the importance of a 3D microenvironment in designing physiologically relevant *in vitro* models of living tissues.

To this purpose, 3D PA HY scaffolds have been realized. Such system was designed in order to confine myoblasts and myotubes inside a 3D microenvironment with physiological properties. In this

way, myoblasts can adhere no more on a flat 2D substrate but to a 3D niche having the same elasticity and compliance of a native muscle tissue. At the same time, the confined 3D microenvironment surrounding cells can promote an higher accumulation of secreted myokines promoting differentiation, thus potentially improving myotube maturation.

This 3D PA HY scaffold (realized according to methods described in § 2.4) contains a series of parallel aligned micrometric channels where cells can be injected. Micrometric channels with different diameters were successfully produced using polymeric cylindrical fillers of different size (ranging from 80 to 160 µm) (Figure 3.5 A, B, D). These dimensions were designed in order to be comparable to the ones of a single myofiber *in vivo*, which measures about 100 µm in diameter in muscles middle section[14]. In addition, in order to allow cell adhesion, inner walls of channels were functionalized with laminin (Figure 3.5 C).

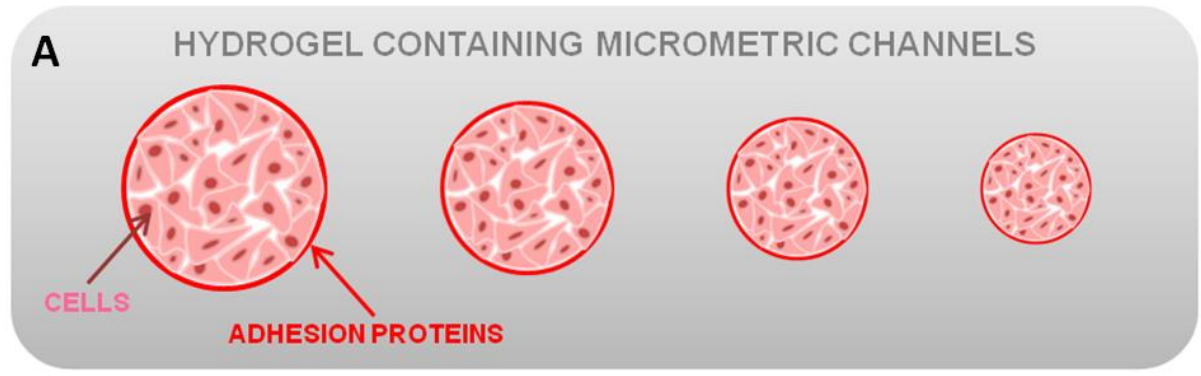

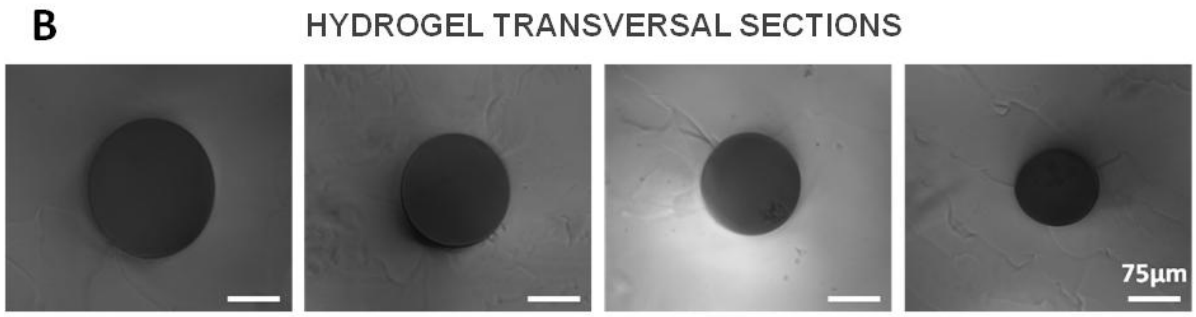

C

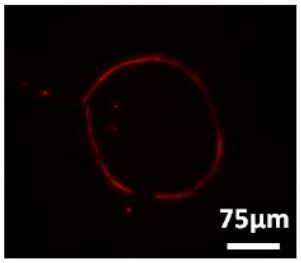

D

cylindrical fillers used	obtained channels
80 µm	80 ± 10 µm
120 µm	120 ± 11 µm
140 µm	140 ± 15 µm
160 µm	160 ± 18 µm

Figure 3.5. (A) Schematic representation of the 3D PA HY scaffold containing micrometric channels. (B) Phase contrast of a transversal section of the micrometric channels with different diameters (before cell injection). (C) Laminin immunofluorescece of a transversal section of a micrometric channel 160 µm in diameter, functionalized with laminin before cell injection. (D) Table reporting dimensions of the cylindrical fillers used and the obtained micrometric channels. Standard deviations were calculated on a total of 5 samples.

3D PA HY biocompatibility was assessed by Live and Dead analysis performed 24 h after myoblast injection (Figure 3.6). Results demonstrated that cell viability in not negatively influenced by the culture inside the micrometric channels. The hydrogel scaffold ensures then mass transport of metabolite and nutrient required for proper myoblasts survival, growth and differentiation.

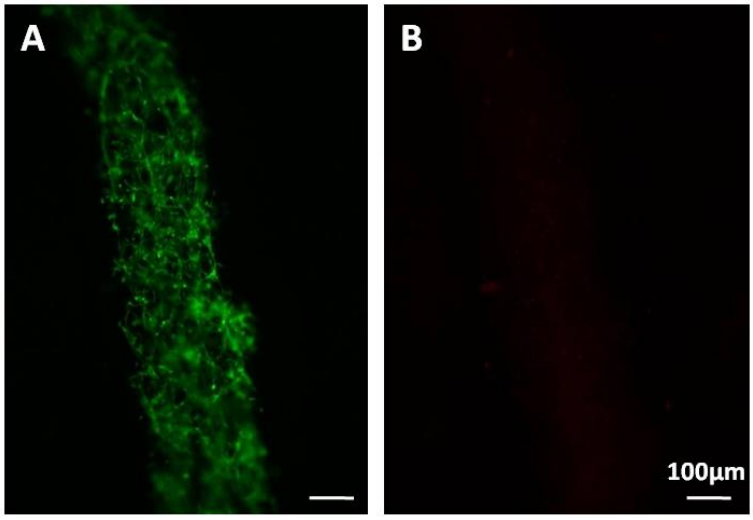

Figure 3.6. Live and Dead analysis on myoblasts cultured inside micrometric channels for 24 h. (A) Cytoplasmic calcein staining of living cells. (B) Nuclear Ethidium Bromide staining of dead cells.

In Figure 3.7 is reported a time course of human myoblasts culture inside the micrometric channels. About 24 h after injection, myoblasts underwent a remarkable morphological change, aligned and adhered to the channels walls (Figure 3.7 B). After about 4 days of culture the formation of elongated structures was observed (Figure 3.7 C). Through immunofluorescence analysis of myosin heavy chain, performed after 5 days of culture on the whole PA HY scaffold, the presence of multinucleated myotubes was revealed (Figure 3.7 D).

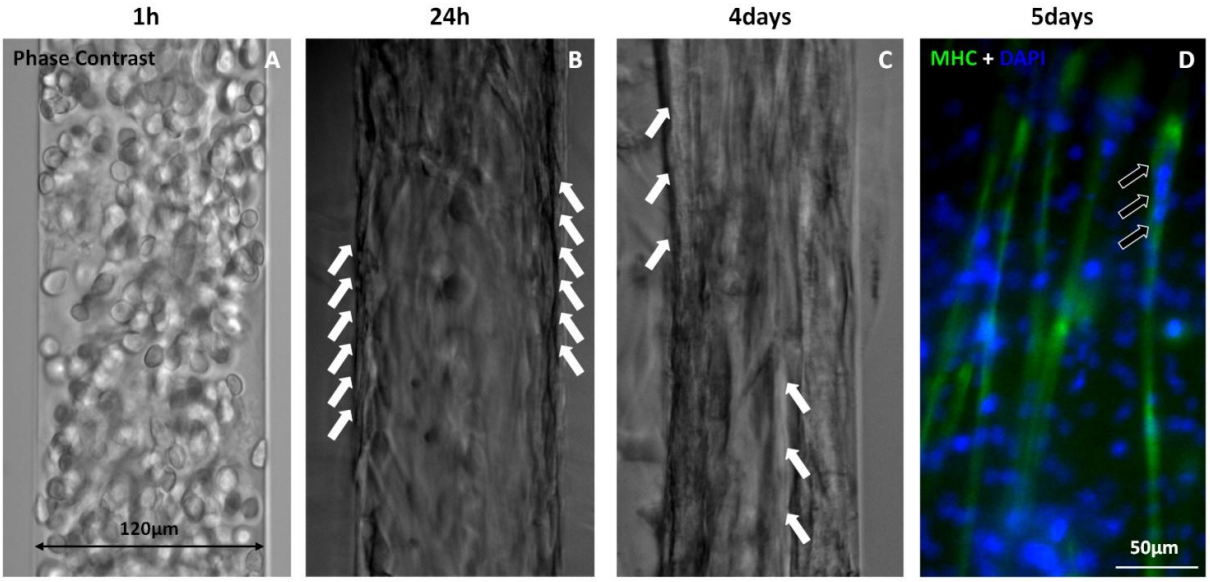

Figure 3.7. Time course of human myoblasts cultured inside the micrometric channels. (A) Myoblasts morphology immediately after the injection inside the micrometric channel. (B) Myoblasts 24h after the injection. Arrows indicate cells adhered to the walls. (C) Myoblasts 4 days after the injection. Arrows indicate the presence of elongated structures. (D) Myosin heavy chain-positive multinucleated myotubes (arrows) 5 days after the injection. Nuclei are counterstained with DAPI.

Expression of myosin heavy chain and α-actinin were observed in cryosections of the 3D PA HY, realized transversally to the channels direction after 10 days of culture (Figure 3.8).

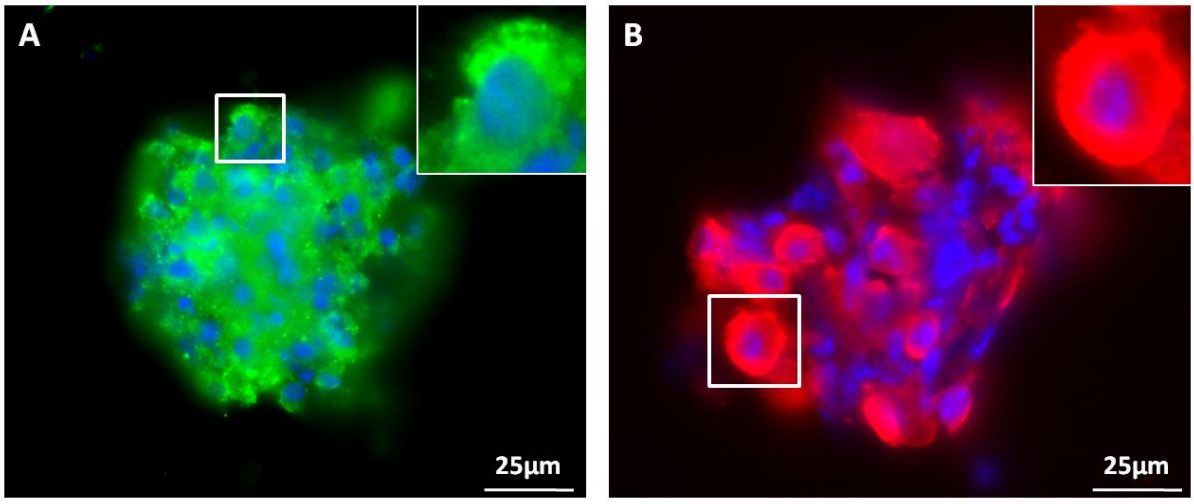

Figure 3.8. Transversal cryosections of micrometric channels cultured with myoblasts for 10 days. (A) Myosin heavy chain immunofluorescence. (B) α-actinin immunofluorescence. Nuclei are counterstained with DAPI.

Human myoblasts can be maintained inside micrometric channels up to 20 days.

Remarkably, these results demonstrate that high-density 3D culture of myoblasts have been obtained inside micrometric channels characterized by myofiber-like dimensions. In these conditions tightly packed myotube bundles have been obtained. Such myotubes express the differentiation markers myosin heavy chain and α-actinin. In addition, they show a morphology completely different from the one obtained in 2D culture.

Cytoskeletal architecture and sarcomeric structures are organized starting from integrin adhesion sites at the membrane. When myoblasts and myotubes adhere to a flat 2D substrate, such adhesion sites are located only on the half of the membrane contacting the substrate. Consequently, the cytoskeletal and sarcomere structures are developed from this side of the cell, pushing nuclei towards the upper-side, where membrane is free from any adhesion point. In a 3D context simulating the *in vivo* situation where ECM completely surround the cell, integrin adhesion sites should be located throughout the cell surface allowing cytoskeletal and sarcomeric structures to organize in a 3D way. As revealed by the analyses of cryosections, myotubes obtained in the micrometric channels resulted to be centronucleated (Figure 3.8, inlets), resembling the morphology of small neo-formed, regenerating myofibers observed in muscle sections of DMD patient or *mdx* mice. This morphology can not be observed in a 2D system.

Many recent works have dealt with the realization of different 3D cell culture systems that can better mimic features of the *in vivo* cell micro-environment if compared to standard 2D *in vitro* culture conditions. In particular, concerning skeletal muscle, most of these works are based on cells encapsulation into gels or matrix[17–19], which are then molded or confined into geometrically-defined holders in order to obtain, after the polymerization, 3D cell aggregates in an open system.

Despite further analyses are needed to assess long term differentiation of the obtained myotubes the 3D model here developed is promising for the obtainment of differentiated myofiber-like structure. If compared to the previously reported methods, our micro-channels-containing 3D PA HY

scaffold present the unique advantage of obtaining myotubes in a confined microenvironment, where they are completely surrounded by an elastic and compliant matrix.

3.3. Testing cell therapy approaches on the *in vitro* model of DMD skeletal muscle

The research strategy to develop a new therapy for DMD or other genetic disease starts from the *in vitro* testing of hypothesis on conventional cell culture and progress towards the assessment of the response of an entire organism through the *in vivo* experimentation on animal models. After many years of research and the obtainment of promising results, the study enters the phase of clinical trial on human patients. However, therapies that looked promising in animal models (such as myoblast transfer) have repeatedly yielded disappointing results in clinical trial[20]. Therefore, the results obtained using *in vivo* models should not be extrapolated to the human disease without caution.

In this scenario, it would be extremely important to have a new model suitable to be coupled with standard research tools and able to: (i) reproduce the human biology and physiology of skeletal muscles; (ii) provide robust and reproducible biological and physiological functional data; (iii) offer a standard background with defined variables, allowing the comparison of different strategies; (iv) be easily transferable to research laboratory for facilitating the therapy development process in reduced time and at lower cost.

As described in § 3.1 a human *in vitro* model of skeletal muscle tissue has been obtained. This human *in vitro* model is made by an array of parallel aligned myotubes presenting a functional differentiation, in terms of sarcomere formation, and carrying the genetic defect of the patient from which myoblasts were derived.

This section describes the investigations on the possibility to exploit the realized *in vitro* model for studying the capability in restoring dystrophin of different myogenic cells. In this study, only the 2D *in vitro* model have been tested since it is better characterized than the 3D one, which still need further analyses before moving to this phase.

An *in vitro* assay was set up, based on our model, having as readout dystrophin expression restoration on engineered myotubes, derived from the co-colture of DMD patient myoblasts with different donor myogenic cells carrying the wild-type copy of the dystrophin gene. Three different myogenic cells with an increasing degree of stemness have been tested: (i) human primary myoblasts, (ii) satellite cells[21] and (iii) mesoangioblasts[22] (Figure 3.9).

Human myoblasts are historically the most investigated cells in the search for a therapy for muscular dystrophies and in particular for DMD. The first pioneer studies and clinical trials were focused on these cells. Satellite cells have been the first stem cells of the skeletal muscle tissue to be isolated. They are still considered the main players in skeletal muscle regeneration. Clinical trials based on satellite cells intramuscular injection were performed in the early 90s. However, both myoblasts and satellite cells were shown to contribute only to a limited muscle regeneration in patients[23–25]. Mesoangioblasts are the cells with the highest degree of stemness among the three tested. Their ability to differentiate into the myogenic lineage and cross the vessel wall, makes them one of the best candidate for clinical applications[26–28]. A phase I clinical trial with mesoangioblasts allotransplantation in DMD patients has already started.

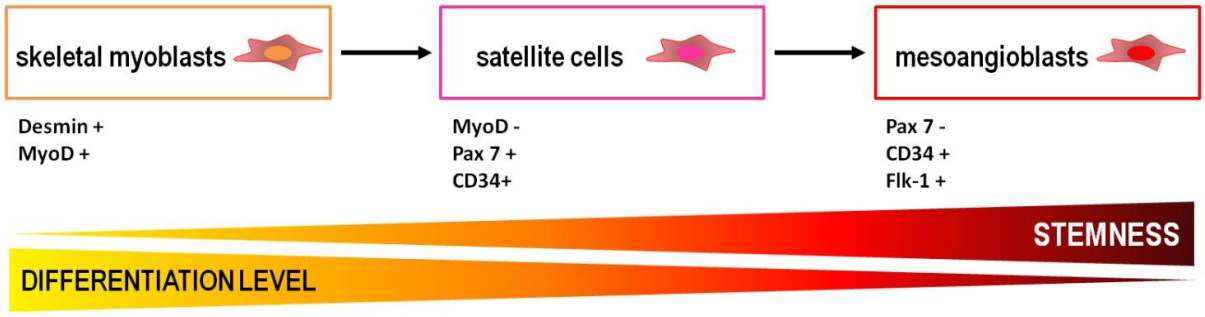

Figure 3.9. The three different types of myogenic cells used: human primary myoblasts, satellite cell and mesoangioblasts. These cells are characterized by an increasing degree of stemness and, at the same time, a decreasing degree of differentiation along the myogenic lineage. Main markers characterizing each cell type are reported.

First of all, it should be considered that in a co-culture between DMD and wild type cells, three different types of multinucleated myotubes can arise: (a) myotubes composed only by DMD myoblasts (DMD-MT); (b) myotubes composed only by wild type myoblasts (WT-MT); (c) "mixed" myotubes composed by the fusion of wild type and DMD myoblasts (mixed-MT).

The capability of wild type cells to restore dystrophin expression in any DMD model is given by the contribution of both WT-MT and mixed-MT. However, a method to distinguish the contribute of the mixed-MT from the total dystrophin production was set up. This is of paramount importance in studying the ability of wild-type nuclei to restore a proper dystrophin expression domain in the context of a whole DMD myotube or myofiber.

To this purpose, lipophilic tracers DiI (red) and DiO (green) were used for staining the myoblasts membrane of wild type and DMD human primary myoblasts, respectively (Figure 3.10). Such tracers were chosen since their high staining efficiency ((75 ± 7) % of the cells are stained with DiI and (88 ± 4) % of the cells are stained with DiO). In addition they do not compromise myoblasts viability and differentiation (unlabeld myoblasts fusion index is (22 ± 6) %, the same myoblasts have a fusion index of (21 ± 4) % if labeled with DiI and of (20 ± 6) % if labeled with DiO).

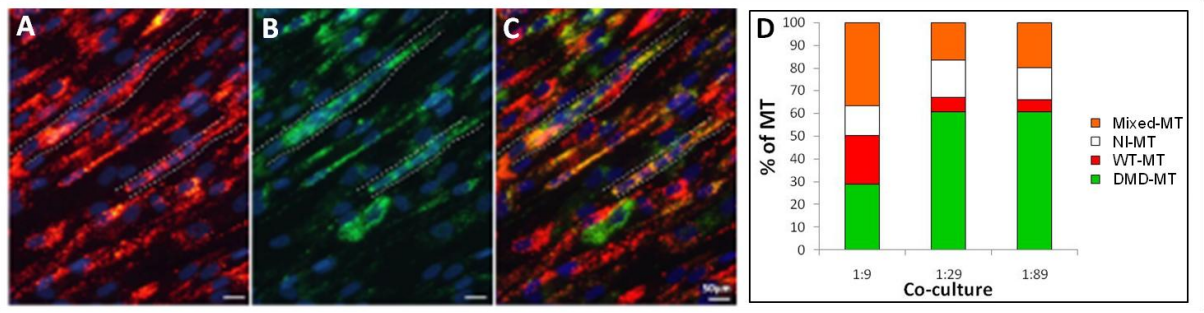

Figure 3.10. Myotubes formation in co-cultures of wild-type human primary myoblasts stained with DiI (red) and DMD human primary myoblasts stained with DiO (green). (A-C) Fluorescent images of red wild-type myotubes (WT-MT) (A), green DMD myotubes (DMD-MT) (B) and orange "mixed" myotubes (mixed-MT) (C) resulting from the overlay of red and green. (D) Quantification of the percentage of four different myotube types in the co-cultures performed with three different ratios: DMD-MT (green), WT-MT (red), mixed-MT (orange), non identified myotubes (NI-MT) (white).

Figure 3.10 reports the percentages of the different myotube types obtained co-culturing the two populations in different ratio (1:9, 1:29 and 1:89, that is 1 wild type myoblast and 9, 29, 89 DMD myoblasts). Since the tracer efficiency was not 100 %, myotubes without any staining were also observed (non identified myotubes, NI-MT). The percentage of mixed myotubes decreases with the

co-culture ratios from about 37% to 16 %. However, the fraction of dystrophin-positive MT (given by the sum between WT-MT and mixed-MT) in the three different co-culture ratios is 58 % in the 1:9 ratio, 22 % in the 1:29 ratio and 25 % in the 1:89 ratio. Taken together these results state that in the co-culture experiments, the mixed-MT are a fraction of about 40 % of all dystrophin-positive myotubes.

This result should be taken into account when the dystrophin will be quantitatively evaluated by western blot. This technique allows the measurement of the whole dystrophin produces, but, obviously, does not discriminate between the MT that produce it. For this reason, while analyzing the western blot results, we should consider that mixed myotubes account for about 40 % of the total dystrophin.

To analyze the capability of the three wild type myogenic cells in restoring dystrophin expression, co-culture experiments were performed using the 1:9 ratio. Immunofluorescence (Figure 3.11) and western blot (Figure 3.12) analyses were performed, in order to verify both the localization and distribution of the protein and the amount of dystrophin produced (in a semi-quantitative manner).

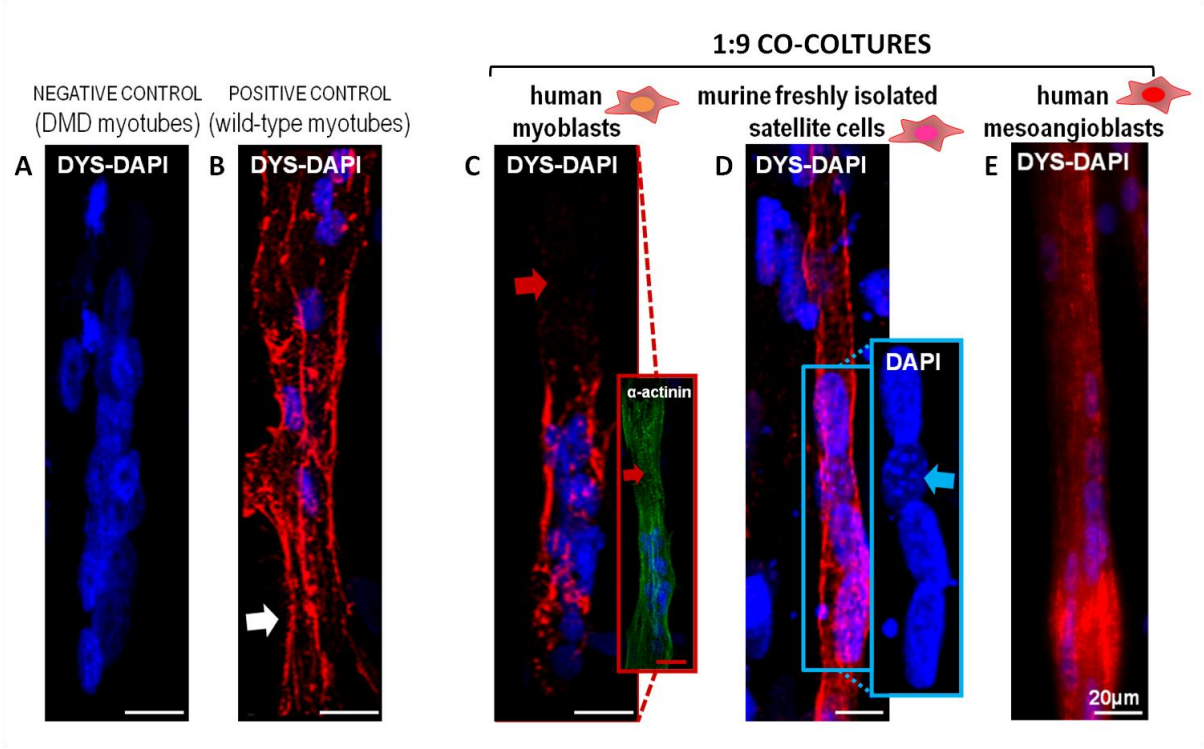

Figure 3.11. Immunofluorescence analyses of dystrophin expression in (A) myotubes obtained by DMD myoblasts (DMD-MT); (B) myotubes obtained from wild-type myoblasts (WT-MT); (C-D) myotubes obtained from 1:9 co-colture of wild-type human primary myoblasts (C), murine satellite cells (D) and human mesoangioblasts (E) with DMD myoblasts.

As expected, DMD-MT do not express dystrophin (Figure 3.11 A), while WT-MT show dystrophin expression correctly localized at the membrane (Figure 3.11 B). In the co-cultures of these two different myoblast populations, mixed-MT with a partial restoration of dystrophin expression were observed (Figure 3.11 C). Dystrophin localization was not uniformly distributed along the entire myotubes length. Figure 3.11 C shows the localization of dystrophin in a defined region of the myotube. Probably, one or more wild type nuclei were present and contribute to the production of dystrophin localized in that area.

The second cell type tested were murine satellite cells. In order to maintain as much as possible the original/*in vivo* myogenicity of these cells, freshly isolated satellite cells should be used, skipping the expansion *in vitro*[29]. For this reason, in this case human satellite cells couldn't be used because the number of required cells is too high and an *in vitro* expansion would have been necessary. Besides being available in high numbers, murine satellite cells allowed the direct identificationof the mixed-MTthrough the localization of the murine nuclei. In fact, murine nuclei, when stained with Hoechst or DAPI, show a peculiar punctate staining, while human nuclei have a uniform stain[30] (Figure 3.11 D, inlet).

In contrast with the human primary myoblasts co-cultures, in the mixed-MT obtained from wild type murine satellite cells and human DMD myoblasts, an uniform distribution of dystrophin along the entire myotube length was observed (Figure 3.11 D). The punctuate staining allowed to clearly identify the contribution of wild type nuclei within a MT. In this case, a single wild-type nucleus direct the expression of dystrophin along wide portion of membrane, almost the entire myotubes length.

The cells with the highest degree of stemness, tested in this study, which are a good myogenic source as well, were the human mesoangioblasts. As for the murine satellite cells, in the mixed-MT obtained from wild type human mesoangioblasts and human DMD myoblasts, a uniform dystrophin expression, well distributed along the entire myotubes length, was observed (Figure 3.11 E).

After a qualitative evaluation of dystrophin localization and distribution by the above reported immufluorescence analyses, the amount of dystrophin produced in the co-cultures was analyzed in a semi-quantitative way by western blot (Figure 3.12).

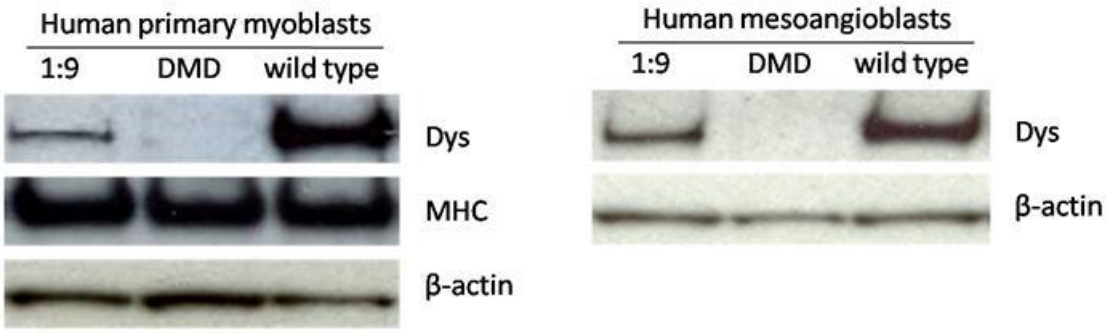

Figure 3.12. Western blot analyses of dystrophin (Dys), myosin heavy chain (MHC) and β-actin in human primary myoblasts and human mesoangioblasts co-culture experiments.

In particular, the amount of dystrophin produced in the 1:9 co-cultures was compared with the amount of dystrophin produced in the wild-type cultures. Quantification of results showed that: (i) the wild type human primary myoblasts in the 1:9 co-culture gave the (14 ± 6) % of dystrophin restoration; (ii) the wild type human mesoangioblasts in the 1:9 co-culture of human primary myoblasts gave the (57 ± 8) % of dystrophin restoration. Considering only the contribution of mixed-MT (which account for about 40 % of all the dystrophin produced, as shown in figure 3.12), wild type human primary myoblasts allow a (6 ± 3) % of dystrophin restoration, while human wild type mesoangioblasts increase their contribution to a (23 ± 4) %. Finally, dystrophin expression restoration by mesoangioblasts results 4 folds higher than the one induced by human primary myoblasts.

All the obtained results can be summarized as follow: (i) human primary myoblasts can restore dystrophin expression only in a limited regions of myotubes (Figure 3.11 C); (ii) murine satellite cells

restore dystrophin in a wider area, almost along the entire myotube length (Figure 3.11 D); (iii) human mesoangioblasts, similarly to the murine satellite cells, are able to restore dystrophin in the entire myotube length (Figure 3.11 E); (iv) in the 1:9 ratio co-culture (1 wild type cells plus 9 DMD cells), human primary myoblasts are able to restore only 6 % of the dystrophin expressed by a culture entirely composed of wild type myoblasts; whereas human mesoangioblasts are able to increase the dystrophin restoration by about 4 folds (23 %) (Figure 3.12).

Taken together these results demonstrate that myogenic cells, with an increasing degree of stemness, have a different capability in restoring dystrophin expression in DMD myotubes. In other words, in a DMD context, the expression of dystrophin seems to be not equal in all myogenic cells, but influenced by the stemness of the considered nucleus.

3.4. References

1. Chargé, S.B.P. & Rudnicki, M.A. Cellular and molecular regulation of muscle regeneration. Physiol. Rev. 84, 209-238 (2004).

2. Sanger, J.W. et al. Myofibrillogenesis in skeletal muscle cells. Clin. Orthop. Relat. Res. S153-162 (2002).

3. Sanger, J.W. et al. How to build a myofibril. J. Muscle Res. Cell. Motil. 26, 343-354 (2005).

4. Sung, J.H. & Shuler, M.L. Microtechnology for Mimicking In Vivo Tissue Environment. Annals of Biomedical Engineering (2012).doi:10.1007/s10439-011-0491-2

5. Carmignac, V. & Durbeej, M. Cell–matrix interactions in muscle disease. The Journal of Pathology 226, 200-218 (2012).

6. Nelson, C.M. et al. Emergent patterns of growth controlled by multicellular form and mechanics. Proc. Natl. Acad. Sci. U.S.A. 102, 11594-11599 (2005).

7. Mazzoleni, G., Di Lorenzo, D. & Steimberg, N. Modelling tissues in 3D: the next future of pharmaco-toxicology and food research? Genes Nutr 4, 13-22 (2009).

8. Yamada, K.M. & Cukierman, E. Modeling tissue morphogenesis and cancer in 3D. Cell 130, 601-610 (2007).

9. Engler, A.J., Humbert, P.O., Wehrle-Haller, B. & Weaver, V.M. Multiscale modeling of form and function. Science 324, 208-212 (2009).

10. Griffin, C.A., Apponi, L.H., Long, K.K. & Pavlath, G.K. Chemokine expression and control of muscle cell migration during myogenesis. J. Cell. Sci. 123, 3052-3060 (2010).

11. Engler, A.J. et al. Myotubes differentiate optimally on substrates with tissue-like stiffness: pathological implications for soft or stiff microenvironments. J. Cell Biol. 166, 877-887 (2004).

12. Sparrow, J.C. & Schöck, F. The initial steps of myofibril assembly: integrins pave the way. Nat. Rev. Mol. Cell Biol. 10, 293-298 (2009).

13. Goyenvalle, A., Seto, J.T., Davies, K.E. & Chamberlain, J. Therapeutic approaches to muscular dystrophy. Hum. Mol. Genet. 20, R69-78 (2011).

14. Sherwood, L. Human Physiology: From Cells to Systems. (Cengage Learning: 2010).

15. Pampaloni, F., Reynaud, E.G. & Stelzer, E.H.K. The third dimension bridges the gap between cell culture and live tissue. Nat. Rev. Mol. Cell Biol. 8, 839-845 (2007).

16. Bian, W., Liau, B., Badie, N. & Bursac, N. Mesoscopic hydrogel molding to control the 3D geometry of bioartificial muscle tissues. Nat Protoc 4, 1522-1534 (2009).

17. Bian, W. & Bursac, N. Engineered skeletal muscle tissue networks with controllable architecture. Biomaterials 30, 1401-1412 (2009).

18. Aubin, H. et al. Directed 3D cell alignment and elongation in microengineered hydrogels. Biomaterials 31, 6941-6951 (2010).

19. Vandenburgh, H. et al. Automated drug screening with contractile muscle tissue engineered from dystrophic myoblasts. FASEB J. 23, 3325-3334 (2009).

20. Collins, C.A. & Morgan, J.E. Duchenne's muscular dystrophy: animal models used to investigate pathogenesis and develop therapeutic strategies. Int J Exp Pathol 84, 165-172 (2003).

21. MAURO, A. Satellite cell of skeletal muscle fibers. J Biophys Biochem Cytol 9, 493-495 (1961).

22. Cossu, G. & Bianco, P. Mesoangioblasts--vascular progenitors for extravascular mesodermal tissues. Curr. Opin. Genet. Dev. 13, 537-542 (2003).

23. Gussoni, E., Blau, H.M. & Kunkel, L.M. The fate of individual myoblasts after transplantation into muscles of DMD patients. Nat. Med. 3, 970-977 (1997).

24. Gussoni, E. et al. Normal dystrophin transcripts detected in Duchenne muscular dystrophy patients after myoblast transplantation. Nature 356, 435-438 (1992).

25. Mendell, J.R. et al. Myoblast transfer in the treatment of Duchenne's muscular dystrophy. N. Engl. J. Med. 333, 832-838 (1995).

26. Sampaolesi, M. et al. Mesoangioblast stem cells ameliorate muscle function in dystrophic dogs. Nature 444, 574-579 (2006).

27. Sampaolesi, M. et al. Cell therapy of alpha-sarcoglycan null dystrophic mice through intra-arterial delivery of mesoangioblasts. Science 301, 487-492 (2003).

28. Tedesco, F.S. et al. Stem cell-mediated transfer of a human artificial chromosome ameliorates muscular dystrophy. Sci Transl Med 3, 96ra78 (2011).

29. Rossi, C.A. et al. In vivo tissue engineering of functional skeletal muscle by freshly isolated satellite cells embedded in a photopolymerizable hydrogel. FASEB J. 25, 2296-2304 (2011).

30. Pomerantz, J.H., Mukherjee, S., Palermo, A.T. & Blau, H.M. Reprogramming to a muscle fate by fusion recapitulates differentiation. J. Cell. Sci. 122, 1045-1053 (2009).

Chapter 4

MICRO-ENGINEERED CARDIAC MUSCLES FOR DMD *IN VITRO* MODELS

This chapter describes the results concerning the development of human *in vitro* model of cardiac muscle. After a brief summary of the motivations and an introduction on the cardiogenic potential of human pluripotent stem cells are provided (§ 4.1); the first part of this chapter (§ 4.2) focuses on human embryonic stem cells-derived cardiomyocytes and their organization into an array of contracting dots through the micro-scale technologies reported in chapter 2. In the second part of this chapter (§ 4.3) results about DMD patient-specific cardiomyocytes derived from human induced pluripotent stem cells are presented. Paragraph § 4.4 reports a study of dystrophin expression restoration on DMD cardiomyocytes genetically corrected by a human artificial chromosome carrying a full-length genomic dystrophin sequence. Finally, as future perspective, preliminary results about the possibility to improve cardiac differentiation from pluripotent stem cells through HAC technology are reported (§ 4.5). Part of this work was performed at the Chromosome Engineering Research Center (Tottori University - Faculty of Medicine, Yonago, Japan) under the supervision of Prof. Mitsuo Oshimura. Results described in § 4.2 are part of a manuscript already submitted for publication (appendix C). Results described in § 4.3 and 4.4 are main part of another manuscript in preparation.

4.1. Cardiogenic potential of human pluripotent stem cells

As previously introduced (§ 1.1, 1.3), in DMD patients heart failure is thought to be responsible for 20% of deaths. Cardiomyopathy, that is present in about 90% of patients, is emerging as a major cause of patient morbidity and mortality due to the increased lifespan allowed by the improvements in treatments of respiratory muscle disease[1]. In addition, many experimental therapies are targeted to skeletal muscle, but failed to improve cardiac function; while therapies restricted to skeletal muscles alone have been shown to accelerate heart disease[2]. From this context it clearly emerges that, in the development of a new therapeutic strategy, skeletal and cardiac muscle should be treated equally, carefully testing its efficiency also at cardiac level. Consequently, a human *in vitro* model of DMD cardiac muscle could represent a powerful tool, beside the *in vivo* testing on animal models, in the process of new therapies development. However, due to the extremely limited proliferative capacity of adult cardiomyocytes, the direct isolation of human cells suitable for an *in vitro* modeling is a challenging issue. Human pluripotent stem cells-derived cardiomyocytes are currently almost the only reliable source of human heart cells[3] suitable for modeling human heart and its development, for high-throughput screening and safety testing of new drugs or treatments and, more in perspective, for cell-based cardiac therapies. As recently reviewed by Laflamme and colleagues[4], human embryonic stem (hES) cells and human induced pluripotent stem (hiPS) cells have

a number of attractive qualities for these applications. In particular: (i) both these pluripotent stem cell types have an unquestioned cardiomyogenic potential, unlike many adult stem cell types for which this capacity is controversial; (ii) hES and hiPS cells retain their pluripotent phenotype through more than a hundred population doublings and their cardiac progeny are readily expandable *in vitro*; (iii) while the isolation of other candidate stem cell populations is frequently difficult and un-reproducible, hES and hiPS cells have been derived by many laboratories using well-established procedures.

In this work hES cells, in particular the HES2 line from WiCell Bank, were used (i) for setting up and optimizing methodologies related to pluripotent stem cells culture and expansion and (ii) for the application of an efficient, well-established procedure of cardiac differentiation[5]. The obtained hES cells-derived CMs were used for the development of a contractile micro-array through the coupling of micro-scale technologies. Subsequently, we focused on hiPS cells. The procedure of cardiac differentiation was optimized in order to obtain DMD patient-specific, hiPS cells-derived CMs. Then, as proof of concept, dystrophin expression restoration was studied on DMD CMs genetically corrected by a human artificial chromosome carrying a full-length genomic dystrophin sequence.

4.2. hES cells-derived CMs micro-array as *in vitro* model of cardiac muscle

4.2.1. hES cells and their differentiation towards the cardiac lineage

The first human embryonic stem (hES) cell lines were derived by Thomson and colleagues in 1998 from the inner cell mass (ICM) of fresh or frozen human embryos at the blastocyst stage, produced by *in vitro* fertilization for clinical purposes and donated by individuals after informed consent and after institutional review board approval[6]. During normal embryonic development, the ICM of blastocyst give rise, to the three germ layers: endoderm, ectoderm and mesoderm that originate all tissue types of the developing embryo. For the derivation of hES cells, the ICM cells are isolated and plated on a mitotically inactivated mouse embryonic fibroblast (MEF) feeder layer where they form colonies, which are then selected, passaged, and expanded. Undifferentiated hES cells retain a normal diploid karyotype and express high levels of telomerase activity during long-term propagation in culture while maintaining the potential to form derivatives of all three embryonic germ layers both *in vivo* and *in vitro*. Injection of hES cells into immunodeficient mice produced teratomas, containing tissues derivatives of endoderm, mesoderm, and ectoderm origin[7]. Similarly, *in vitro*, hES cells spontaneously differentiated when cultured in the absence of MEF feeder layer, forming three-dimensional cell clusters termed embryoid bodies (EBs) which can be maintained in suspension and contain as well, cell derivatives of the three germ layers[8]. Since 1998, when the first hES cell lines were reported, a great number of genetically diverse cell lines have been derived from human blastocysts. In order to assess the similarities and differences in the expression of commonly used markers of hES cells among different lines and to identify a set of well-validated markers to establish hES cell identity, the International Stem Cell Initiative (ISCI) was established and carried out a comparative study on a large and diverse set of hES cell lines. This allow the identification of a widely accepted, set of pluripotency markers, commonly expressed by hES cells lines: the glycolipid antigens SSEA3 and SSEA4, the keratan sulfate antigens TRA-1-60, TRA-1-81, GCTM2 and GCT343, and the protein antigens CD9, CD90, tissue-nonspecific alkaline phosphatase and class 1 HLA and the strongly developmentally regulated genes NANOG, OCT4, TDGF1, DNMT3B, GABRB3 and GDF3[9].

In recent years, several highly efficient cardiac differentiation protocols of hES cells have been developed. Using lessons from the embryogenesis, three main approaches have been developed to direct hES cells towards the cardiac lineage *in vitro*[4,10].

The first approach is based on the spontaneous differentiation through EBs formation which is enhanced and specifically directed down the cardiac lineage by the addition of growth factors and repressors known to influence heart development in the embryo (Figure 4.1). Such soluble molecules include in particular members of the TGF-β (transforming growth β) family, such as BMP (bone morphogenetic protein) and activin A; members of the Wnt family and FGF (fibroblast growth factor) family, all of which are major regulators in cardiac development. In addition, VEGF (vascular endothelial cells growth factor), the Wnt-inhibitor Dkk1 (added late to the culture) and ascorbic acid have been shown to be important.

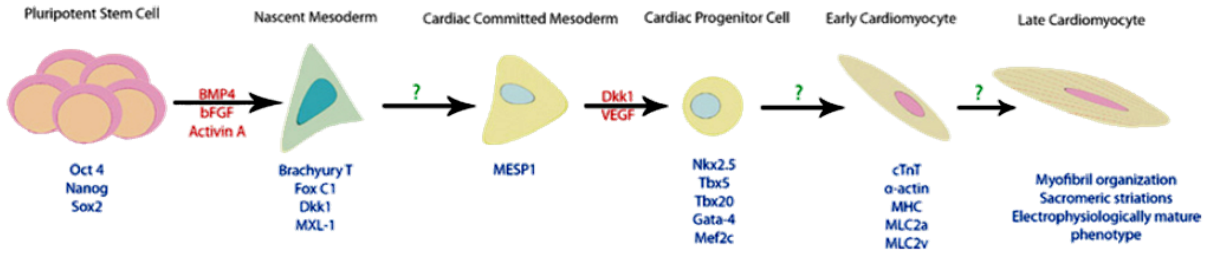

Figure 4.1. Schematic representation of the pluripotent stem cell differentiation into cardiomyocytes. This process may be considered as a series of steps distinguished by the expression of various transcription factors and which progression is controlled by different soluble molecules. Although all the steps in the process are not clear, the time of introduction of these factors is very important. In particular, initial introduction of BMP4, activin A and βFGF will start the directed differentiation and later introduction of a Wnt signal inhibitor (Dkk1) and VEGF will help to push the cells further to form cardiomyocytes. *(From Dambrot et al, 2011[10])*.

In particular, Yang and colleagues designed a staged protocol (Figure 4.2) based on a combination of these soluble factors added in a precise temporal sequence, which is, at the moment, the most efficient for cardiomyocytes derivation from hES cells. In this protocol, the combination of activin A and BMP4 induces a primitive-streak-like population and mesoderm (stage 1), as demonstrated by the upregulation and transient expression of specific genes such as brachyury (T). Then, the WNT inhibitor DKK1 is added to specify cardiac mesoderm and VEGF is included to promote the expansion and maturation of the a KDR-positive population (stage 2). Finally, bFGF is added again at day 8 of differentiation to support the continued expansion of the developing cardiovascular lineages (stage 3)[5].

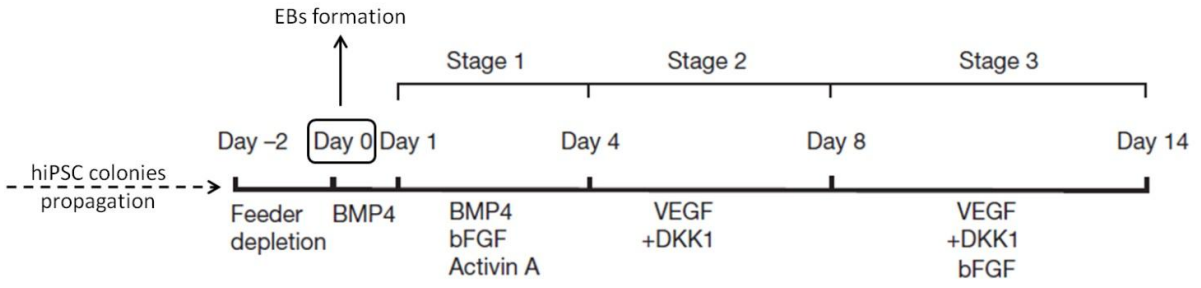

Figure 4.2. Outline of the three-stage protocol designed by Yang and colleagues for the differentiation of hES cells towards the cardiac lineage. *(Adapted from Yang et al, 2008[5])*.

A second approach for cardiac differentiation of hES cells is based on stromal cell co-culture. This exploits the instructive influence of endoderm for cardiac differentiation during embryogenesis and uses co-culture with endoderm-like cell lines or their conditioned medium[11,12].

A third method utilizes a high-density monolayer model supplemented only with BMP4 and activin A in a defined serum free medium. Laflamme et al. reported this method to be much more efficient than EB-based methods, although to date the number of publications describing its use is limited and its reproducibility across different hES cell lines is still unclear[13].

In this PhD work, hES cells-derived CMs were combined with *ad-hoc* micro-scale technologies to obtained an *in vitro* engineered cardiac muscle tissue.

4.2.2. Obtainment of a micro-array of contracting hES cells-derived CMs

Human CMs were obtained from the human embryonic stem cell line HES2, through the protocol described by Yang and colleagues, above reported (§ 4.2.1, Figure 4.2).

EBs obtained from HES2, after application of such differentiation procedure, were disgregated through enzymatic and mechanical treatments (see appendix C for detailed method) and seeded on a micro-patterned PA HY. This PA HY, specifically tailored for muscle cells as described in § 2.2, was characterized by an elastic modulus of 15 kPa, that is a substrate elasticity maximizing cardiomyocytes work. Adhesion proteins were micro-patterned on the PA HY surface into a defined geometries of circular spots, 300 µm in diameter and 700 µm center to center spaced. As described in § 2.3, this geometry minimize the mechanical stress of beating cells that is equally distributed in all the directions, reducing the detachment risk.

The resulting micro-engineered culture was a 20×20 array of circular spots of contracting CMs, defined with micrometric precision (Figure 4.3 A). The percentage of cardiomyocytes per spot was high, around 90% (based on the percentage of cardiac Troponin T positive cells), with a good distribution on the entire array. The maintenance of cardiac markers on micropatterned cells was verified after 5-7 days of culture onto the micro-patterned hydrogel. cTnT, α-actinin, and Cx43 and were analyzed by immunofluorescence (Figure 4.3 B). At this time point, spontaneous and electrically induced contractions were observed.

Usually, *in vitro* studies involving human CMs use clusters of cardiomyocyte derived by the dissection of the EB's contracting area or by co-culture with other cell types[14,15]. Only few *in vitro* cardiac models have been developed until now based on hES cell-derived cardiomyocytes (hCMs)[16–19] and all these human models were developed at the macro-scale, requiring an high number of cardiomyocytes per construct (at least 4×10^5 cells). The realized *in vitro* cardiac model presents then the unique advantage to be designed at the micro-scale. A reduced number of human CMs are needed for its realization, increasing the number of samples per batch and enhancing the high troughputness of the developed model. In addition, each micro-structured human CMs spot could represent an independent sample deriving from the same batch of cells. Consequently, the array offers the possibility of analyzing different spots at the same time, exposed to identical conditions, with a consistent/repeatable number of hCMs per spot. The developed *in vitro* model could thus give a high number of output information per experiment and reduce the high variability usually observed when working with a primary human cell source[20].

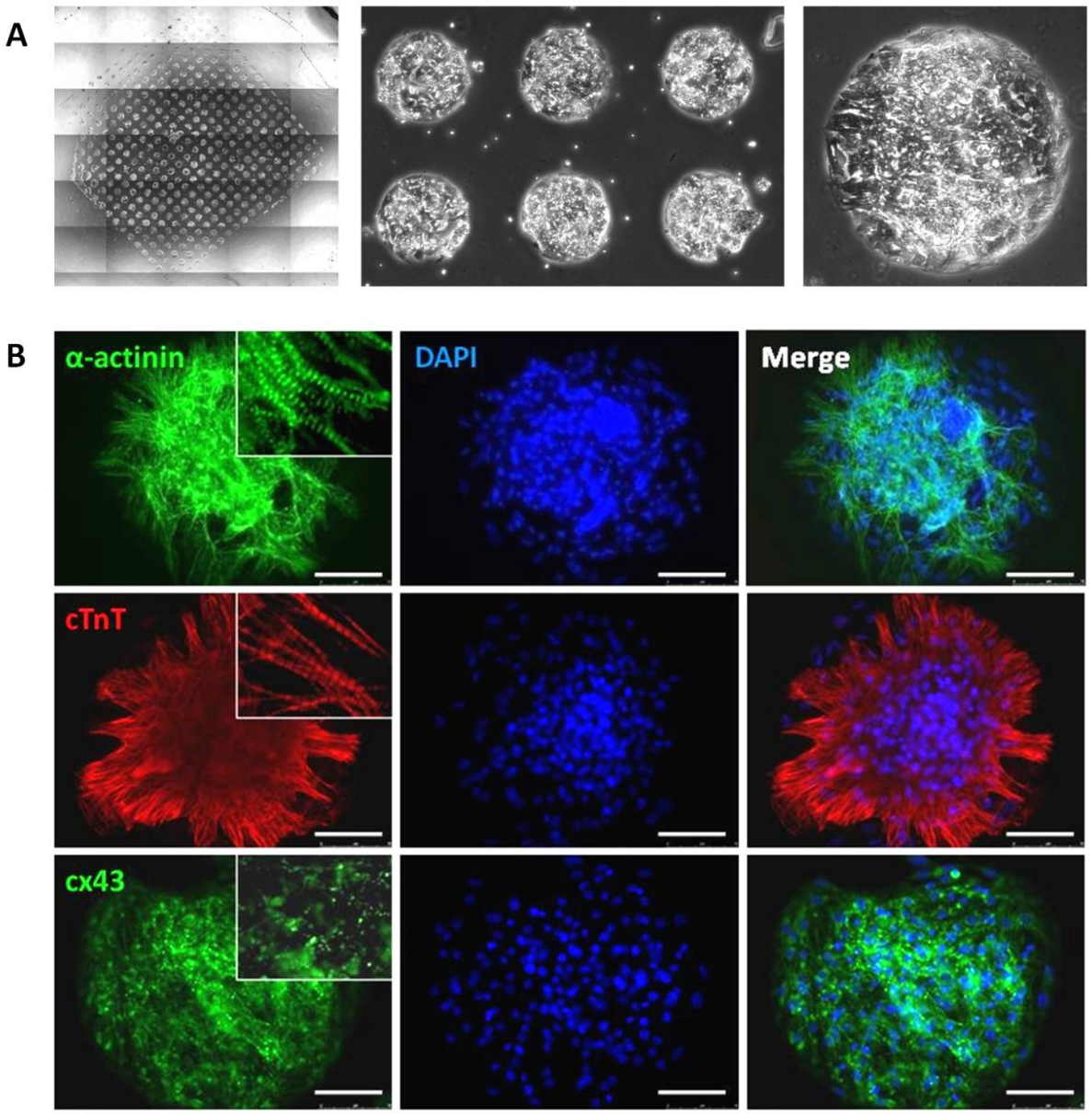

Figure 4.3. (A) Micro-array of contracting CMs spots in three different magnifications. Spots are 300 µm in diameter and 700 µm center to center spaced. (B) Expression of cardiac markers on hES cells-derived CMs cultured for 5-7 days onto the micro-patterned hydrogel.

4.3. DMD patient-specific cardiomyocytes from hiPS cells

4.3.1. hiPS cells and the derivation of patient- or disease-specific stem cells

Almost a decade after the derivation of hES cells, the efficient reprogramming of differentiated human somatic cells into a pluripotent state by Yamanaka and colleagues in 2007[21] was heralded as one of the most important scientific findings of the last decade. They demonstrate that retroviral transduction of adult human dermal fibroblasts with four defined factors (Oct4, Sox2, Klf4, and c-Myc) allow the obtainment of pluripotent cells, the human induced pluripotent stem (hiPS) cells. hiPS cells, like hES cells, can self-renew indefinitely while maintaining the capacity to differentiate into cell types of the three germ layers *in vitro* and *in vivo* in teratomas and are similar to hES cells in morphology, proliferation, surface antigens, gene expression, epigenetic status of pluripotent cell-specific genes, and telomerase activity. Since this first report, reprogramming of many other somatic cell types using different methods of transcription-factor introduction have been published in quick succession.

hiPS cells overcome the ethical controversies related to hES cells and, more remarkably, since such cells can be generated from the individual's own tissues, open for the first time the perspective of deriving patient- and disease-specific stem cell lines.

In a recent work, originated from the collaboration between the Yamanaka's laboratory and the Oshimura's one[22], hiPS cells were derived for the first time from a DMD patient and then the genetic deficiency was completely corrected by the transfer, via microcell-mediated chromosome transfer (MMCT), of a human artificial chromosome (HAC) carrying a full-length genomic dystrophin sequence (DYS-HAC), including the associated regulatory elements[23]. DMD patient-specific hiPSc with the DYS-HAC gave rise to the three germ layers in the teratoma, and human dystrophin expression was detected in muscle-like tissues. Furthermore, chimeric mice from *mdx*-derived iPSc with DYS-HAC were produced and DYS-HAC was detected in all tissues examined, with tissue-specific expression of dystrophin.

Only recently hiPS cells have been successfully differentiated into CMs. In addition, it has been shown that the differentiation procedure should be optimized for different hiPS cell lines[24].

4.3.2. hiPS cells expansion, characterization and differentiation into CMs

During the research activity, the following hiPS cell lines, were successfully cultured and expanded: (i) hiPS cells derived from an healthy individual, carrying a normal genotype with a wild-type copy of the dystrophin gene (WT hiPS cells); (ii) hiPS cells derived from a DMD patient with deletion of exons 4-43 (DMD hiPS cells); (iii) hiPS cells derived from the same DMD patient and genetically corrected by a human artificial chromosome carrying the full-length genomic dystrophin sequence (DYS-HAC hiPS cells). These hiPSc lines were derived by Prof. Oshimura Laboratory at the Chromosome Engineering Research Center (Tottori University - Faculty of Medicine, Yonago, Japan) as reported in their recent work[22].

hiPS cells are sensitive cells, which propagation and expansion should be performed carefully and precisely to avoid spontaneous differentiation. These aspects make their maintenance a laborious and time demanding process. Furthermore, under the same culture conditions, hiPS cell lines derived from different original clones may differ considerably in growth rate and tendency towards

differentiation. Being pluripotent stem cells, hiPSc colonies have a high metabolism and fast deplete the medium nutrients that should be changed daily. During expansion, large and spread differentiated cells may appear at the edges or in the center of colonies, that should be completely or partially removed by mechanical picking, daily.

The three above reported hiPS cell lines were successfully cultured and expanded for about 10 passages in their undifferentiated state. Expression of pluripotency markers was evaluated during expansion by immunofluorescence analyses. All hiPS cell lines resulted to express the transcription factors Oct4, Sox2, c-myc and the surface markers TRA-1-60 and TRA-1-81 (Figure 4.4 A). In addition, the DYS-HAC hiPS cell line was monitored for the expression of the enhanced green fluorescent protein (EGFP), a marker contained in the dystrophin-human artificial chromosome (Figure 4.4 B).

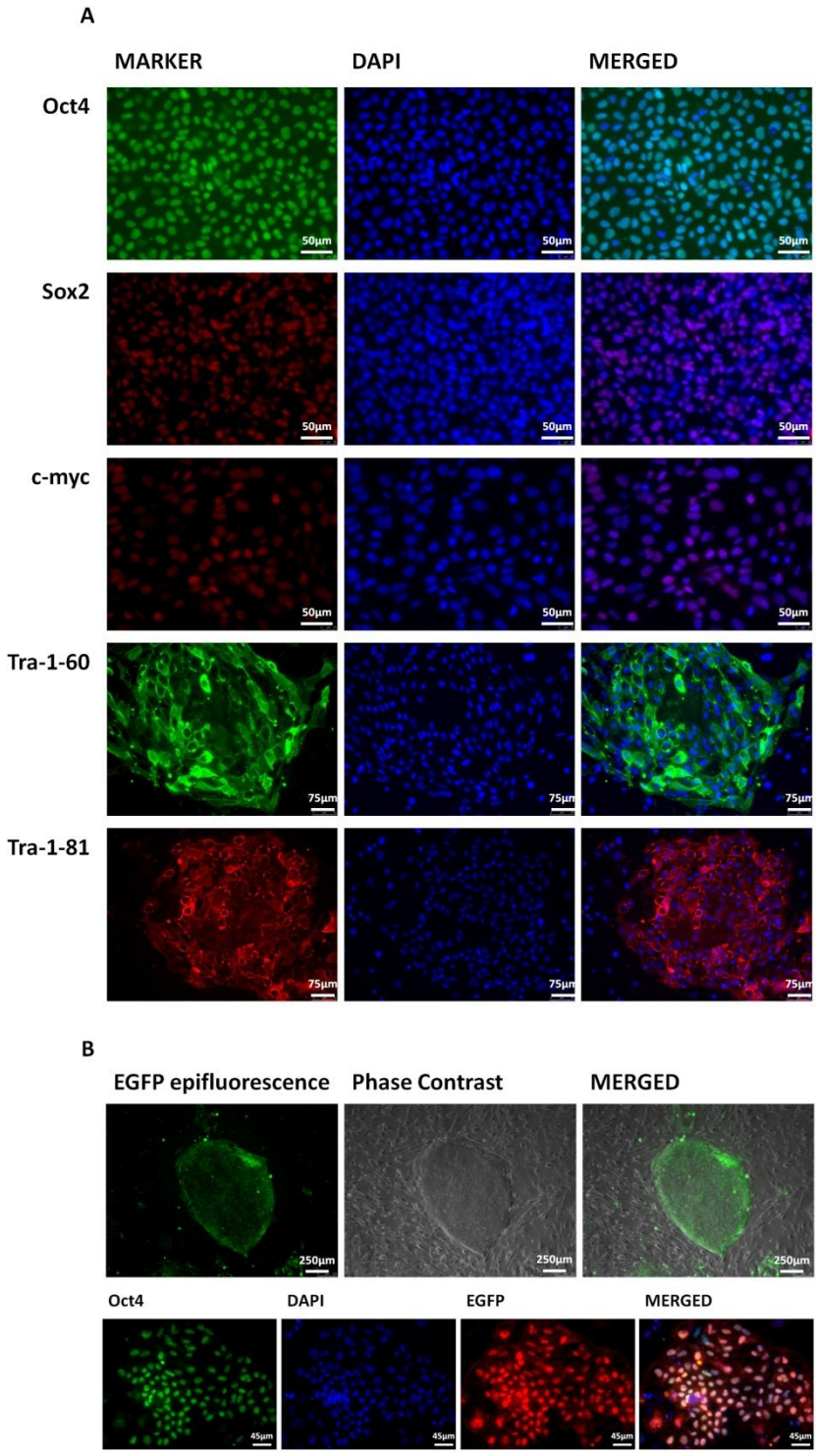

Figure 4.4. (A) Expression of pluripotency markers hiPS cell colonies. (B) Maintenance of enhanced green fluorescent protein (EGFP) in DYS-HAC hiPS cell colonies, a marker contained in the dystrophin-human artificial chromosome.

Embryoid bodies (EBs) were successfully generated from all the three hiPSc lines. The obtained EBs were differentiated towards the cardiac lineage through an *ad-hoc* optimized procedure. Overall outline of this procedure is reported in figure 4.5 D.

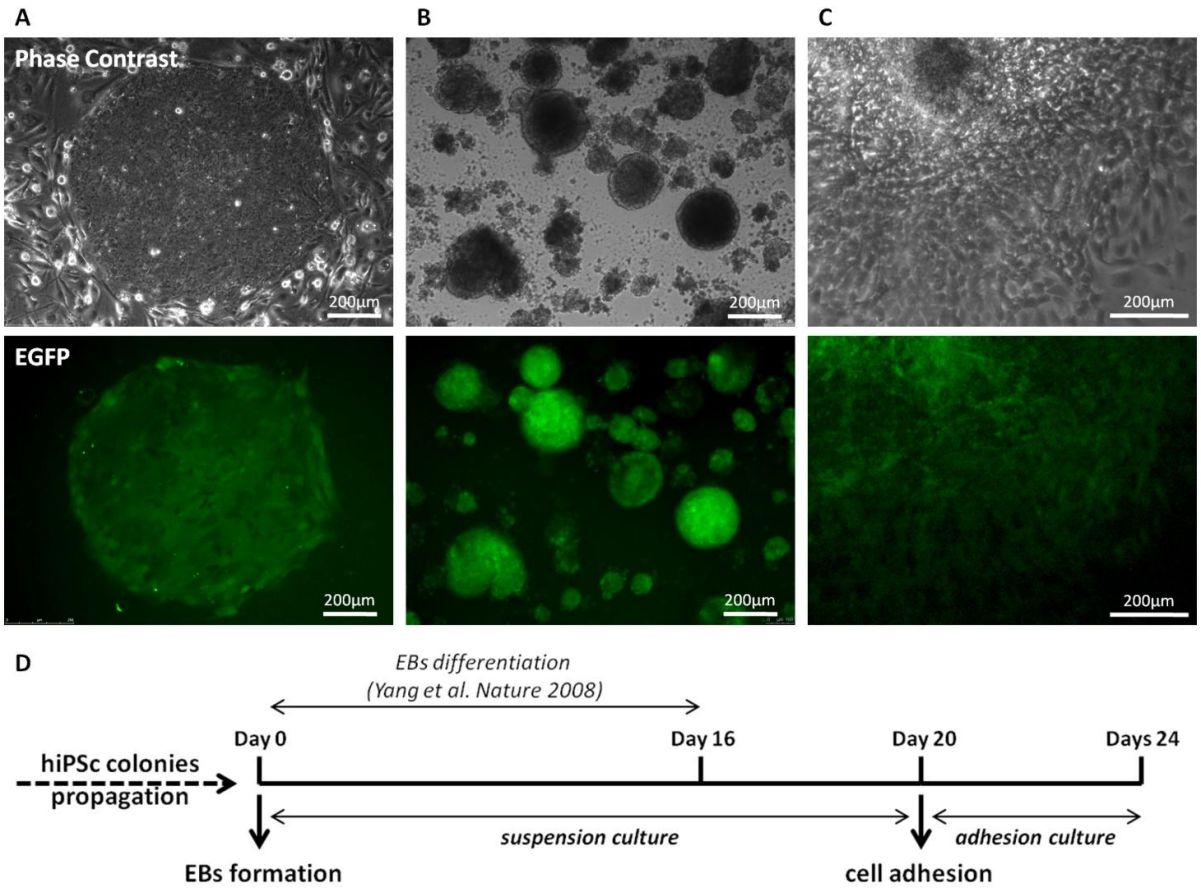

Figure 4.5. Differentiation of hiPSc. (A) DYS-HAC hiPSc undifferentiated colonies cultured on MEF feeder cells. (B) EBs generated from DYS-HAC hiPSc colonies at day 4 of the differentiation procedure. (C) Cultured cells 2 days after EBs adhesion. Epifluorescence images (lower panel) show the expression of EGFP in each condition, indicating the presence of the DYS-HAC. (D) Overview of the differentiation procedure.

Once completed the differentiation of EBs cultured in suspension (day 16), according to the protocol described by Yang and colleagues (§ 4.2.1, Figure 4.2) and previously applied for the obtainment of hES cells-derived CMs, EBs were cultured for additional 4 days in suspension and then seeded on substrate with physiological stiffness for 4 days.

The application of a 16-days differentiation procedure, resulted in the obtainment of a relevant percentage of spontaneously-contracting EBs, ranging from a minimum of 14% for DMD hiPS cells-derived EBs to a maximum of 44% for WT hiPS cells-derived EBs (Table 4.1). Such differences probably rely mainly on the intrinsic variability existing between hiPS cell lines derived from different original clones.

Table 4.1. Percentage of spontaneously contracting EBs and cTnT-positive cells obtained for each cell line used.

hES/hiPS cell line	Contracting EBs obtained (% ± SD) - day16	cTnT-positive cells (% ± SD) - day 24
DMD hiPS cells	14 ± 4	7,6 ± 0,7
WT hiPS cells	44 ± 2	9,8 ± 4,6
DYS-HAC hiPS cells	19 ± 5	8,2 ± 1,5

SD = standard deviation calculated on data obtained from 5 independent analyses.
cTnT = cardiac Troponin T

In order to allow a complete maturation of CMs, contracting EBs at day 20 were seeded on substrate with physiological stiffness for 4 days.

As above reported, it has been demonstrated that the development of sarcomeric structures of human striated muscles (appendix B) and the contractile functionality of chicken cardiomyocytes[25] are influenced by the substrate stiffness. Furthermore, in our group it has been recently demonstrated that adhesion on substrate with a physiological stiffness promote functional maturation of human CMs, allowing a shortening of calcium transients[26].

Following adhesion, a functional maturation of CMs was observed (Figure 4.6). CMs obtained at day 24 were characterized by a remarkable sarcomeric cytoskeletal architecture, as revealed by immunofluorescence analyses of α-actinin (Figure 4.6 A), cardiac troponin T (cTnT) and F actin (Figure 4.6 B); and GAP-junction formation, as revealed by immunfluorescence analyses of connexin 43 (Figure 4.6 C). The percentage of cTnT-positive CMs obtained on the overall population was near 10% (Table 4.1). For DYS-HAC hiPS cells-derived CMs the same percentage increase to (44 ± 2) % when only contracting EBs are selected.

Expression of sarcomeric proteins, in particular cTnT and atrial myosin light chain (MLC2A), in adhered CMs, was also confirmed by RT-PCR (Figure 4.6 G). On the contrary, for DMD and DYS-HAC hiPS cells-derived CMs, expression ML2A, a marker of terminally-differentiated atrial CMs, was not revealed before CMs adhesion, in EBs suspension culture. Only WT hiPS cells-derived CMs already express this marker before adhesion, probably due to the higher efficiency of the overall differentiation procedure obtained for this hiPS cell line, as demonstrated by the higher percentage of contracting CMs.

Adhered CMs also displayed calcium transients upon electrical stimulation, typical of calcium cycling during contraction (Figure 4.6 F) together with a diffuse intracellular distribution of sarco-endoplasmic reticulum calcium-ATPase (SERCA) (Figure 4.6 D), a key element of the calcium handling machinery, needed for calcium re-uptake after contraction.

Transcription factors NKX2.5 and GATA4 were also expressed in all conditions tested, as revealed by RT-PCR (Figure 4.6 G) and immunofluorescence analyses (Figure 4.6 E), respectively. On the opposite of what observed for MLC2A, NKX 2.5 seems to be down-regulated in DYS-HAC hiPS cells-derived CMs after adhesion.

In DYS-HAC hiPS cells-derived CMs, the down-regulation of NKX2.5 expression, moving from suspension to adhesion culture condition, and the concomitant expression of the contractile protein ML2A, specific of terminally-differentiated atrial CMs, is consistent with a maturation of the cardiac phenotype, as reported in figure 4.1. Such differences were not detected for NORMAL hiPS cells-derived CMs, probably because they are override by the higher efficiency of the overall differentiation procedure for this line and, at the same time, by the greater heterogeneity in the phenotypes of the obtained CMs.

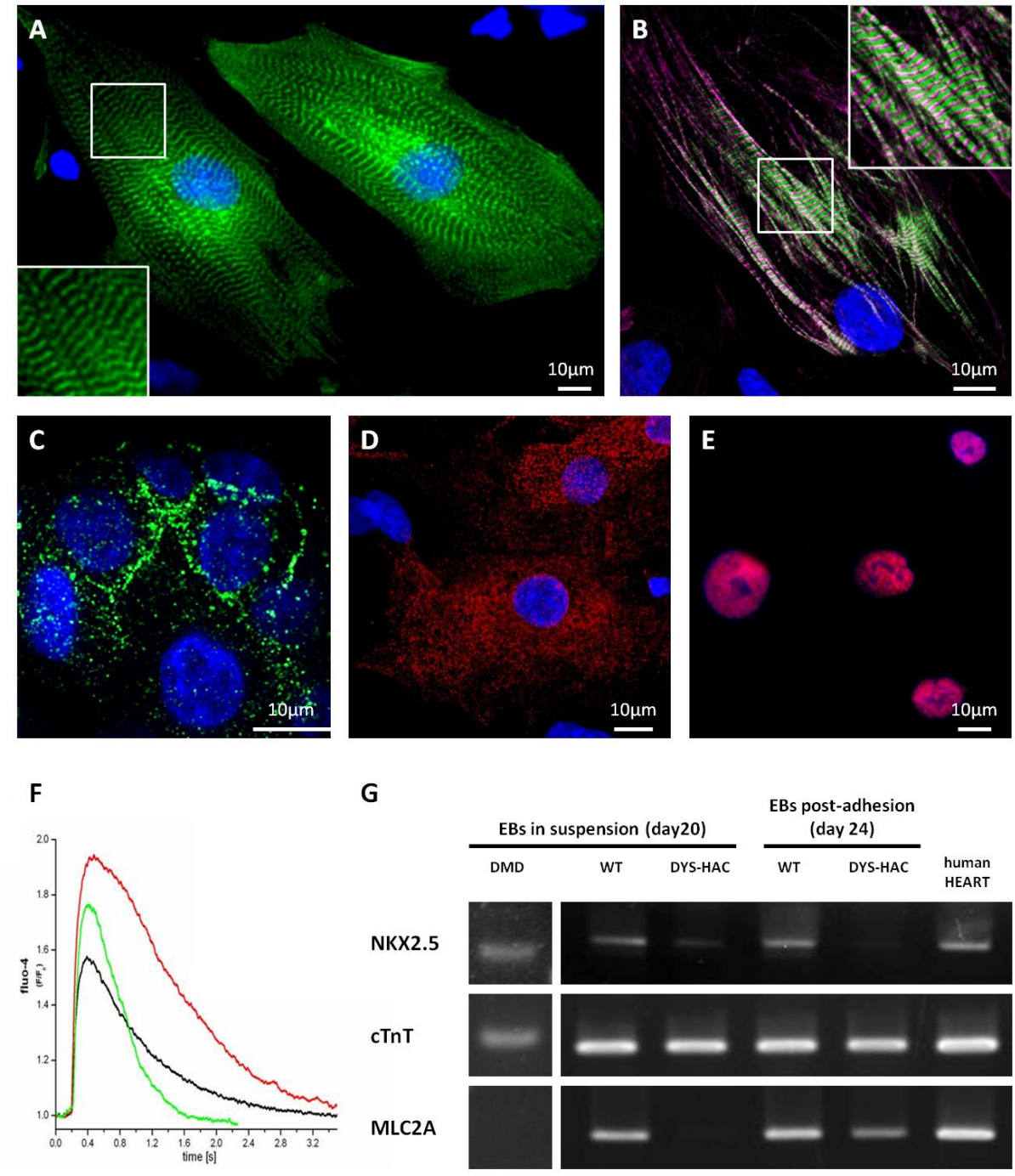

Figure 4.6. Immunofuorescence analyses of α-actinin (A), cardiac troponin T (green) and F-actin (violet) (B), Cnx43 (C), SERCA (D) and GATA4 (E) in adhered CMs at day 24 of the differentiation procedure. (F) Calcium transients from three unrelated cardiomyocytes day 24 of the differentiation procedure. (G) RT-PCR analyses show the expression of NKX2.5, cTnT and MLC2A in EBs obtained from DMD, WT and DYS-HAC hiPSc, cultured in suspension, at day 20 and on the EBs-derived adhered cells at day 24 of the differentiation procedure.

Taken together these results show the obtainment of functionally-differentiated CMs from hiPS cells. In particular, through an *ad-hoc* optimized differentiation procedure, human CMs derived from both healthy individuals and DMD patients were obtained. The obtained DMD patient-specific, hiPS cells-derived CMs represent the ideal cell source for an *in vitro* modeling of DMD cardiac muscle. In addition, DMD patient genetically corrected CMs have been obtained.

The genetically corrected CMs are the focus of the investigations, reported in the following paragraphs, aimed at testing dystrophin expression restoration at cardiac level, by a human artificial chromosome.

4.4. Testing dystrophin expression restoration on DMD patient-specific CMs by HAC

The dystrophin human artificial chromosome (DYS-HAC) is the first vector carrying the whole dystrophin genomic locus including also the associated regulatory elements (REF). This potentially allows the correct activation of the complex mechanism regulating dystrophin expression, including the activities of multiple promoters and the exon-skipping and exon-scrambling events, that are finely regulated in a development- and tissue-specific way. The possibility to restore dystrophin expression in a tissue specific manner, following native regulation mechanism, makes the DYS-HAC a promising tool for the treatment of DMD also at cardiac muscle level.

First of all, dystrophin expression was verified during the cardiac differentiation procedure on WT, DMD and genetically corrected DYS-HAC hiPSc, by RT-PCR using specific primers designed in order to spam exon-exon junction localized inside the sequences that result to be deleted on the DMD patient (from exon 4 to 43) (Figure 4.7). mRNA from human heart and skeletal muscle was used as positive control.

WT EBs displayed dystrophin expression both when cultured in suspension and after adhesion. On DMD EBs no dystrophin expression was revealed in any conditions. On genetically-corrected DYS-HAC EBs dystrophin expression is restored both when cultured in suspension and after adhesion. A positive result was obtained for each of the five exon junctions checked, distributed on the whole deleted region.

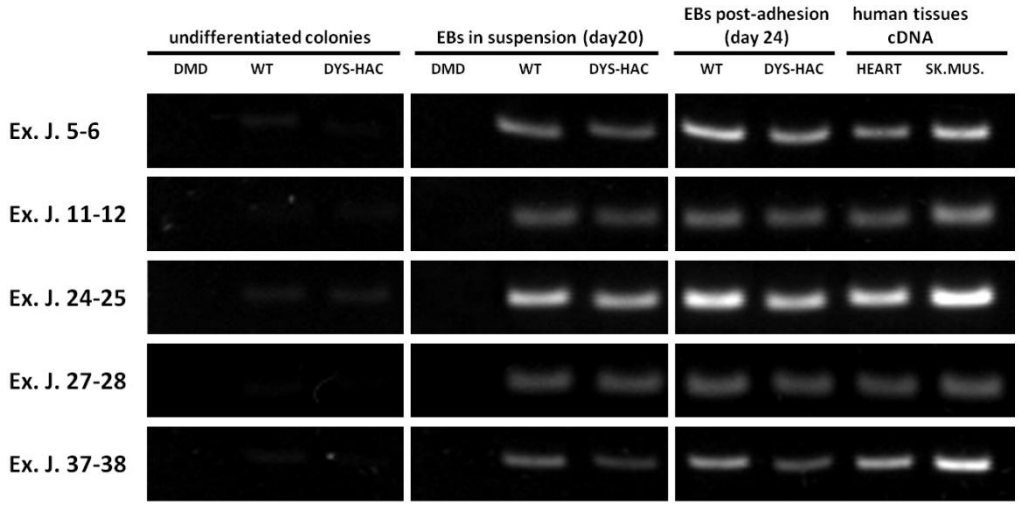

Figure 4.7. RT-PCR analyses of specific dystrophin sequences localized inside the patient deletion (exons 4-43). Primers were constructed in order to spam exon-exon junctions (Ex. J.). cDNA from human hearth and skeletal muscle was used as positive control.

In vivo, cardiomyocytes are known to express the full-length muscle dystrophin isoform (Dp427m), together with other isoforms, such as the Dp427I (that has been shown to be expressed in the hearth of chimeric mice from *mdx*-derived iPSc with DYS-HAC[22]) and the Dp71, that is ubiquitously expressed also in many other non-muscle tissues.

In order to (i) assess the expression of different dystrophin cardiac isoforms and (ii) verify the presence of other cell types in the obtained preparation; the expression of the dystrophin isoforms Dp427m, Dp427I, Dp140 and Dp71 was analyzed by RT-PCR during the cardiac differentiation procedure on WT, DMD and genetically corrected DYS-HAC hiPSc (Figure 4.8). mRNA from human tissues was used as positive control.

WT EBs (both in suspension and adhesion) displayed the expression of all the four different dystrophin isoforms analyzed. The expression of isoform Dp140 indicates the presence of other cell types further to cardiomyocytes, which are expected in this type of differentiation procedures[5]. On the contrary, on DMD EBs the expression of these isoforms were not revealed, except for Dp71. The promoter of this short isoform is in fact located in intron 62, while patient deletion include sequences from exon 4 to 43. On genetically-corrected DYS-HAC EBs (both in suspension and adhesion), expression of all the four isoforms is restored. In this case also a slight expression of dystrophin isoforms Dp427I, Dp140 and Dp71 was observed in colonies.

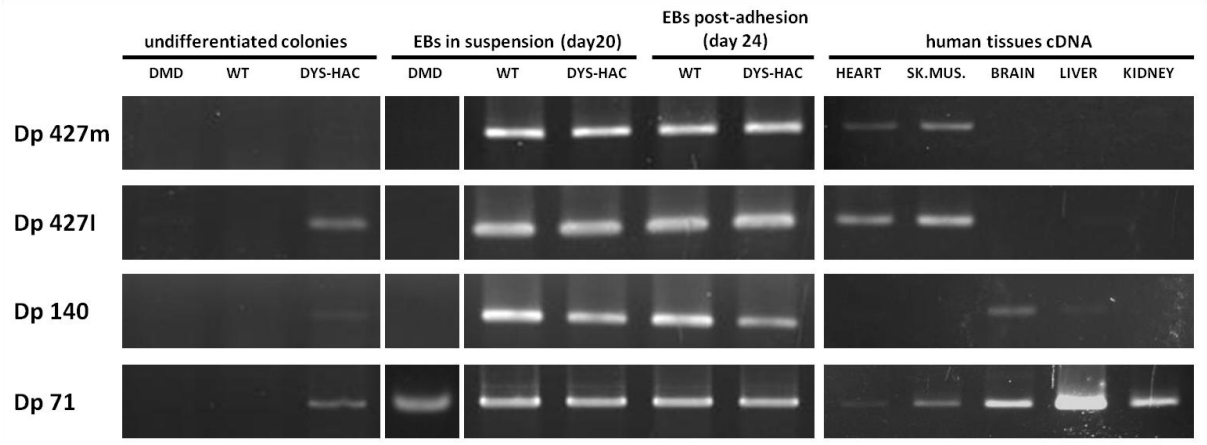

Figure 4.8. RT-PCR analyses of dystrophin isoforms at three different stages of the differentiation process: undifferentiated colonies, differentiated EBs cultured in suspension (day 18) and adhered cells (day 24), for each hiPSc line (DMD, WT, DYS-HAC). cDNA from human tissues was used as positive control.

Taken together these RT-PCR analyses, showed that, during the cardiac differentiation protocol, (i) dystrophin expression (at mRNA level) is correctly restored by the DYS-HAC and (ii) multiple dystrophin isoforms are expressed.

Subsequently, a proper restoration of the dystrophin protein and its correct subcellular localization was verified by immunofluorescence analyses. To this purpose a polyclonal antibody recognizing both the full-length muscle isoforms and other shorter isoforms, such as the Dp71, was used.

At first EBs were analyzed at day 20, immediately after adhesion (Figure 4.9 A). At the same time point, the analyses were performed also on cytospin preparation of disgregated EBs. Finally, the analyses was performed 4 days after EBs adhesion (Figure 4.9 B).

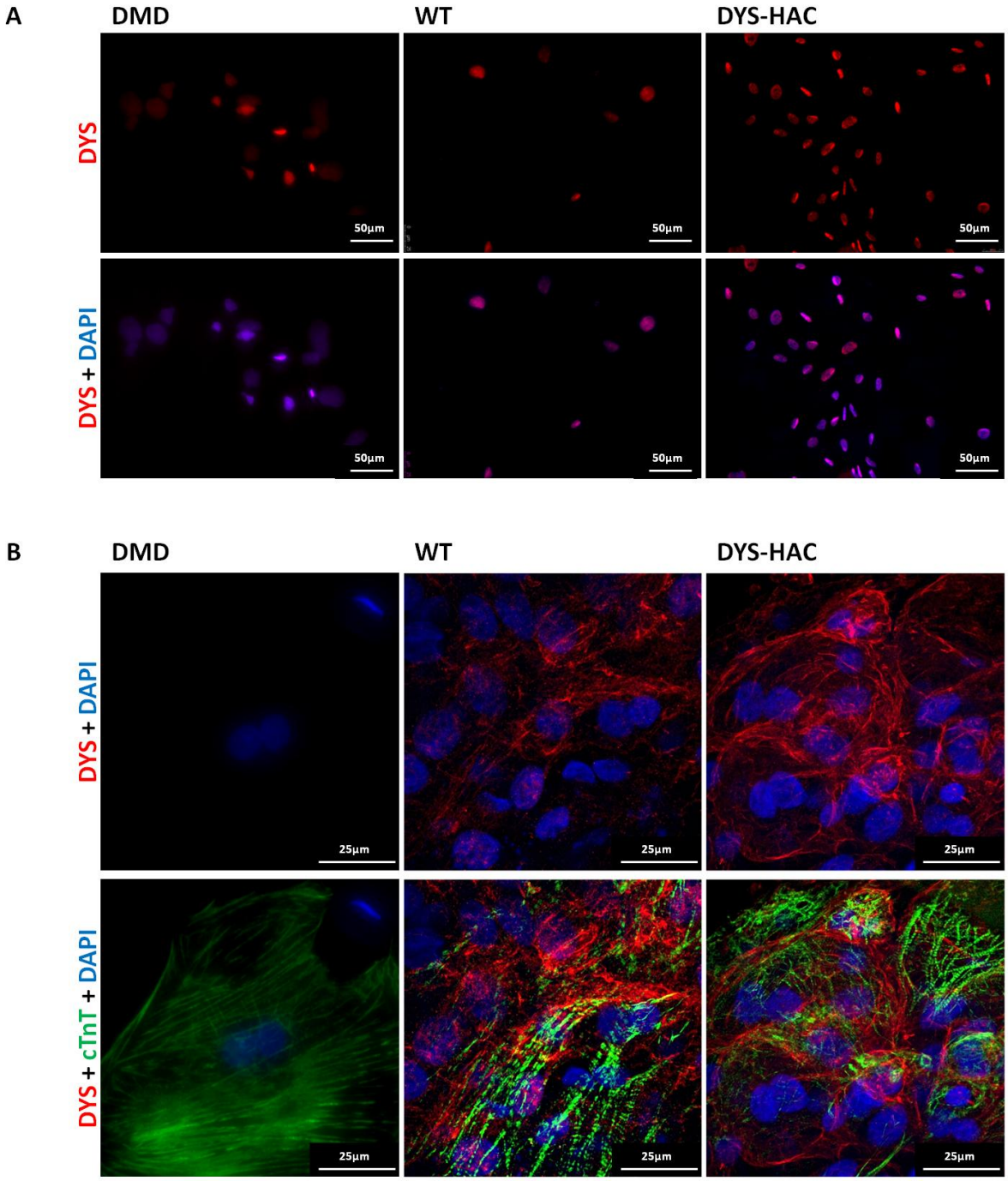

Figure 4.9. Dystrophin expression at day 20 (A) and at day 24 (B) on DMD, WT and DYS-HAC EBs.

Interestingly, WT EBs analyzed at day 20, immediately after adhesion, displayed a nuclear dystrophin staining. Quantitative evaluation from cytospin preparation revealed that a nuclear dystrophin staining was present in 63% of total cells. Of these, a 51% expressed also cTnT. At day 24, further to the nuclear staining of cTnT-negative cells, also membrane localization of dystrophin was observed in cTnT-positive cells. On DMD EBs, only a nuclear dystrophin staining was observed, both at day 20 and 24. On genetically-corrected DYS-HAC EBs, similarly to what observed for WT EBs, at day 20 most of the cells presented a nuclear dystrophin staining (45%) and, of these, 56% expressed also cTnT. At day 24, a remarkable dystrophin expression at membrane level was observed on cTnT-positive cells.

Different studies have provided experimental evidence of the nuclear localization of dystrophin Dp71, and several dystrophin-associated proteins in a variety of cell models[27–29], in different non-muscle cell types, arising the possibility that these proteins play an alternative function inside nuclei. In addition, Ramirez and colleagues recently demonstrated that Dp71 localizes at Nuclear and Nuclear Envelope level during myogenesis in C2C12 muscle cells, where it interacts with dystrophin-associated proteins to form a complex[30].

Our findings are in line with these studies, showing that a dystrophin isoform, probably Dp71, is expressed at nuclear level, both in cardiac and non cardiac cells, during the differentiation of hiPSc.

Summarizing, we demonstrated that: **(a)** the DYS-HAC do not hinder cardiac differentiation of hiPS cells; **(b)** dystrophin expression (at mRNA level) is correctly restored by the DYS-HAC during hiPS cardiac differentiation procedure, (in particular, the expression of specific sequences deleted in the patient was observed); **(c)** the DYS-HAC drives the expression of multiple dystrophin isoforms in cardiomyocytes, in particular the full-length muscle isoform Dp427m and the initiating isoform Dp427I, which are not expressed in the DMD patient with deletion of exons 4-43; **(d)** different dystrophin isoforms are expressed during hiPS cardiac differentiation procedure, in particular a nuclear localization was observed in CMs at an intermediate differentiation stage (day 20) and a membrane localization was observed in CMs at a late differentiation stage (day 24).

4.5. Development of an HAC for the obtainment of reversible reporter hiPS cells lines

Although the huge potential of hiPSc-derived cardiomyocytes, the biggest roadblock for their applications (both for *in vitro* disease modeling and, more in perspective, for an *in vivo* treatment), are (i) the current inability to exactly quantify the extent of cardiomyocyte differentiation and (ii) the difficulty in selecting pure or nearly pure population of cardiomyocytes without destroying the cells[31,32]. In this context, the realization of tools to detect cardiac cells among other cell types (such as endothelial cells and vascular smooth muscle cells), that are inevitably present in the populations obtained during the differentiation processes, could be of paramount importance. To this purpose, a HAC carrying the EGFP reporter gene under the control of NKX2.5 regulatory sequence was designed and realized.

Briefly, BAC clone RP11-466H21 containing the human NKX2.5 gene and their regulatory elements (including all upstream and downstream enhancer required for a cardiac specific expression) was modified targeting a modification cassette containing EGFP reporter gene and neomycin selection inside the coding sequence of exon 1. Also a loxP-3' HPRT site was inserted in the BAC sequence. The modified BAC was cloned into an HAC vector, the 21HAC1[33], (containing a loxP-5' HPRT site) by the Cre/loxP system in CHO cells (Figure 4.10 A). Thanks to the reconstitution of a complete HPRT gene, CHO cells were selected by HAT medium. FISH analyses (Figure 4.10 B) confirmed the presence of the HAC containing BAC sequences in CHO cell. To exclude rearrangements, the presence of key sequences of the modified BAC was verified by genomic PCR analyses in CHO cells (Figure 4.10 C).

The obtained CHO cells can be used for microcell mediated chromosome transfer. Using this technique, the HAC carrying EGFP reporter gene under the control of NKX2.5 regulatory sequences can be transfer to hiPC cells, thus obtaining reporter lines. Furthermore, the HAC vector used contains a conditional centromere[34] and can be then potentially removed once selection of cardiac cells is performed.

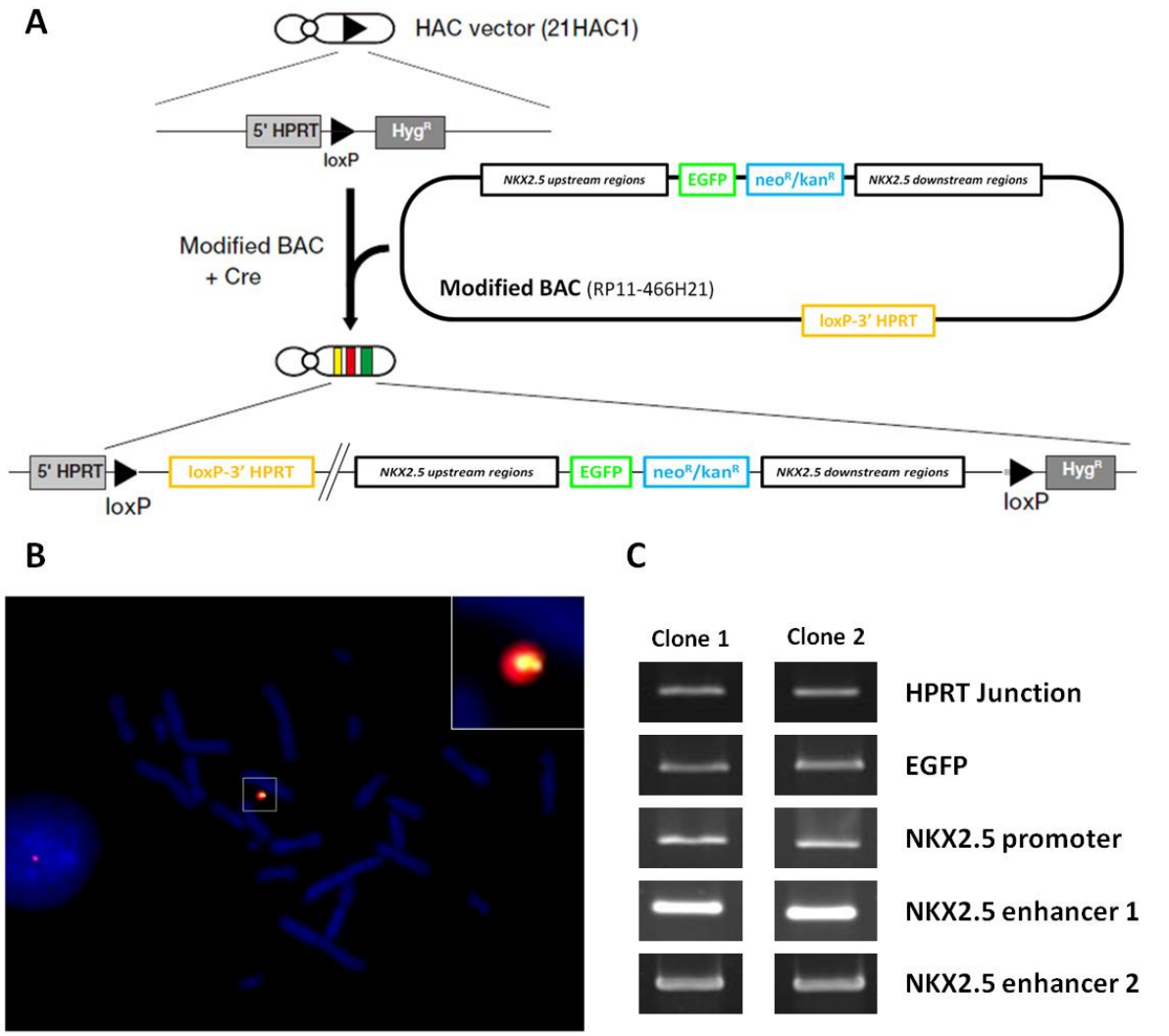

Figure 4.10. (A) Strategy of BAC modification and introduction into the HAC vector; (B) FISH analyses in CHO cells. Red: Human Cot-1; Green: NKX 2.5 BAC; Blu: DAPI; (C) Genomic PCR analyses in CHO cell for specific BAC sequences.

4.6. References

1. Spurney, C.F. Cardiomyopathy of Duchenne muscular dystrophy: current understanding and future directions. Muscle Nerve 44, 8-19 (2011).

2. Fayssoil, A., Nardi, O., Orlikowski, D. & Annane, D. Cardiomyopathy in Duchenne muscular dystrophy: pathogenesis and therapeutics. Heart Fail Rev 15, 103-107 (2010).

3. Jiang, J., Han, P., Zhang, Q., Zhao, J. & Ma, Y. Cardiac Differentiation of Human Pluripotent Stem Cells. Journal of Cellular and Molecular Medicine (2012).doi:10.1111/j.1582-4934.2012.01528.x

4. Shiba, Y., Hauch, K.D. & Laflamme, M.A. Cardiac applications for human pluripotent stem cells. Curr. Pharm. Des. 15, 2791-2806 (2009).

5. Yang, L. et al. Human cardiovascular progenitor cells develop from a KDR+ embryonic-stem-cell-derived population. Nature 453, 524-528 (2008).

6. Thomson, J.A. et al. Embryonic stem cell lines derived from human blastocysts. Science 282, 1145-1147 (1998).

7. Amit, M. et al. Clonally derived human embryonic stem cell lines maintain pluripotency and proliferative potential for prolonged periods of culture. Dev. Biol. 227, 271-278 (2000).

8. Itskovitz-Eldor, J. et al. Differentiation of human embryonic stem cells into embryoid bodies compromising the three embryonic germ layers. Mol. Med. 6, 88-95 (2000).

9. Adewumi, O. et al. Characterization of human embryonic stem cell lines by the International Stem Cell Initiative. Nat. Biotechnol. 25, 803-816 (2007).

10. Dambrot, C., Passier, R., Atsma, D. & Mummery, C.L. Cardiomyocyte differentiation of pluripotent stem cells and their use as cardiac disease models. Biochem. J. 434, 25-35 (2011).

11. Mummery, C. et al. Differentiation of human embryonic stem cells to cardiomyocytes: role of coculture with visceral endoderm-like cells. Circulation 107, 2733-2740 (2003).

12. Passier, R. et al. Increased cardiomyocyte differentiation from human embryonic stem cells in serum-free cultures. Stem Cells 23, 772-780 (2005).

13. Laflamme, M.A. et al. Cardiomyocytes derived from human embryonic stem cells in pro-survival factors enhance function of infarcted rat hearts. Nat. Biotechnol. 25, 1015-1024 (2007).

14. Braam, S.R. et al. Prediction of drug-induced cardiotoxicity using human embryonic stem cell-derived cardiomyocytes. Stem Cell Res 4, 107-116 (2010).

15. Jonsson, M.K.B. et al. Quantified proarrhythmic potential of selected human embryonic stem cell-derived cardiomyocytes. Stem Cell Res 4, 189-200 (2010).

16. Shapira-Schweitzer, K., Habib, M., Gepstein, L. & Seliktar, D. A photopolymerizable hydrogel for 3-D culture of human embryonic stem cell-derived cardiomyocytes and rat neonatal cardiac cells. J. Mol. Cell. Cardiol. 46, 213-224 (2009).

17. Caspi, O. et al. Tissue engineering of vascularized cardiac muscle from human embryonic stem cells. Circ. Res. 100, 263-272 (2007).

18. Tulloch, N.L. et al. Growth of engineered human myocardium with mechanical loading and vascular coculture. Circ. Res. 109, 47-59 (2011).

19. Schaaf, S. et al. Human engineered heart tissue as a versatile tool in basic research and preclinical toxicology. PLoS ONE 6, e26397 (2011).

20. Pera, M.F. & Tam, P.P.L. Extrinsic regulation of pluripotent stem cells. Nature 465, 713-720 (2010).

21. Takahashi, K. et al. Induction of pluripotent stem cells from adult human fibroblasts by defined factors. Cell 131, 861-872 (2007).

22. Kazuki, Y. et al. Complete genetic correction of ips cells from Duchenne muscular dystrophy. Mol. Ther. 18, 386-393 (2010).

23. Hoshiya, H. et al. A highly stable and nonintegrated human artificial chromosome (HAC) containing the 2.4 Mb entire human dystrophin gene. Mol. Ther. 17, 309-317 (2009).

24. Kattman, S.J. et al. Stage-specific optimization of activin/nodal and BMP signaling promotes cardiac differentiation of mouse and human pluripotent stem cell lines. Cell Stem Cell 8, 228-240 (2011).

25. Engler, A.J. et al. Embryonic cardiomyocytes beat best on a matrix with heart-like elasticity: scar-like rigidity inhibits beating. J. Cell. Sci. 121, 3794-3802 (2008).

26. Serena, E. et al. hESC-CM maturation is driven by the cell-substrate interaction. (2011).

27. Hogan, A. et al. Interaction of gamma 1-syntrophin with diacylglycerol kinase-zeta. Regulation of nuclear localization by PDZ interactions. J. Biol. Chem. 276, 26526-26533 (2001).

28. Kulyte, A. et al. Characterization of human alpha-dystrobrevin isoforms in HL-60 human promyelocytic leukemia cells undergoing granulocytic differentiation. Mol. Biol. Cell 13, 4195-4205 (2002).

29. Marquez, F.G. et al. Differential expression and subcellular distribution of dystrophin Dp71 isoforms during differentiation process. Neuroscience 118, 957-966 (2003).

30. González-Ramírez, R., Morales-Lázaro, S.L., Tapia-Ramírez, V., Mornet, D. & Cisneros, B. Nuclear and nuclear envelope localization of dystrophin Dp71 and dystrophin-associated proteins (DAPs) in the C2C12 muscle cells: DAPs nuclear localization is modulated during myogenesis. J. Cell. Biochem. 105, 735-745 (2008).

31. Huber, I. et al. Identification and selection of cardiomyocytes during human embryonic stem cell differentiation. FASEB J. 21, 2551-2563 (2007).

32. Moore, J.C. et al. A P19Cl6 GFP reporter line to quantify cardiomyocyte differentiation of stem cells. Int. J. Dev. Biol. 48, 47-55 (2004).

33. Kazuki, Y. et al. Refined human artificial chromosome vectors for gene therapy and animal transgenesis. Gene Ther. 18, 384-393 (2011).

34. Iida, Y. et al. Human artificial chromosome with a conditional centromere for gene delivery and gene expression. DNA Res. 17, 293-301 (2010).

CONCLUSIONS

DMD is one of the most common and severe inherited neuromuscular disorder, affecting 1 in 3500 newborn males. DMD is caused by mutations in the dystrophin gene, encoding a key structural protein of connecting the contracting cytoskeletal machinery of skeletal and cardiac muscle fibers to the extracellular matrix scaffold. The absence of dystrophin leads to a progressive skeletal muscle degeneration and a series of cardiac complications. Patients usually die in their early twenties for respiratory complications or cardiomyopathy[1].

DMD is among the most difficult diseases to treat[2]. More than twenty years have passed since the identification of the molecular defect underling DMD[3]. Many progresses have been made in understanding the genetics and pathogenesis of the disease and several studies has been conducted both *in vitro*, on bench-top cell cultures, and *in vivo*, on different animal models identified as genetic homologues of the human pathology. Despite some promising outcomes coming from recent clinical trials, this has not, so far, resulted in an effective and definitive cure significantly altering the relentless progression of this disease, which has still a 100% mortality rate.

In understanding the reasons of this delay, it should be considered that the process of new therapies development for a genetic disease, such as DMD, requires high costs and long time before the researchers' efforts could effectively be translated into benefits for patients. This could be at least partly attributed to the fact that the majority of research is carried out in systems which do not adequately model the human physiology and pathology[4].

Furthermore, it should be considered that a definitive therapy for DMD patients, effective both at skeletal and cardiac muscle level, will be probably based on a combined approach, integrating different of the previously described strategies. Testing similar combined approaches in a single pre-clinical trial, based on the currently available tools and technologies, can become extremely challenging. In this sight, one of the most promising strategy, that can be coupled with conventional tools for lowering time and costs required in the process of new therapies development, is the *in vitro* testing on engineered systems able to give a prediction of the therapy effects on human tissue and their functionality.

The aim of this PhD thesis is then the development of micro-engineered human skeletal and cardiac muscles representing *in vitro* models of DMD patient tissues useful for testing therapeutic strategies aimed at restoring a proper dystrophin expression. These human *in vitro* models wants to couple the

simplicity and rapidity of conventional cell cultures with a correct representation of human tissues and their functionality. Beside pre-clinical trials on animal models, testing therapies on these human *in vitro* models could mean obtaining a prediction of the effects on patient tissues directly on bench top, before moving to clinical trials. In these perspectives, they could potentially represent a complementary tool in the process of new therapies development bridging the existing gaps between Petri-dish cultures, animal models and clinical trials on patients.

Such *in vitro* models should be obtained through combining a human cell source with micro-scale technologies. Two different approaches have been developed for the *in vitro* modeling of skeletal and cardiac muscles, relying to the different human cell source.

Concerning skeletal muscles, the cell source for *in vitro* modeling was represented by human primary myoblasts directly derived from biopsies of DMD patients. In order to efficiently drive their differentiation to a stage representative of DMD patient skeletal muscles biology and functionality, the main environmental cues directing key phases of myogenesis *in vivo* were reproduced *in vitro* using micro-scale technologies. In particular: (i) the higly aligned myofibers architecture were reproduced by micro-patterning adhesion proteins into defined geometries of parallel lanes, directing myoblast alignment and fusion in the early stages of myogenesis; (ii) mechanical properties of *in vivo* microenvironment were reproduced using an elastic hydrogel substrate, allowing a functional differentiation of myotubes in the late phases of myogenesis. In this way, an *in vitro* model of human DMD skeletal muscle was obtained. Such *in vitro* model was made of an array of parallel aligned myotubes presenting a functional differentiation, in terms of sarcomere formation, and carrying the genetic defect of the patient from which they derive.

As proof of concept, the realized *in vitro* model was used to set up an *in vitro* assay which readout was dystrophin expression restoration on the engineered DMD myotubes obtained after the co-colture with different donor myogenic cells carrying the wild-type copy of the dystrophin gene (Figure 5.1). Three different myogenic cells with an increasing degree of stemness were tested: (i) human primary myoblasts, (ii) satellite cells and (iii) mesoangioblasts.

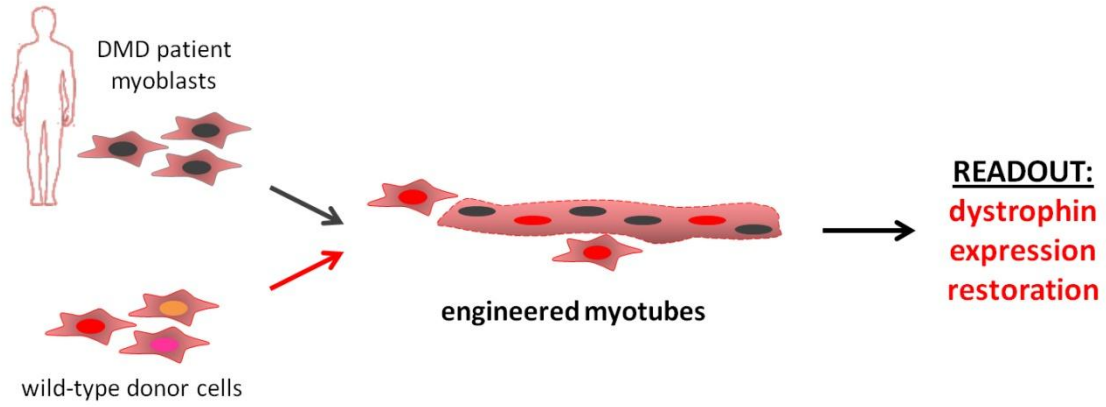

Figure 5.1. Testing cell therapy approaches *in vitro* on the micro-engineered DMD skeletal muscle.

The obtained results demonstrate that different myogenic cells have a different capability in restoring dystrophin expression on the DMD engineered myotubes. In particular human primary myoblasts were shown to restore dystrophin expression only in a limited region of myotubes, allowing the recovery of only a 7% of the dystrophin expressed by a culture entirely composed of

wild type myotubes. On the other hand, human mesoangioblasts were able to restore dystrophin in almost the entire myotubes length and to increase the dystrophin restoration by about 4 folds than human primary myoblasts (27%).

From these results, the expression of dystrophin in a DMD context seems to be not equal for all myogenic cells, but influenced by the stemness of the considered nucleus. In the developed *in vitro* model of DMD skeletal muscle, these differences can be evaluated by two factors: the portion of the myotube membrane restored with dystrophin (eg. proximal to the wild type nucleus for primary myoblasts; spanning the entire myotube for mesoangioblasts) and the yield of the expressed protein (eg. 7 % for primary myoblasts; 27 % for mesoangioblasts).

These finding show how results obtained testing these cell therapy approaches on a human *in vitro* model could be useful in the design of an hypothetical *in vivo* application. For instance, based on the obtained results, a lower number of wild-type mesoangioblasts could be used to restore dystrophin expression in a dystrophic muscle, while an higher amount of myoblasts should be use to obtain the same restoration.

In these perspective, the developed human *in vitro* model can represent a robust platform for performing preliminary or pre-clinical tests of different therapeutic strategy for DMD. In addition, it can be used as complementary tool in a clinical trial, for test different batches of cells before using them on patients.

As further improvement, also a 3D *in vitro* model of skeletal muscle have been realized. In this 3D *in vitro* model myoblasts were confined inside micrometric channels of an elastic and compliant hydrogel matrix. In these conditions tightly packed myotube bundles have been obtained. Such myotubes express the differentiation markers myosin heavy chain and α-actinin. In addition, they show a morphology completely different from the one obtained in 2D culture. Despite further analyses are needed to assess long term differentiation of the obtained myotubes the 3D model here developed is promising for the obtainment of differentiated myofiber-like structure useful for functional study.

Concerning DMD cardiac muscle, the first critical step for its *in vitro* modeling, is the choice of an adequate cell source. Due to the extremely limited proliferative capacity of adult cardiomyocytes, the direct isolation of human cells suitable for *in vitro* cardiac muscle engineereing is a challenging issue. Human pluripotent stem cells-derived cardiomyocytes are currently almost the only reliable source of human heart cells[5] suitable for this application.

Also in this case the coupling of micro-scale technologies with the appropriate cells source, i.e. human embryonic stem cell derived cardiomyocytes, resulted in the obtainment of a human *in vitro* model. The realized *in vitro* model of cardiac muscle was made of an array of contracting cardiomyocytes.

Despite being representative of cardiac tissue functionality and offering an high number of output information per single experiment, this *in vitro* model, since obtained from an “healthy” cell source, was still not representative of the pathologic DMD condition.

The efficient reprogramming of differentiated human somatic cells into a pluripotent state by Yamanaka and colleagues in 2007[6] was heralded as one of the most important scientific findings of the last decade and open for the first time the perspective of deriving patient- and disease-specific

stem cell lines. Furthermore, in a recent work, human induced pluripotent stem (hiPS) cells were derived for the first time from a DMD patient and then the genetic deficiency was completely corrected by a human artificial chromosome carrying a full-lenght genomic dystrophin sequence.

Starting from this cell source, in this work, DMD patient-specific cardiomyocytes were obtained through the application of a cardiac differentiation procedure based on the one firstly developed by Yang and colleagues, that is at the moment the most efficient for cardiomyocytes derivation from human embryonic stem cells. Then, these DMD cardiomyocytes were used as *in vitro* model to study how the human artificial chromosome (HAC) can restore multiple dystrophin expression at cardiac level (Figure 5.2).

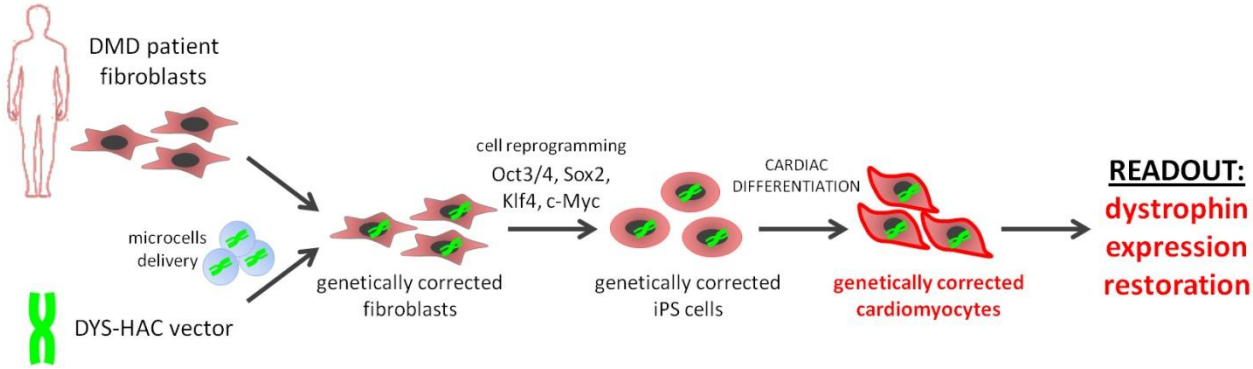

Figure 5.2. Testing dystrophyn expression restoration by HAC on DMD patient-specific cardiomyocytes.

From this study emerged that: (i) the DYS-HAC do not hinder cardiac differentiation of hiPS cells; (ii) dystrophin expression is correctly restored by the DYS-HAC during hiPS cardiac differentiation procedure; (iii) the DYS-HAC drive the expression of multiple dystrophin isoforms in cardiomyocytes.

As future perspective, it is of paramount importance to overcome the intrinsic limitation related to the cardiac differentiation procedure of pluripotent stem cells, in particular (i) the inability to exactly quantify the extent of cardiomyocyte differentiation and (ii) the difficulty in selecting pure or nearly pure population of cardiomyocytes without destroying the cells[7,8]. For this purpose, preliminary results about the application of HAC technonolgy for the obtainment of reversible reporter hiPSc lines has been reported.

References

1. Blake, D.J., Weir, A., Newey, S.E. & Davies, K.E. Function and genetics of dystrophin and dystrophin-related proteins in muscle. Physiol. Rev. 82, 291-329 (2002).

2. Cossu, G. & Sampaolesi, M. New therapies for Duchenne muscular dystrophy: challenges, prospects and clinical trials. Trends Mol Med 13, 520-526 (2007).

3. Hoffman, E.P., Brown, R.H., Jr & Kunkel, L.M. Dystrophin: the protein product of the Duchenne muscular dystrophy locus. Cell 51, 919-928 (1987).

4. Collins, C.A. & Morgan, J.E. Duchenne's muscular dystrophy: animal models used to investigate pathogenesis and develop therapeutic strategies. Int J Exp Pathol 84, 165-172 (2003).

5. Jiang, J., Han, P., Zhang, Q., Zhao, J. & Ma, Y. Cardiac Differentiation of Human Pluripotent Stem Cells. Journal of Cellular and Molecular Medicine (2012).doi:10.1111/j.1582-4934.2012.01528.x

6. Takahashi, K. et al. Induction of pluripotent stem cells from adult human fibroblasts by defined factors. Cell 131, 861-872 (2007).

7. Huber, I. et al. Identification and selection of cardiomyocytes during human embryonic stem cell differentiation. FASEB J. 21, 2551-2563 (2007).

8. Moore, J.C. et al. A P19Cl6 GFP reporter line to quantify cardiomyocyte differentiation of stem cells. Int. J. Dev. Biol. 48, 47-55 (2004).

APPENDIX A:
Micropatterning topology on soft substrates affects myoblast proliferation and differentiation

Susi Zatti[1,2], Alice Zoso[1,2], Elena Serena[1,2], Camilla Luni[1,2], Elisa Cimetta[1] and Nicola Elvassore[*,1,2]

[1]Department of Industrial Engineering (DII), University of Padova, via Marzolo 9, 35131 Padova, Italy
[2]Venetian Institute of Molecular Medicine (VIMM), via Orus 2, 35129 Padova, Italy
[*]Corresponding author Tel.: +39 049 827 5469. Fax: +39 049 827 5461. E-mail address: nicola.elvassore@unipd.it

Langmuir 2012

DOI: 10.1021/la204776e

ABSTRACT:

Micropatterning techniques and substrate engineering are becoming useful tools to investigate several aspects of cell−cell interaction biology. In this work, we rationally study how different micropatterning geometries can affect myoblast behavior in the early stage of *in vitro* myogenesis. Soft hydrogels with physiological elastic modulus (E = 15 kPa) were micropatterned in parallel lanes (100, 300, and 500 μm width) resulting in different local and global myoblast densities. Proliferation and differentiation into multinucleated myotubes were evaluated for murine and human myoblasts. Wider lanes showed a decrease in murine myoblast proliferation: (69 ± 8)% in 100 μm wide lanes compared to (39 ± 7)% in 500 μm lanes. Conversely, fusion index increased in wider lanes: from (46 ± 7)% to (66 ± 7)% for murine myoblasts, and from (15 ± 3)% to (36 ± 2)% for human primary myoblasts, using a patterning width of 100 and 500 μm, respectively. These results are consistent with both computational modeling data and conditioned medium experiments, which demonstrated that wider lanes favor the accumulation of endogenous secreted factors. Interestingly, human primary myoblast proliferation is not affected by patterning width, which may be because the high serum content of their culture medium overrides the effect of secreted factors. These data highlight the role of micropatterning in shaping the cellular niche through secreted factor accumulation, and are of paramount importance in rationally understanding myogenesis *in vitro* for the correct design of *in vitro* skeletal muscle models.

1. INTRODUCTION

The realization of functionally differentiated skeletal muscle *in vitro* is one of the major challenges in tissue engineering and regenerative medicine.[1] Engineered substitutes for skeletal muscle tissue hold promise for the *in vivo* treatment of a variety of muscle defects and diseases.[2] Furthermore,

microengineered muscles could represent a powerful tool suitable for the investigation of complex physiological processes,[3] for drugscreening applications,[4] and for testing new gene and cell therapy approaches, lowering the costs and time required to develop widely available personalized treatments for larger numbers of patients.[5] Knowing the factors that influence myogenesis *in vitro* is of paramount importance in order to engineer a skeletal muscle tissue.

In vivo skeletal muscle development is a process characterized by a defined series of events that includes myoblast proliferation, alignment and fusion into multinucleated myotubes,[6] and their further differentiation into functional myofibers.[7] Simulating myogenesis *in vitro* requires the consideration of several key factors: cell−cell interaction, extracellular matrix composition and architecture, mechanotransduction signals, medium composition, and electrical stimulation.[7,8] Early studies demonstrated that myoblasts need to interact with their fusion partner cells to differentiate into myotubes.[9] This interaction could occur either by direct contact of neighboring cell membrane proteins (such as members of the cadherin family and Ig superfamily)[10] or through mediation by myokines,[6] which are soluble factors secreted by myoblasts and acting in an auto/paracrine manner. To our knowledge, an experimental investigation of how these two aspects individually affect myogenesis has not yet been reported. Direct cell−cell interaction could be relatively simple to study by changing myoblast density in culture, whereas the effect of secreted soluble factors may be more experimentally complex to investigate, because it requires a fine control of the cell culture topology and of the local accumulation of secreted soluble factors.

However, notwithstanding this experimental complexity, it is well-known that myokines maintain a balance between growth and differentiation of muscle cells.[6] A recent work by Griffin[11] demonstrated by quantitative proteomic approaches that a large number of chemokines, chemokine receptors, and signaling molecules are expressed *in vitro* by muscle cells. This recent result shows that these endogenous secreted proteins may have a greater role in influencing the extracellular milieu and in myogenesis than previously appreciated.[11] On the other hand, besides myoblast-secreted factors, the extracellular soluble environment also includes exogenous mitogens from the serum fraction of the culture medium that normally promote proliferation and act as inhibitors of myogenic differentiation via the down-regulation of myogenic determination factors.[12−15]

In order to decouple the effect of the cell−cell contact from the secretoma-derived auto/paracrine signaling on early myogenesis *in vitro*, we envisioned controlling cell topology and cell pattern by independently changing the local cell density (and, consequently, the cell−cell contact probability) and the size of the cell cluster which may influence the local accumulation of soluble secreted factors.

In this scenario, microtechnologies can be a powerful tool in studying the role of the soluble niche of myoblasts in myogenesis *in vitro*. Currently, recent works investigating myoblast topology and myogenesis were either focused on the effect of substrate stiffness,[16] on the effect of different topology geometries,[17] or on the elongation of C2C12 myoblasts in 3D microchannels.[18] However, experimental evidence, which isolates the role of myoblast secreted factors from all other phenomena, has not yet been reported.

Therefore, in this work we aimed to study the effects of myokine accumulation produced by myoblasts on their proliferation and differentiation. We exploited micropatterning techniques to organize myoblasts in parallel lanes of increasing width and interspacing size. We used a permeable

and soft culture substrate. In particular, a permeable substrate absorbs cell secreted molecules, enhancing the local accumulation of secreted factors, whereas a soft substrate with a physiological elastic modulus (15 kPa) promotes skeletal muscle functional differentiation, in terms of sarcomeric striations of myotubes, and skeletal muscle stem cell self-renewal in culture.[16,19,20]

The patterned geometries have been designed in order to change local and global cell density. We defined the local cell density as the specific number of cells within the micropatterned area and it refers to the cell density at local level. The global cell density is defined as the ratio between the number of counted cells and the total area (which is the area including both micropatterned lanes and interspacing). This parameter refers to the overall cell density of the whole culture surface. In this way we could rationally investigate how the imposed micropattern constraints could be associated with an accumulation, at local level, of cell secreted factors produced by cells and how they could compete with the exogenous mitogens provided by medium.

2. EXPERIMENTAL METHODS

2.1. Cell Culture

2.1.1. C2C12 Culture Expansion

The murine skeletal muscle immortalized cell line C2C12 (ATCC) was expanded in standard conditions with proliferation medium: Dulbecco's modified Eagle's medium (DMEM, Sigma-Aldrich) supplemented with 10% fetal bovine serum (FBS, Gibco-Invitrogen) and 1% penicillin−streptomycin mix solution (Gibco-Invitrogen). C2C12 were induced to form myotubes in differentiating medium: DMEM supplemented with 2% horse serum (Gibco-Invitrogen) and 1% penicillin−streptomycin mix solution.

2.1.2. Human Primary Myoblasts Cultures Expansion

Human primary myoblasts were provided by the ''Telethon BioBank'' (Telethon Research Service, Istituto Nazionale Neurologico ''Carlo Besta'', Milano, Italy). Myoblasts were expanded with proliferation medium: 60% High-Glucose Dulbecco's Modified Eagle's Medium (DMEM Glutamax, Gibco-Invitrogen), 20% Medium M199 (Sigma-Aldrich), 20% fetal bovine serum (FBS, Gibco-Invitrogen), 10 ng/mL EGF (PeproTech), 2 ng/mL β-FGF (PeproTech), 10 µg/mL insulin (insulin from bovine pancreas, Sigma-Aldrich) and 1% penicillin−streptomycin−glutamine mix solution (Invitrogen); on standard 100 mm tissue culture Petri dishes previously coated with 0.5% gelatin solution (gelatin from porcine skin, Sigma-Aldrich). Human primary myoblasts were induced to form myotubes in differentiating medium: 98% DMEM Glutamax, 2% horse serum (Gibco-Invitrogen), 30 mg/mL insulin and 1% penicillin−streptomycin−glutamine mix solution.

2.2. Microstructured Culture Engineering

2.2.1. Hydrogel

Film Preparation. Microcontact printing of adhesion proteins was performed onto the nonfouling surface of poly acrylamide hydrogel films with an average thickness of 100 µm, the elastic modulus of which (15.00 ± 0.75 kPa) reproduces the stiffness of native skeletal muscle.[19] Hydrogel films were prepared as previously described[16] on chemically modified glass slides 25 mm in diameter. Briefly, 20 µL of the liquid prepolymer solution, composed of acrylamide/bisacrylamide 29:1 40% solution

(Sigma-Aldrich) diluted in phosphate-buffered saline (PBS, Gibco-Invitrogen) to the final concentration of 10% and supplemented with 20 mg/mL photoinitiator (Irgacure 2959; Ciba Specialty Chemicals), was polymerized by UV light exposure for 3 min (high-pressure mercury vapor lamp (Philips HPR 125 W) emitting at 365 nm. Glass slides with covalently bound hydrogel films were immersed in ultrapure distilled water for 48 h to ensure complete removal of the unreacted monomeric units or photoinitiator. After rinsing with ultrapure distilled water, hydrogels were allowed to dry completely for 1 h and then sterilized by exposure to UV light for 20 min under a sterile hood.

2.2.2. Microcontact Printing

A micropattern of adhesion proteins was printed onto the hydrogel surface as previously described using an elastomeric PDMS stamp reproducing the desired geometry in relief.[16,21] Briefly, the PDMS stamp was inked in the protein solution (mouse-laminin 100 µg/mL in PBS, Sigma-Aldrich) for a few seconds and the excess solution was removed. Conformal contact between the dry hydrogel surface and the stamp was then achieved by applying a gentle pressure, thus transferring the protein micropattern onto the substrate. Microcontact printed hydrogels were then transferred into 35 mm Petri dishes for cell seeding.

2.2.3. Cell Seeding and Culture Maintenance

Two different seeding densities were used: 200 cell/mm^2 (low seeding density) and 400 cell/mm^2 (high seeding density) (Table 1). 300 µL aliquots of cell suspension were dropped over the hydrogel and cells were allowed to adhere overnight to the laminin micropattern. The day after, 3 mL aliquots of proliferation medium were gently added and then cultures were kept in a 95% humidified and 5% CO2 atmosphere at 37°C. After 2 days under proliferating conditions, cultures were used for BrdU pulse and chase analyses or switched to differentiating condition with the appropriate medium. Proliferation data reported in Table 1 were evaluated 48 h after seeding by image analysis. For each value, a minimum of 3 to a maximum of 8 independent images were analyzed.

Table 1.1. Summary of the parameters characterizing each microstructured culture

lane–interspacing widths [µm]	one-lane area [mm^2] (ratio of lane to interspacing areas)	local seeding density [cell/ mm2]	experimental local cell density [cell/ mm2]	experimental global cell density [cell/ mm2]
100-100	72 (1/2 total area)	400	3300 ± 500	1700 ± 200
		200	1500 ± 200	800 ± 100
300-300	72 (1/2 total area)	400	3100 ± 500	1600 ± 200
		200	2000 ± 300	1000 ± 200
500-500	72 (1/2 total area)	400	3200 ± 500	1600 ± 200
		200	2300 ± 400	1200 ± 200
100-50	96 (2/3 total area)	200	1700 ± 300	1200 ± 200
100-200	48 (1/3 total area)	200	1900 ± 400	700 ± 100

[a]Local cell density is the ratio between the number of counted cells and the cell patterning area. Global cell density is the ratio between the number of counted cells and the total area. All data values reported are means ± standard deviations

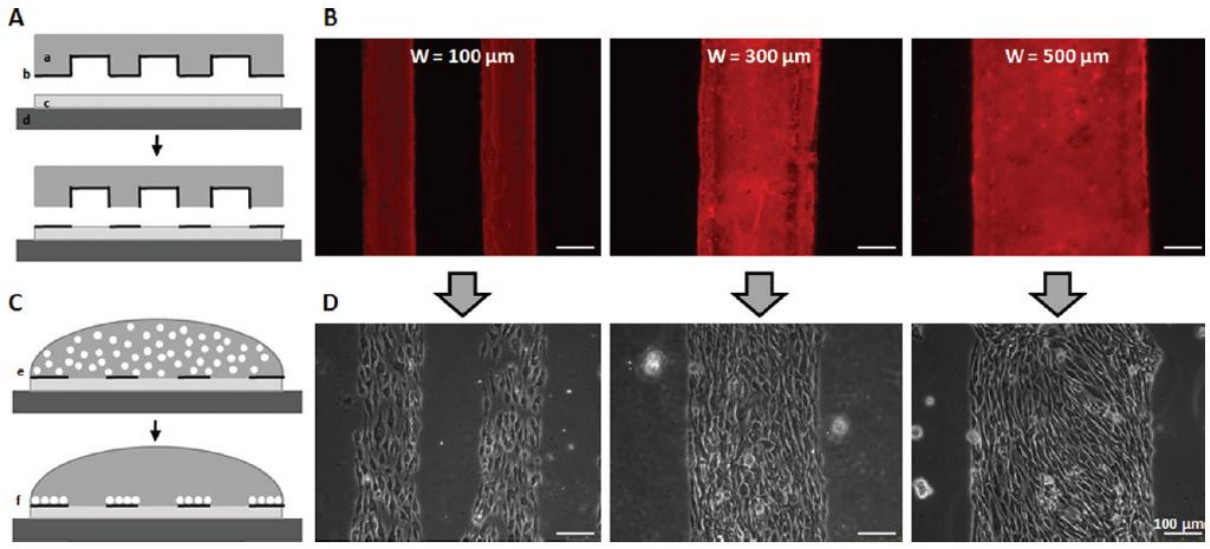

Figure 1. Micrometric control of cell culture topology by adhesion protein micropatterning on hydrogel surfaces. (A) Microcontact printing. Adhesion proteins (b) are patterned with a PDMS mold (a), carrying a geometry of parallel lanes, onto the hydrogel surface (c) polymerized on a glass slide (d). (B) Laminin immunofluorescence on microprinted hydrogels. The indicated value of W represents both lane and interspacing widths, which are the same for each configuration. (C) Cell seeding on the patterned hydrogel substrates. Cell suspension is dropped over the micropatterned hydrogel surface forming a droplet-like structure (e). After overnight incubation, cells adhere only to the protein-patterned areas (f). (D) Phase contrast images of C2C12 cultures within the geometries shown in B.

2.3. Evaluation of Cell Proliferation

BrdU pulse and chase experiments were performed on the microstructured cultures 48 h after seeding. Cell cultures were incubated with 10 µM BrdU (Sigma-Aldrich) for 3 h (C2C12) and 5 h (human primary yoblasts) and fixed with PBS-70% EtOH (Sigma-Aldrich) for 30 min at −20 °C. Cultures were then incubated with HCl 2 N for 45 min at 37 °C in order to denature DNA and rinsed twice in borate buffer 0.1 M pH 8.5 for 5 min. Mouse primary antibody against BrdU (Roche) 5 µg/mL in PBS-0.1% BSA (Sigma-Aldrich) was then applied for 1 h at 37 °C. Alexa488 fluorescence-conjugated antimouse IgG secondary antibody (Invitrogen) was applied for 45 min at 37 °C. Finally, nuclei were counterstained with DAPI (Sigma Aldrich). Samples were mounted with Elvanol and viewed under a fluorescence microscope. The fraction of proliferating cells was calculated as the number of BrdUpositive nuclei on total nuclei. Collected data were analyzed through one-way and two-way analyses of variance (ANOVA), using MatLab software, with a p-value of 0.01 as a threshold for significance. All data values reported are means ± standard deviation. For each group, a minimum of 3 to a maximum of 8 independent images were analyzed.

2.4. Evaluation of Cell Differentiation

Microstructured cultures maintained for 6 days (for C2C12) or 8 days (for human primary myoblasts) in differentiating medium were then analyzed for the expression of myosin heavy chain. Mouse monoclonal primary antibody against myosin heavy chain II (MHC, Sigma-Aldrich) was applied for 1 h at 37 °C, while the Alexa488 fluorescence-conjugated antimouse IgG secondary antibody (Invitrogen) was applied for 45 min at 37 °C. Nuclei were counterstained with DAPI. Samples were mounted with Elvanol and viewed under a fluorescence microscope. The fusion index was calculated as the percentage of nuclei inside MHC-positive myotubes of all nuclei, by image analyses. Collected data were analyzed through one-way ANOVA, using MatLab software, with a p-value of 0.01 as a

threshold for significance. All data values reported are means ± standard deviation of the mean. For each group, a minimum of 3 to a maximum of 8 independent images were analyzed.

2.5. Computational Model

A computational model was developed and solved in quasi-steady-state conditions. The system geometry includes hydrogel and medium volumes, whose heights are 100 μm and 3 mm, respectively. At their interface, a cell layer of negligible volume, reproducing various patterns (parallel lanes of different sizes, triangular shape), constitutes a homogeneous source of a representative exogenous factor. We neglected cell division and assumed a constant secretion of soluble factor, taking advantage of mathematical modeling capability to study a phenomenon without the overlap of other physical and biological processes. The concentration field of the exogenous factor was obtained by solving its equation of continuity. The diffusivity in the hydrogel was assumed to be 1/10 of its value in the medium ($10^{-}6$ cm^2/s). The model was implemented in Comsol Multiphysics v 3.4 (COMSOL, Inc., Stockholm, Sweden) using a relative tolerance of $10^{-}6$ for the solution. Coarsening and refining the mesh space grid ensured that the results were independent of the spatial discretization.

3. RESULTS AND DISCUSSION

3.1. Rational Design of Micropatterning and Computational Analyses of Secreted Factor Concentrations.

Micropatterning allows precise control over the shape of the area of cell adhesion. We designed a pattern geometry that is organized into 12-mm-long parallel lanes, over a total area of 144 mm^2. Cells attach on lanes, adsorbed with adhesion proteins, with micrometric spatial resolution, while the interspacing between the lanes is cell-repellent (Figure 1). In the following, we will refer to cell density within the lanes as local cell density, and to that averaged on the whole surface as global.

We designed five configurations differing in lane and interspace widths. In three of them, lane and interspace widths are the same (100, 300, and 500 μm) (Figure 1). Thus, when two configurations have equal local cell density, they also have equal global cell density (Table 1). On the contrary, in the other two configurations, lane width is maintained fixed (100 μm), while the interspace varies (50 and 200 μm). Thus, even for the same local cell density, the global density is still different. Table 1 summarizes the geometric parameters and the local cell density of seeding used in the experiments.

With this setup, we aimed at studying how different microstructured cultures and conditions of local and global cell density can affect myoblast proliferation and differentiation. Analyses of different conditions of local and global densities could be important for decoupling the role of cell–cell interaction from the role of soluble secreted factors on myoblast behavior.

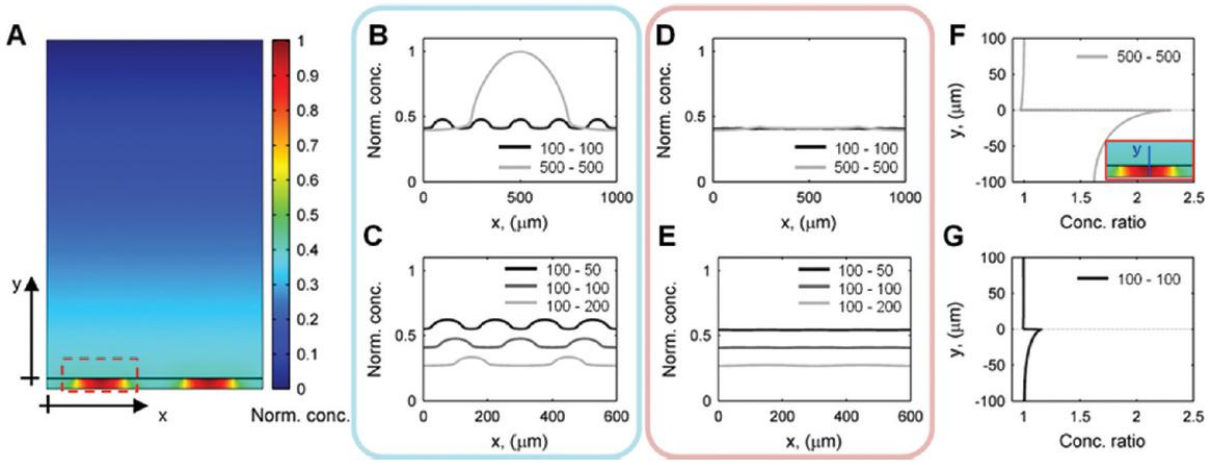

Figure 2. Concentration profiles of a representative secreted factor resulting from numerical simulations for different micropatterning sizes. (A) Transversal section of a two-lane cell culture on hydrogel. The coordinate system used in B–G is also indicated. The plane y = 0 represents the interface between hydrogel and medium. Normalized concentration in A–E refers to the ratio of concentration to its maximum value in A, where lane and interspace widths are 500 μm. (B) Comparison between two different lane/interspace widths at 5 μm below the medium–hydrogel interface (y = −5 μm). Five 100-μm lanes and one 500-μm lane are shown. Legend: first number indicates lane width, second number interspacing size. (C) Comparison between two different interspacing widths at 5 μm below the medium–hydrogel interface (y = −5 μm). Four, three, and two 100-μm lanes are shown, interspaced by 50, 100, and 200 μm, respectively. (D) Same as B, above medium–hydrogel interface (y = 5 μm). (E) Same as C, above medium–hydrogel interface (y = 5 μm). (F–G) Ratios of the concentration at the center of the lane to that at the edge, plotted along the y-direction (as indicated in the inset figure), for the micropatterning sizes indicated in the respective legends.

First, we performed a computational study to simulate how the soluble extracellular environment is affected by the different patterning geometries. Specifically, we evaluated the concentration profile of a representative factor secreted by the cells (Figure 2). Because of the simplified structure of the model, the simulated results give only a qualitative understanding of the processes involved; nonetheless, they assist the interpretation of the experimental data.

Figure 2A shows a color map indicating the concentration of the secreted factor within the whole volume of culture, including the hydrogel underneath the cells. A higher concentration is reached in the proximity of the cell-patterned area, in particular within the hydrogel domain, where the secreted factor diffuses more slowly and accumulates.

We studied the effect of lane width, keeping constant the global cell density (Figures 2B). The accumulation of secreted factor for 500-μm-wide lanes is significantly larger, with a maximum concentration at the lane center which is approximately double the concentration for 100-μm-wide lanes. Furthermore, wider lanes show a larger concentration change between the center and the lateral edge of the lane, producing a more heterogeneous environment for the cells therein (Figure 2F and G). On the contrary, the pattern size has a negligible effect on the medium above the cells, because of the fast diffusion that homogenizes secreted factor concentration (Figure 2D).

We also evaluated the effect of the interlane width when the lane size is held constant and the local cell density is the same. The results show a less remarkable influence on factor accumulation in this case, not only in medium above the cells (Figure 2C), but also below the cells in the hydrogel (Figure 2E).

Thus, the different accumulation of secreted factors is highly influenced by the presence of a substrate, the hydrogel, having low diffusion coefficient and then acting as a reservoir. However, for this same substrate, the extent of this accumulation can be tuned by changing the width of the lanes where cells attach, allowing the study of the effect of secreted factors on cell behavior.

3.2. Micropatterning Affects C2C12 Proliferation

C2C12 proliferation was investigated in the three geometries with equal lane width and interspacing. We observed that C2C12 cultures in 100 μm lane geometry showed the highest percentage of proliferating cells ((52 ± 1)% for the higher seeding density and (69 ± 8)% for the lower seeding density) (Figure 3C). BrdU-positive and negative cells were uniformly distributed inside the 100 μm patterning lanes (Figure 3A, left panel). The percentage of proliferating cells significantly decreased using the 300 and 500 μm lane geometry ((31 ± 2)% and (27 ± 4)%, respectively, for the higher seeding density; (58 ± 3)% and (39 ± 7)%, respectively, for the lower seeding density) (Figure 3C) and BrdU immunofluorescence analyses revealed negative regions inside these wider patterning lanes (Figure 3A, middle and right panels).

As expected, the proliferation rate was negatively influenced by an increased seeding density (p-value <0.01, two-way ANOVA), regardless of the patterning geometry. We also observed that micropatterning lane width strongly affects cell proliferation, for the same seeding density (p-value <0.01). However, cell seeding density and pattern geometry do not act synergistically in affecting proliferation (p-value >0.01).

We then investigated how the global density influences myoblast proliferation, using the geometry that induces the highest percentage of proliferating cells (lane width 100 μm; interspacing 50, 100, and 200 μm; see Table 1). We observed that the percentage of proliferating cells remained unchanged on the three microstructured cultures, despite a different global cell density (Figure 3D).

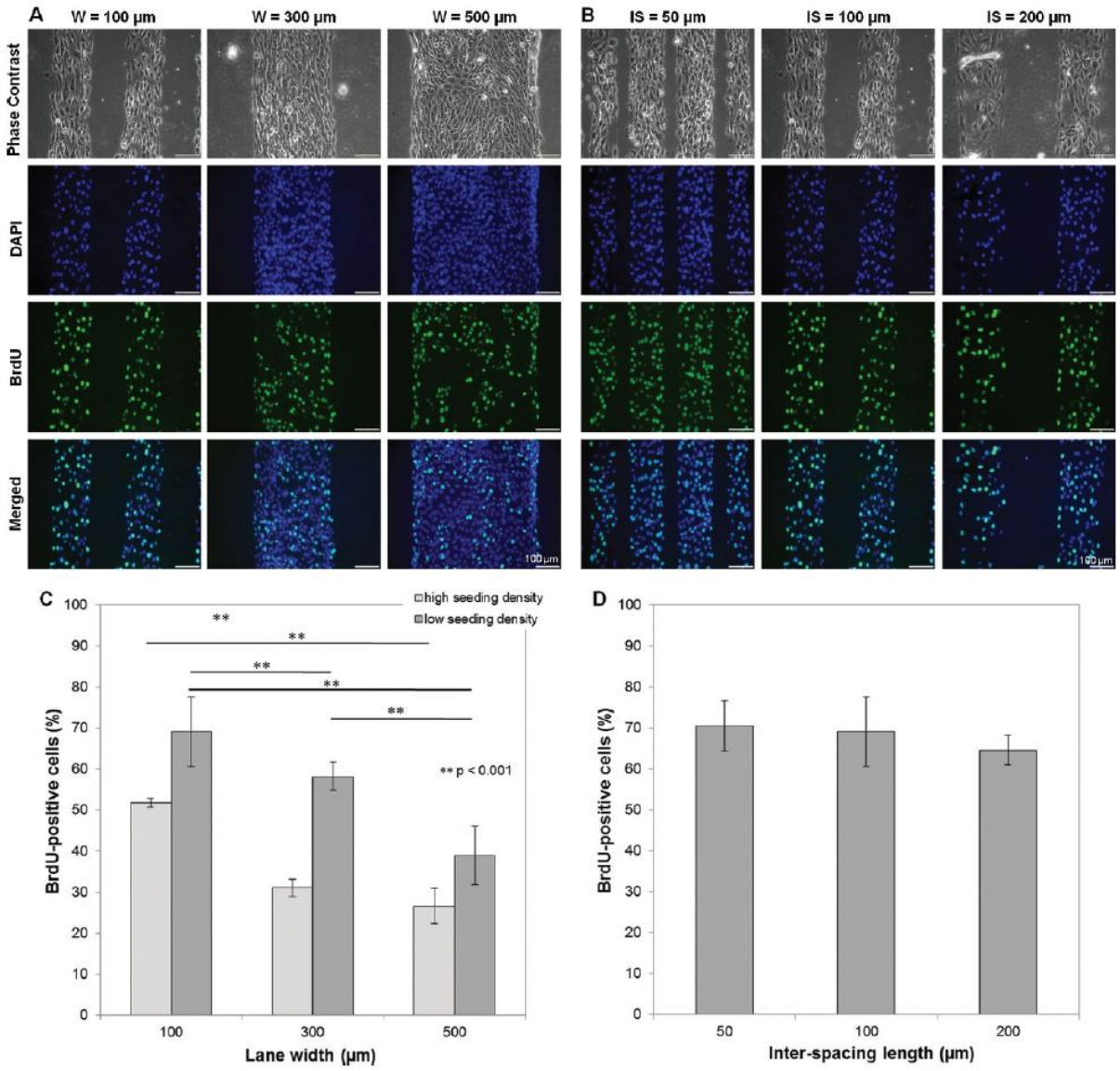

Figure 3. Effect of micropatterning on C2C12 proliferation. (A,B) BrdU immunofluorescence on microstructured C2C12 cultures 48 h after seeding on micropatterning lanes (A) with 100, 300, and 500 µm width (W) and with 100 µm width and 50, 100, and 200 µm interspace length (IS). Nuclei are counterstained with DAPI. (C) Histogram reporting the percentage of BrdU-positive C2C12 cells for each micropatterning lane width and for two different seeding densities. The number of proliferating cells decreases in microstructured cultures with wider lanes geometries. (D) Histogram reporting the percentage of BrdU-positive C2C12 cells for each micropatterning interspacing length. The number of proliferating cells is the same for microstructured cultures with wider interspacing length geometries. Reported p-values were obtained by one-way ANOVA analyses of 5 (C) and 3 (D) independent images. Error bars represent standard deviations.

A great number of studies have shown that cell behavior, in terms of differentiation fate, can be influenced by modulating the culture topology and the cell shape by micropatterning techniques.[22,23] Human embryonic stem cells (hESC) were induced to different fates through micropatterning of colonies.[24]

These results show that (i) cell density and micropatterning width affect myoblast proliferation; (ii) the effect of micropatterning width is predominant; (iii) the interspace length does not affect myoblast proliferation. They are fully consistent with the computational model, showing that accumulation of secreted factor increases when wider lanes are used (Figure 2B), whereas there is less significant accumulation of the secreted factor when varying the interspacing size (Figure 2D).

3.3. Micropatterning Lane Width Positively Influences

C2C12 Differentiation into Myotubes. During early myogenesis *in vitro*, myoblast fusion into multinucleated myotubes is preceded by cell withdrawal from cell cycle. This is usually induced by reduction of the serum concentration in the culture medium.

C2C12 cells were cultured on micropatterned surfaces characterized by 100, 300, and 500 µm lane widths using a high seeding density (400 cells/mm^2), which is required for efficient muscle differentiation. In all the microstructured cultures a remarkable formation of myotubes, arranged in independent parallel bundles, was observed (Figure 4A,B).

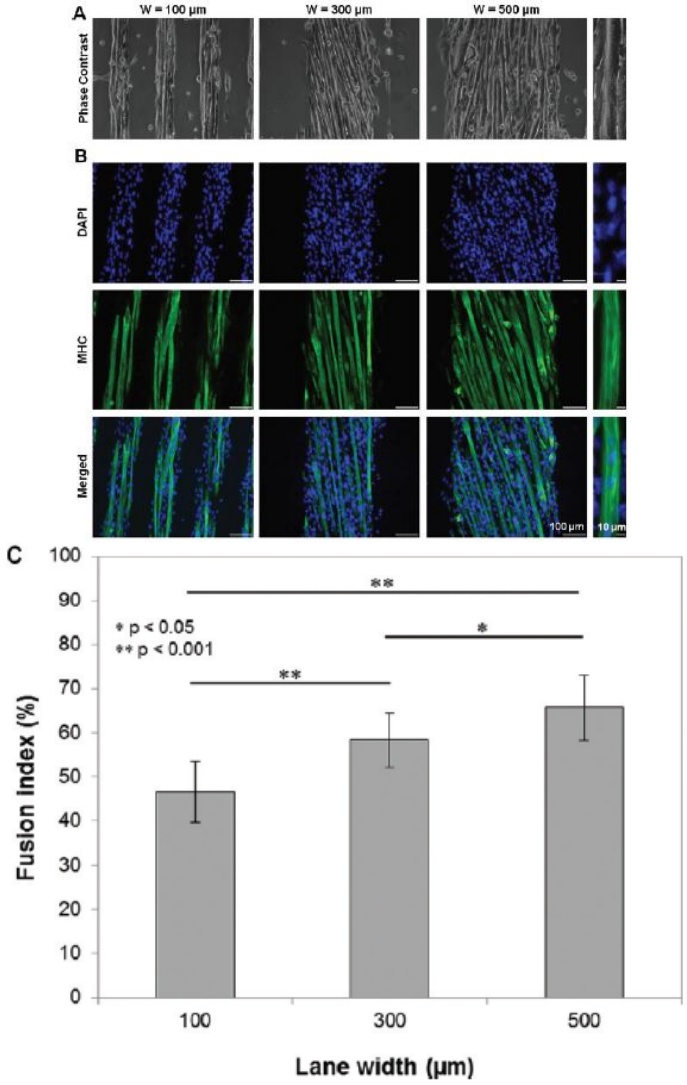

Figure 4. Effect of micropatterning lane width on C2C12 differentiation. (A) Phase contrast of live C2C12 myotubes on the different microstructured cultures characterized by 100, 300, and 500 µm lane widths, 8 days after seeding (2 days of proliferating conditions and 6 days of differentiating conditions). (B) Myosin heavy chain (MHC) immunofluorescence on C2C12 myotubes obtained in the same conditions. Nuclei are counterstained with DAPI. Right column reports magnification showing MHC sarcomeric organization. (C) Histogram reporting C2C12 fusion index for each micropatterning lane width. Fusion index increases for microstructured cultures with wider lane geometries. Reported p-values were obtained by one-way ANOVA analyses of 8 independent images. Error bars represents standard deviations.

Myotubes were similar in size, with a characteristic width of about 30 µm, and a length ranging from 300 to 800 µm. MHC immunofluorescence analyses showed the sarcomeric organ organization of MHC (Figure A,B – magnifications), in agreement with our previously reported data.[16]

We observed that the C2C12 fusion index increased with patterning lane width, from a minimum of (46 ± 8)% for 100-µm-wide lanes to a maximum of (66 ± 7)% for 500-µm-wide lanes (Figure 4C).

As expected, myoblasts differentiation showed an opposite trend compared to proliferation rate. The wider the micropatterning lanes are, the more the effect on myoblasts withdrawal from cell cycle and consequent fusion into myotubes is relevant. These data are consistent with myogenic differentiation process, in which secreted factors self-regulated myoblasts differentiation, as reported in a recent work published during the revision of this paper.[17]

3.4. Myokine-Containing Conditioned Medium Negatively

Affect C2C12 Proliferation. The results showed so far, both experimental and computational, suggest the hypothesis that there is a correlation between accumulation of secreted factors on different patterning geometries and myoblast proliferation and differentiation.

In order to test if soluble secreted factors have an autocrine/paracrine influence on myoblast behavior, we performed the same proliferation experiment using a preconditioned medium (Figure 5).

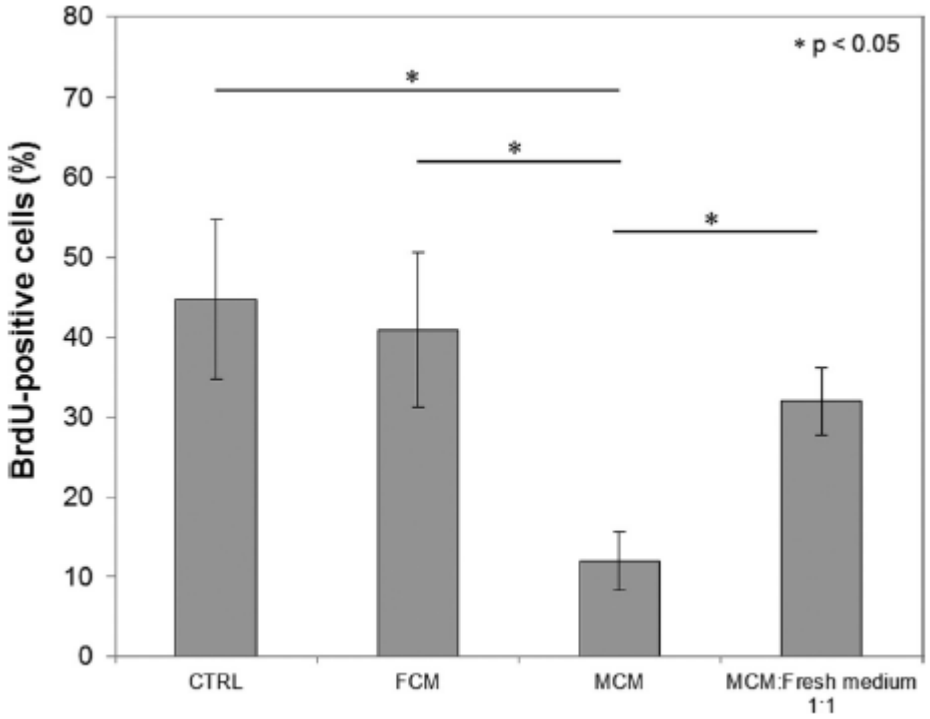

Figure 5. Effect of conditioned medium on C2C12 proliferation. Histogram reporting the percentage of BrdU-positive C2C12 cells on micropatterned surfaces characterized by 500 µm lanes cultured with freshly prepared medium, as control (CTRL), HFF fibroblast conditioned medium (FCM); C2C12 myoblast conditioned medium (MCM); medium obtained by mixing in a 1:1 ratio MCM and fresh medium. Reported p-values were obtained by one-way ANOVA analyses of 5 independent images. Error bars represent standard deviations.

In particular, we compared C2C12 proliferation on micropatterned surfaces characterized by 500 µm lanes cultured using (i) fresh medium (CTRL), (ii) medium preconditioned by a confluent culture of C2C12 myoblasts (MCM), (iii) medium preconditioned by a confluent culture of human foreskin fibroblasts (FCM), and (iv) a mix of C2C12 conditioned medium and fresh medium in a 1:1 ratio (MCM:fresh medium = 1:1) (seeding density: 400 cells/mm^2).

The results showed that C2C12 conditioned medium remarkably decreases myoblast proliferation, if compared to myoblasts cultured with fresh medium. On the other hand, medium preconditioned by fibroblasts do not have any effect on cell proliferation, meaning that (a) the observed differences are not due to an exhausted medium; (b) the solely soluble secreted factors specifically produced by myoblasts (myokines) remarkably affect C2C12 behavior. Consistent with this, using the mixed medium (1:1 ratio) we observed only a partial decrease in myoblast proliferation.

These results strengthen the hypothesis that an increase in myokine concentration, which is likely to happen in wider patterning, negatively affects cell proliferation and enhances cell differentiation, regardless of the cell density and, consequently, from cell−cell cross-talk through cell adhesion molecules.

It could be important to emphasize that the hydrogel underneath the cells could have a major role in accumulating secreted factors, as reported in Figure 2F,G. This hypothesis is consistent with the results published by Bajaj and colleagues that report no difference when increasing patterning width. Since they used glass as myoblast substrate, they could not observe any significant accumulation.[17] Nevertheless, a direct comparison between these two substrates is difficult, because hydrogels create a myogenic environment also in terms of elastic modulus and favor myoblast differentiation through protein micropatterning, as reported in our recent work.[16]

Another important consideration concerns the role of secreted factors when translating from a two-dimensional to a three-dimensional model,[18,25−27] which can better mimic the features of the *in vivo* cell microenvironment. In this latter case, the system is confined and the accumulation of secreted factors could be even higher than in a 2D system. Therefore, in a 3D system, it is likely that the matrix of encapsulated cells can act as a reservoir of soluble molecules, shaping local cell niche composition. This issue is extremely relevant when translating a conventional 2D culture to 3D cell culture system.

3.5. Establishment of a Gradient in C2C12 Proliferationby ad Hoc Patterning Design.

It would be interesting to understand if there is a threshold of patterning width that distinguishes between proliferating and nonproliferating myoblasts. For this reason we developed a “sunrays-like” structure, in which a single ray shows a continuous gradient of width (Figure 6A). These geometries were made of circles with 7 rays. Each ray in the circle was a triangle characterized by 1 mm height and a base width of 500 µm. C2C12 myoblasts were cultured on these micropatterned surfaces (Figure 6B) using a seeding density of 400 cells/mm^2.

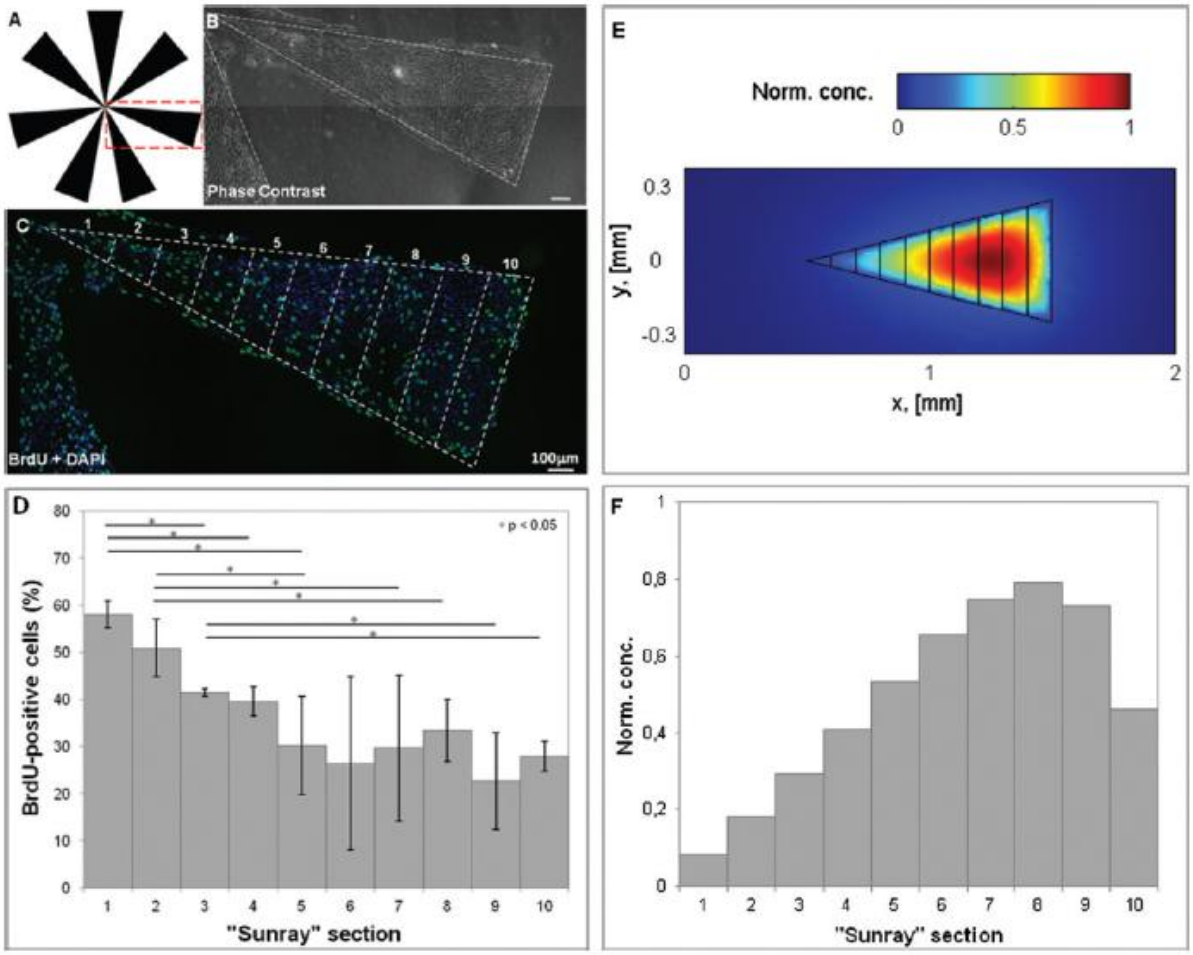

Figure 6. Establishment of a gradient in C2C12 proliferation by micropatterning lane gradual enlargement. (A) Schematic representation of the "sunrays-like" patterning geometry. (B) Phase contrast of C2C12 cultured in the microstructured cultures. (C) BrdU immunofluorescence on microstructured C2C12 cultures 48 h after seeding. Nuclei are counterstained with DAPI. The "sunray" area was divided into 10 portions as shown here. (D) Histogram reporting the percentage of BrdU-positive C2C12 cells in each of the 10 portions, mediated for 4 different "sunrays". Reported p-values were obtained by one-way ANOVA analyses of the 4 independent data. Error bars represent standard deviations. (E) Surface plot of the normalized concentration of a representative exogenous factor, as indicated by the color map, on the plane below the cells. (F) Mean concentration of the exogenous factor in each sector of the "sunray" indicated in E.

First, we observed that BrdU-positive cells were uniformly distributed inside the thinner region of the rays, whereas BrdUnegative regions appeared in the wider portion. A similar phenomenon was previously observed for the 300 and 500 µm lane geometries (Figure 3A). For the proliferation analysis, we divided the ray area into 10 segments (Figure 6C) and evaluated the percentage of proliferating cells inside each one. The reported data result from the analyses of 4 repeated experiments. The results show that myoblast proliferation decreases moving from the inner to the outer edge (Figure 6D), confirming the trend previously obtained with the discrete values of patterning width.

These results are consistent with the outcome of the computational model (Figure 6E,F). Figure 6E shows the concentration field of a representative factor secreted by the cells cultured within a triangular geometry. The factor is accumulated in the hydrogel below the cells with a quasi-linear dependence on the width of the triangle (Figure 6F). The decrease in the last segments (9−10 in Figure 6F) is due to the boundary effect.

3.6. Effect of Micropatterning Lanes Width on Human

Myoblasts Behavior. We replicated the experiments using human primary myoblasts. These cells were cultured on the three different micropatterned surfaces (100, 300, and 500 μm lanes) using a seeding density of 400 cells/mm^2.

We observed that human myoblasts proliferation was the same in all micropatterning widths (about 40% BrdU positive cells, independent from patterning width) (Figure 7A). The discrepancy between C2C12 (Figure 3C) and human myoblast behavior may be dependent on the different proliferation medium used for cell cultures. Human primary myoblast medium contains mitogenic factors (β-FGF and EGF) and a double amount of serum.

We thus hypothesized that the proliferation of human myoblasts could be mainly affected by medium composition (high serum and growth factors) rather than by myokines, secreted factors. To test this hypothesis, C2C12 were cultured in human myoblast medium, on 500 μm lanes, and with a seeding density of 400 cells/mm^2. In particular, C2C12 were treated with three different media: (1) DMEM supplemented with 10% FBS (conventional medium for C2C12 proliferation); (2) DMEM supplemented with 10% FBS and the mitogenic factors β-FGF and EGF (2 and 10 ng/mL respectively); (3) DMEM High Glucose supplemented with 20% FBS, the mitogenic factors β-FGF and EGF (2 and 10 ng/mL respectively) and insulin (10 μg/mL) (medium reproducing the conditions used for human myoblasts proliferation). Figure 2B showed that C2C12 proliferation is highly increased by the presence of serum and mitogenic factors.

Concerning differentiation, the evaluation of human myoblast fusion index on the three different microstructured cultures confirmed the positive trend previously obtained for C2C12. In this case, a more relevant increase of fusion index was observed in wider patterning lanes, from a minimum of (15 ± 4)% for 100 μm lane microstructured cultures to a maximum of (36 ± 2)% for 500 μm lane microstructured cultures (Figure 7C). The values of fusion index for human primary myoblasts obtained in this work were consistent with the data reported in our recent work.[16]

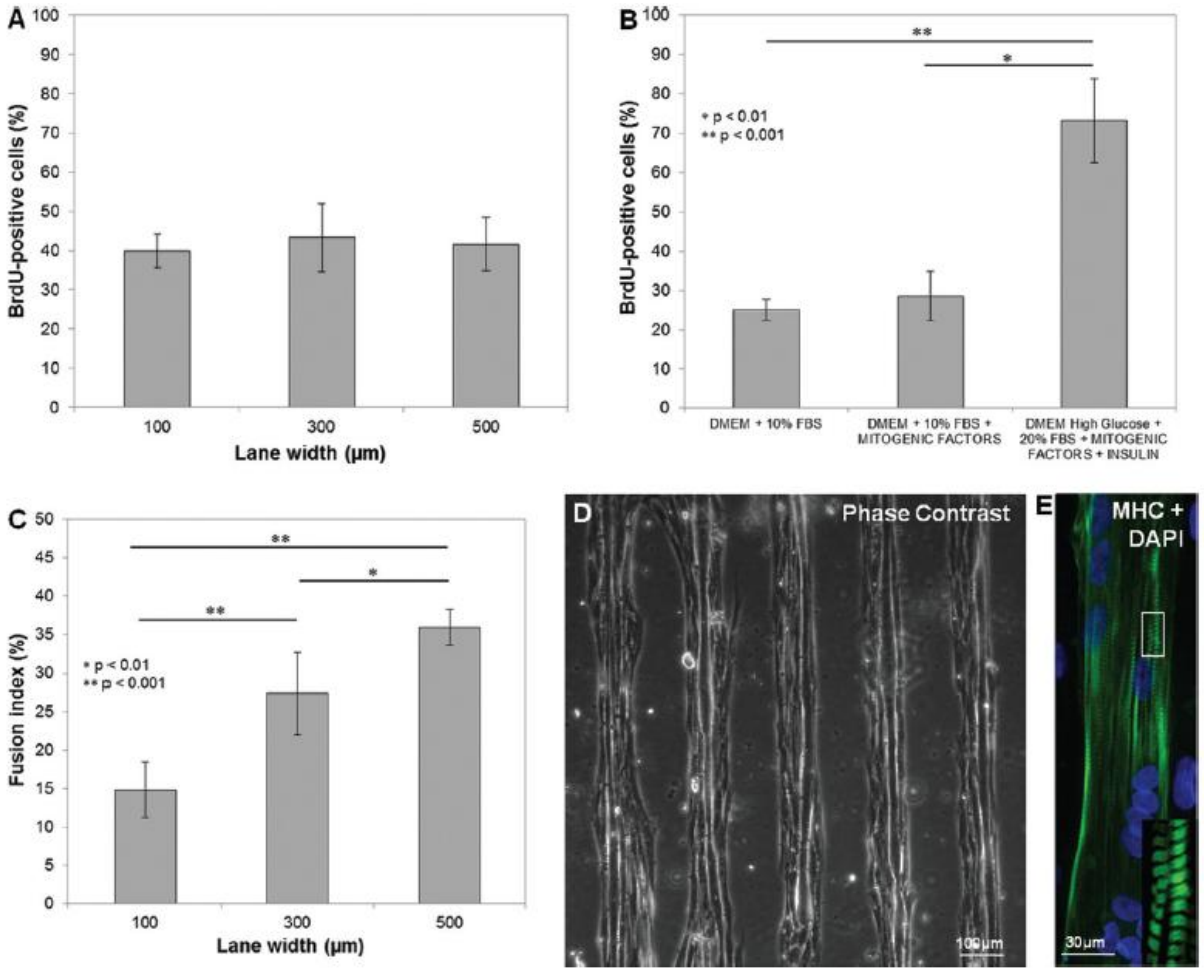

Figure 7. Effect of micropatterning lane width on human myoblast proliferation and differentiation. (A) Histogram reporting the percentage of BrdU-positive human myoblasts for different micropatterning lane widths. The number of proliferating cells is the same for microstructured cultures with wider lane geometries. (B) Effect of serum mitogens on C2C12 proliferation. The histogram reports the percentage of BrdU-positive C2C12 cells on microstructured cultures characterized by 500 µm lane width, treated with different media. Human myoblast proliferation medium, containing a double amount of serum, causes a significant increase in C2C12 proliferation. (C) Histogram reporting human myoblast fusion index for different micropatterning lane widths. Fusion index increases for microstructured cultures with wider lanes geometries. (D) Myotube formation on a microstructured culture characterized by a 100 µm lane geometry, after 8 days of differentiation. (E) Myosin heavy chain (MHC) immunofluorescence on human myotubes obtained on the microstructured cultures after 8 days of differentiation. Sarcomeric organization indicating functional differentiation was revealed in each patterning condition. For each histogram, reported p-values were obtained by one-way ANOVA analyses of 5 independent images. Error bars represent standard deviations.

Human myotubes obtained in all the microstructured cultures (with a characteristic width of about 30 µm and a length ranging from 500 µm to 1 mm) revealed a remarkable level of sarcomeric organization. Again, MHC immunofluorescence analyses showed myotube sarcomeric striations on portions or on their entire length (Figure 7D,E).

4. CONCLUSIONS

In conclusion, we demonstrated that (i) micropatterning affects myoblast proliferation and differentiation; (ii) micropatterning width, but not interspacing length, can affect myoblasts behavior in terms of both proliferation and differentiation; (iii) these effects can be due to an accumulation of secreted factors, as demonstrated by both the computational analysis and the experiments performed with conditioned medium; (iv) the accumulation of soluble secreted factors could be due to the presence of the hydrogel; (v) the same effects concerning myoblast differentiation are true for human myoblasts, while concerning their proliferation the exogenous factors (medium composition) override the accumulation of endogenous secreted factors; (vi) studies conducted varying micropatterning geometry and myoblast behavior can give useful information for translating from 2D to 3D model of skeletal muscle in order to obtain an *in vitro* model that highly recapitulates the myogenesis *in vitro*.

ACKNOWLEDGMENTS

This work was supported by Telethon (grant n. GGP08140); Città della Speranza; Fondazione CARIPARO and Regione Veneto (Azione Biotech II/III).

REFERENCES

1. Liao, H.; Zhou, G.-Q. Tissue Eng. Part B Rev. 2009, 15, 319−331.

2. Bach, A. D.; Beier, J. P.; Stern-Staeter, J.; Horch, R. E. J. Cell. Mol. Med. 2004, 8, 413−422.

3. Baar, K. Exp. Physiol. 2005, 90, 799−806.

4. Vandenburgh, H. Tissue Eng. Part B Rev. 2010, 16, 55−64.

5. Cossu, G.; Sampaolesi, M. Trends Mol. Med. 2007, 13, 520−526.

6. Chargé, S. B. P.; Rudnicki, M. A. Physiol. Rev. 2004, 84, 209−238.

7. Sanger, J. W.; Kang, S.; Siebrands, C. C.; Freeman, N.; Du, A.; Wang, J.; Stout, A. L.; Sanger, J. M. J. Muscle Res. Cell. Motil. 2005, 26, 343−354.

8. Dupont, S.; Morsut, L.; Aragona, M.; Enzo, E.; Giulitti, S.; Cordenonsi, M.; Zanconato, F.; Le Digabel, J.; Forcato, M.; Bicciato, S.; Elvassore, N.; Piccolo, S. Nature 2011, 474, 179−183.

9. Gurdon, J. B.; Tiller, E.; Roberts, J.; Kato, K. Curr. Biol. 1993, 3, 1−11.

10. Krauss, R. S.; Cole, F.; Gaio, U.; Takaesu, G.; Zhang, W.; Kang, J.-S. J. Cell. Sci. 2005, 118, 2355−2362.

11. Griffin, C. A.; Apponi, L. H.; Long, K. K.; Pavlath, G. K. J. Cell. Sci 2010, 123, 3052−3060.

12. Li, L.; Zhou, J.; James, G.; Heller-Harrison, R.; Czech, M. P.; Olson, E. N. Cell 1992, 71, 1181−1194.

13. Olwin, B. B.; Rapraeger, A. J. Cell Biol. 1992, 118, 631−639.

14. Szalay, K.; Rázga, Z.; Duda, E. Eur. J. Cell Biol. 1997, 74, 391−398.

15. De Angelis, L.; Borghi, S.; Melchionna, R.; Berghella, L.; Baccarani-Contri, M.; Parise, F.; Ferrari, S.; Cossu, G. Proc. Natl. Acad. Sci. U.S.A. 1998, 95, 12358−12363.

16. Serena, E.; Zatti, S.; Reghelin, E.; Pasut, A.; Cimetta, E.; Elvassore, N. Integr. Biol. (Camb.) 2010, 2, 193−201.

17. Bajaj, P.; Reddy, B Jr.; Millet, L.; Wei, C.; Zorlutuna, P.; Bao, G.; Bashir, R. Integr. Biol. (Camb.) 2011, 3, 897−909.

18. Aubin, H.; Nichol, J. W.; Hutson, C. B.; Bae, H.; Sieminski, A. L.; Cropek, D. M.; Akhyari, P.; Khademhosseini, A. Biomaterials 2010, 31, 6941−6951.

19. Engler, A. J.; Griffin, M. A.; Sen, S.; Bönnemann, C. G.; Sweeney, H. L.; Discher, D. E. J. Cell Biol. 2004, 166, 877−887.

20. Gilbert, P. M.; Havenstrite, K. L.; Magnusson, K. E. G.; Sacco, A.; Leonardi, N. A.; Kraft, P.; Nguyen, N. K.; Thrun, S.; Lutolf, M. P.; Blau, H. M. Science 2010, 329, 1078−1081.

21. Cimetta, E.; Pizzato, S.; Bollini, S.; Serena, E.; De Coppi, P.; Elvassore, N. Biomed. Microdevices 2009, 11, 89−400.

22. McBeath, R.; Pirone, D. M.; Nelson, C. M.; Bhadriraju, K.; Chen, C. S. Dev. Cell 2004, 6, 483−495.

23. Li, F.; Li, B.; Wang, Q.-M.; Wang, J. H.-C. Cell Motil. Cytoskeleton 2008, 65, 332−341.

24. Lee, L. H.; Peerani, R.; Ungrin, M.; Joshi, C.; Kumacheva, E.; Zandstra, P. Stem Cell Res. 2009, 2, 155−162.

25. Engler, A. J.; Humbert, P. O.; Wehrle-Haller, B.; Weaver, V. M. Science 2009, 324, 208−212

26. Bian, W.; Liau, B.; Badie, N.; Bursac, N. Nat. Protoc. 2009, 4, 1522−1534.

27. Vandenburgh, H.; Shansky, J.; Benesch-Lee, F.; Skelly, K.; Spinazzola, J. M.; Saponjian, Y.; Tseng, B. S. FASEB J. 2009, 23, 3325−3334.

APPENDIX B:
Soft substrates drive optimal differentiation of human healthy and dystrophic myotubes

Elena Serena[1,2], Susi Zatti[1,2], Elena Reghelin[1,2], Alessandra Pasut[1,2], Elisa Cimetta[1] and Nicola Elvassore[*,1,2]

[1]Dipartimento di Principi e Impianti di Ingegneria Chimica DIPIC, University of Padova, Padova, Italy.[2]Venetian Institute of
[2]Venetian Institute of Molecular Medicine, Padova, Italy
[*]Corresponding author Tel.: +39 049 827 5469. Fax: +39 049 827 5461. E-mail address: nicola.elvassore@unipd.it

Integrative Biology 2010

DOI: 10.1039/b921401a

ABSTRACT:

The *in vitro* development of human myotubes carrying genetic diseases, such as Duchenne Muscular Dystrophy, will open new perspectives in the identification of innovative therapeutic strategies. Through the proper design of the substrate, we guided the differentiation of human healthy and dystrophic myoblasts into myotubes exhibiting marked functional differentiation and highly defined sarcomeric organization. A thin film of photo cross-linkable elastic poly-acrylamide hydrogel with physiological-like and tunable mechanical properties (elastic moduli, E: 12, 15, 18 and 21 kPa) was used as substrate. The functionalization of its surface by micro-patterning in parallel lanes (75 mm wide, 100 mm spaced) of three adhesion proteins (laminin, fibronectin and matrigel®) was meant to maximize human myoblasts fusion. Myotubes formed onto the hydrogel showed a remarkable sarcomere formation, with the highest percentage (60.0% ± 3.8) of myotubes exhibiting sarcomeric organization, of myosin heavy chain II and α-actinin, after 7 days of culture onto an elastic (15 kPa) hydrogel and a matrigel® patterning. In addition, healthy myotubes cultured in these conditions showed a significant membrane-localized dystrophin expression. In this study, the culture substrate has been adapted to human myoblasts differentiation, through an easy and rapid methodology, and has led to the development of *in vitro* human functional skeletal muscle myotubes useful for clinical purposes and *in vitro* physiological study, where to carry out a broad range of studies on human muscle physiopathology.

Insight, innovation, integration: Skeletal muscle differentiation *in vitro* is greatly influenced by microenvironmental culture conditions, but the underlying mechanisms remain poorly understood. We developed an easy and rapid technology for cell substrate design, in terms of biochemical, topological and mechanical properties, which allowed the accurate control of the specific interaction between substrate and myoblast membrane, the nucleation site for the scaffolding of sarcomeric proteins. Our technology allowed the investigation of the effects of substrate properties on functional maturation of human dystrophicmyotubes. The system has been biologically inspired: it was developed ad hoc taking into account the biological requirements of myoblasts culture and all the technological improvements were designed for having accurate readout from the cell culture. Our results show that substrate stiffness has a key role in regulating human myotubes differentiation and maturation. This system could thus represent a powerful tool for the development of new therapies and drugs on a human target.

1. INTRODUCTION

Micro-engineering of human functional skeletal muscle myotubes ‘‘on bench side’’ is a relevant challenge in regenerative and translational medicine.[1] A cost-effective and highthroughput production of micro-scale muscle models showing human physiological and biological response is a fundamental issue in speeding up the development process of new drugs or innovative therapies.[2] Furthermore, new perspectives in such therapeutic strategies development[3] may arise from the fabrication of human myotubes from myoblasts of patients with important and unsolved genetic diseases, such as Duchenne Muscular Dystrophy (DMD), the most severe among muscular dystrophies.[4,5]

The process of skeletal myoblast differentiation *in vitro* has been widely investigated over the last decades, whether with the aim of studying the physiology and regulatory mechanisms of the process[6,7] and the microenvironment of muscle stem cell niche,[8,9] or in sight of developing a tissue engineered graft.[10] Several species (mouse, rat, chicken) and cell types (satellite cells, muscle precursor cells, embryonic stem cells) have been investigated, as well as different substrates (Petri dish; two and three dimensional, natural or synthetic scaffolds). These studies have produced valuable knowledge in the fields of myofibrillogenesis and, consequently, in skeletal muscle tissue engineering. However, they were mainly performed using *in vitro* non-human cells or *in vivo* animal models. They both have several advantages, such as being, respectively, a low-cost and high-speed testing tool and a good representation of the complexity of an entire organism, but researching on a human tissue could give correct insights into the human biology and could greatly accelerate the process of research translation into clinic.[11–13]

Only few studies on human myoblast differentiation *in vitro* are reported,[14–16] despite their valuable contribution in sight of clinical applications and translational medicine.

Muscle regeneration *in vivo* is highly regulated in a spatial and temporal manner by the expression of different muscle specific proteins[17] and by not yet fully characterized cell–microenvironment interactions.[18] In skeletal muscle, the extracellular matrix not only displays adhesive ligands important to cells anchorage, but also presents a number of potentially influential physical properties responsible for the acquisition of the contractile phenotype. Recently, it has been reported that the substrate mechanical properties, in terms of elastic modulus, have a key role in muscle differentiation and, in general, in stem cell lineage specification.[19] Engler and colleagues proved that murine myoblasts cultured *in vitro* require a substrate with muscle-like mechanical properties to optimally differentiate ($E = 12 \pm 4$ kPa).[20] Cell topology is another key element in myoblasts differentiation. Skeletal muscle tissue is in fact comprised of highly oriented myofibers formed from numerous fused mononucleated cells: it is well known that structure and organization of muscle fibers dictate tissue function. Thus, muscle cell alignment that permits organized myotube formation is a crucial step in the musculoskeletal myogenesis.[21] The ability to topologically guide muscle cells would greatly maximize the formation of aligned myotubes.

In this scenario, we investigated the effects of these key factors in the differentiation of human myoblasts derived from DMD patients for the derivation of functional human myotubes reporting the genetic disorder. We also proved that the technology here developed could be easily extended to myoblasts derived from healthy donors. In particular, following a biologically inspired approach, we engineered three different properties of the cell culture microenvironment in sight of a proper *in*

vitro differentiation of human myoblasts: (i) cell topology through micro-patterning of adhesion protein, in order to guide myoblast adhesion in parallel lanes and promote their alignment and fusion; (ii) substrate elasticity, in order to reproduce the correct mechanical stimuli of native skeletal muscles; (iii) extra cellular matrix proteins, in order to maximize the differentiation potential of human myoblasts. We observed a strong influence of the substrate mechanical properties onto sarcomeric architecture formation: myoblasts cultured onto a stiff substrate, glass, formed myotubes that showed few sarcomere striations only when they grew on top of an underneath cell layer, while the typical pattern of sarcomere was visible for the entire length of the myotubes when cultured onto a soft hydrogel. In particular we demonstrated that human myoblasts need a substrate with E ≈ 15 kPa and a patterning of matrigel® (2.5% v/v) to optimally differentiate (percentage of striated myotubes 60.3 ± 3.8%) after 7 days of culture.

2. Experimental methods

2.1 Human myoblast expansion

Human myoblasts were provided by the ''Telethon BioBank'' (Telethon Research Service, Istituto Nazionale Neurologico ''Carlo Besta'', Milano, Italy). Myoblasts were expanded in gelatin-coated dish with proliferation medium: 60% highglucose Dulbecco's Modified Eagle's Medium (Glutamax, Invitrogen), 20% Medium M199 (Sigma), 20% FBS (Invitrogen), 10 ng ml^{-1} EGF (PeproTech), 2 ng ml^{-1} β-FGF (PeproTech), 10 μg ml^{-1} insulin (insulin from bovine pancreas, Sigma), Penicillin-Streptomycin-Glutamine (Invitrogen). Before reaching the confluence, cells were trypsinized (Tripsina-EDTA 0.25%, Invitrogen) and replated either in a new dish or onto the hydrogel surfaces. Myoblasts were induced to form myotubes in differentiating medium: 98% High-Glucose DMEM, 2% horse serum (Invitrogen), 30 μg mL^{-1} insulin, penicillin, streptomycin and glutamine.

2.2 Hydrogel preparation

Hydrogels were prepared as previously described.[22] Briefly, clean and dry glass slide surfaces were chemically modified by subsequent deposition of a solution of 3-aminopropyltriethoxysilane (Sigma-Aldrich) and glutaraldehyde 0.5% in PBS 1X; this resulted in the formation of a hydrophobic layer ensuring covalent binding of the hydrogel films. Acrylamide/bisacrylamide 29 : 1 40% solution (Sigma-Aldrich) was diluted in phosphatebuffered saline (PBS, Sigma-Aldrich) to the final concentrations of 8%, 10%, 12% and 14%. The photoinitiator (Irgacure 2959; Ciba Specialty Chemicals) was initially dissolved in methanol at 200 mg ml^{-1} and then added to the acrylamide/ bis-acrylamide solution in order to obtain a final concentration of 20 μg ml^{-1}, and mixed thoroughly. 20 ml of the prepolymer solution were dropped over the functionalized glass surface. Hydrogel polymerization occurred by exposing the prepolymer solution to UV light for 3 min (high-pressure mercury vapor lamp (Philips HPR 125 W) emitting at 365 nm with an incident light intensity of 20 mW cm^{-2}). Selective photo-polymerization of acrylamide solutions on the glass surface was achieved by interposing a photomask with the desired geometry between the light source and the glass slide. Non-polymerized acrylamide was removed using distilled water. Such procedures resulted in homogeneous hydrogel films with 16 mm diameter and an average thickness of 40 mm. Glass slides with covalently bonded hydrogel films were immersed in ultra-pure distilled water for 48 h to ensure complete removal of the unreacted monomeric units or photoinitiator and then soaked in a 70% ethanol solution. After rinsing with ultra-pure distilled water, hydrogels were allowed to dry

completely overnight; final sterilization occurred after 20 min exposure to UV light under a sterile hood.

2.3 Protein micropatterning and cell seeding

A micropattern of adhesion proteins was performed onto the hydrogel surface as previously described.[22] Laminin and fibronectin (both from Sigma Aldrich) were used at a concentration of 100 mg ml^{-1} in PBS, while matrigels (BD Bioscience) was diluted at 2.5% v/v in DMEM. Briefly, the PDMS stamp, microstructured with a geometry of parallel lanes (75 mm wide and 100 mm spaced), was inked in the protein solution for a few seconds, and the excess solution was removed. Conformal contact between the dry hydrogel surface and the stamp was then achieved by applying a gentle pressure, thus transferring the desired protein micropattern onto the hydrogel surface. 300 µL of cell suspension (1 x 10^5 cells mL^{-1}) was dropped over the hydrogel and the myoblasts allowed to adhere to the patterned surface. Cell cultures were kept at 37°C, 5% CO_2. After 3 days of culture, the medium was switched to a differentiating medium.

2.4 Immunohistochemistry

Primary antibodies used in this study were against MyoD (rabbit polyclonal, Santa Cruz Biotech), desmin (rabbit polyclonal, Abcam), myosin heavy chain II (mouse monoclonal, Sigma-Aldrich), a-actinin (mouse monoclonal, Sigma-Aldrich) and dystrophin (rabbit polyclonal, Abcam). Cells were fixed with 2% PFA (Sigma-Aldrich) for 7 min at room temperature and permeabilized with 0.5% Triton X-100 (Sigma-Aldrich) and blocked in PBS-2% horse serum (HS) for 45 min at room temperature. Primary antibodies were individually applied for 1 h at 37°C. Cells were washed and incubated with Alexa488 and Alexa495 fluorescence-conjugated secondary antibody (Invitrogen) against mouse or rabbit, depending on primary antibody for 45 min at 37°C. Finally, nuclei were counterstained with DAPI (Sigma Aldrich) and samples were mounted with Elvanols, and viewed under a fluorescence microscope.

2.5 Topologic analysis

Images of desmin immunostaining, 24 and 48 h after seeding, were analyzed in order to evaluate the angles formed between each myofiber axis and the direction of the pattern. Evenly dividing the orientation angles range, we defined the ratio between myotubes falling into the same class of orientation and the total number of myotubes; a polar graph was then plotted, reporting myotubes frequency as a function of the orientation angle. In the case of culture onto glass the preferential direction was chosen randomly.

3. Results and discussion

3.1 Substrate design and engineering

In sight of mimicking the physiological mechanical cues of native skeletal muscle tissue, an elastic poly-acrylamide hydrogel (PAh), produced by photo-polymerization of a 29 : 1 v/v acrylamide/bis-acrylamide solution, was used as cell culture substrate. The non-fouling PAh surface was then successfully functionalized through micro-contact printing (mCP) of parallel lanes (75 mm wide and 100 mm spaced) of adhesion proteins, allowing to topologically organize the cell culture with micrometric spatial resolution and in order to promote myoblasts alignment and fusion.

The PAh production and micro-patterning protocols were optimized from previously described procedures[22] (Fig. 1). Briefly, the prepolymer solution with a biocompatible photoinitiator, was photo-polymerized through a selective photomask, resulting in a circular hydrogel of 16 mm diameter (Fig. 1A–B). In order to tune the mechanical properties of the hydrogel with human cell culture, the PAh composition was optimized by varying the percentage of acrylamide/bis-acrylamide mixture in the prepolymer solution, leading to elastic hydrogels with increasing stiffness. PAh prepared with 8%, 10%, 12% and 14% of such mixture resulted in hydrogels with elastic moduli (E) of 12 kPa, 15 kPa, 18 kPa and 21 kPa, respectively (Fig. 1C). According to literature data, the elastic modulus of 10% PAh is consistent with the stiffness of a native skeletal muscle.[20]

The µCP technique simply required conformational contact between the dried hydrogel surface and the microstructured poly(dimethyl)-siloxane (PDMS) stamp previously coated with adhesion protein solution; application of gentle pressure ranging from 10 to 100 kPa allowed to selectively transfer the protein onto the substrate (Fig. 1D). In order to optimize extracellular matrix composition for human myoblasts, we analyzed the effect of laminin, fibronectin (both at 100 mg ml^{-1}) and matrigels (2.5% v/v), commonly used in myoblasts culture *in vitro*. The obtained patterning led to a highly defined myoblasts array (Fig. 1E–F). This methodology is simple, easy, rapid and effective, as, in addition, all the reagents and chemicals needed for PAh production and µCP are typically available in a biological laboratory.

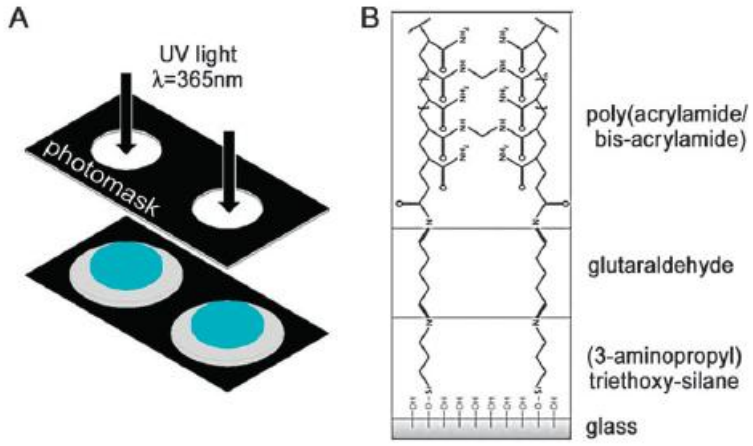

Acrylamide/bis-acrylamide (%)	Young's modulus (kPa)
8	12±0.60
10	15±0.75
12	18±0.90
14	21±1.05

Figure 1. Hydrogel production and topological control of human dystrophic myoblasts adhesion. (A–B) PA Hydrogel production. (A) The PAh are prepared by photo-polymerization of the acrylamide/bisacrylamide solution under UV light. (B) The circular PAh, 16 mm in diameter, was covalently bound to a glass coverslip through 3-aminopropyltriethoxysilane and glutaraldehyde, as shown in the schematic representation of the chemistry. (C) The table reports the elastic modulus (Young's modulus) of the PAh as a function of the pre-polymer solution composition (acrylamide/bis-acrylamide). (D–F) Micro-contact printing and cell topology. (D) The PAh surface is functionalized by micro-contact printing: the proteins (red)

are transferred to the hydrogel surface (light blue) through conformal contact between a PDMS stamp (white), carrying a geometry of parallel lanes (75 mm width, 100 mm spaced), and the PAh. Immunofluorescence against laminin (E) indicates that this technique results in a highly defined patterning, which enables a micrometric control over human myoblasts adhesion topology (F).

3.2 The sarcomeric architecture in human myotubes isimproved by cell pattern and tissue-like substrate elastic modulus

Human myoblasts were derived from biopsies of both healthy and DMD affected donors for a total of seven individuals (Table 1), provided by Telethon Biobank (Istituto Besta, Milan, Italy). The culture had high myogenic potential within early passages *in vitro*: >84% desmin positive cells, >90% MyoD positive cells (Fig. 2). The fusion index was highlyrelated to biopsy and ranges from an average of 50 ± 4.8% for healthy myoblasts to 20 ± 3.2% for DMD myoblasts.

Table 1.1. Biopsy characterization. Biopsy identification number, age and sex are reported

	Biopsy	Sex	Age
DMD	9445	M	6
	9374	M	2
	9450	M	2
	7475	M	2
Healthy	9208	M	2
	9347	F	3
	9420	M	7

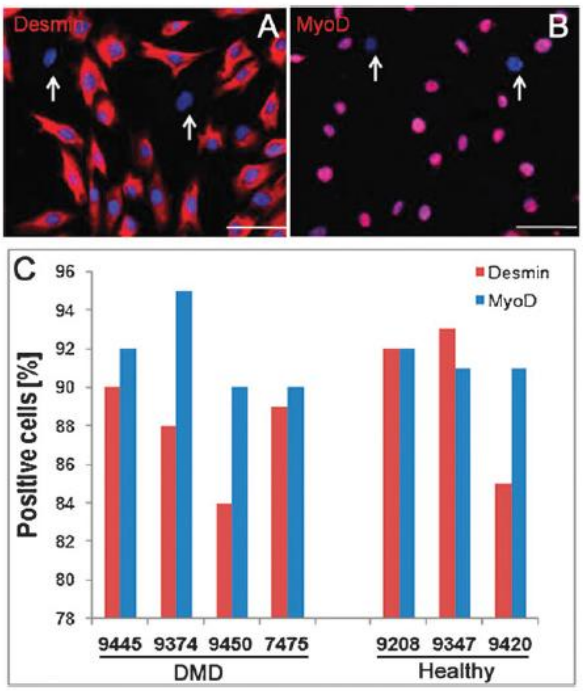

Figure 1. Human primary myoblasts characterization. Immunofluorescence on desmin (A) and MyoD (B). Arrows indicate negative cells. Nuclei are counterstained with DAPI. Scale bar = 75 mm. (C) Histogram reporting the percentage of desmin and MyoD positive cells in each biopsy.

We observed that human myoblasts from DMD patients cultured onto conventional cell culture surfaces (e.g.: not patterned glass or polystyrene) started to align in random directions 48 h after seeding and fused after 3 days, only when switched to differentiating medium (Fig. 3A–E). On the contrary, human myoblasts seeded onto micro-patterned PAh (EE15 kPa) either with laminin, fibronectin or matrigels were guided in adhesion with micrometric precision since the first hours after seeding (Fig. 3F–J). After 72 h, myoblasts showed the typical elongated morphology and were fully confluent within the patterned lanes (Fig. 3I). Human myotubes formation started 72 h after cell seeding in proliferation medium, without switching to the differentiating medium (inset in Fig. 3I). Myogenic markers (Fig. 3E and J) and differentiation capacity were maintained in both substrates. The analysis of myoblasts orientation 1 and 48 h after seeding confirmed that the protein micro-patterning enables the control over cell orientation and allows the maximization of myoblasts adhesion along a predefined direction (Fig. 3 K–L). Together, these results indicate how the use of micro-patterned PAh as culture substrates: (i) ensured the formation of a single layer of cells, thus increasing the uniformity of conditions and the influence of the substrate properties on cell differentiation, (ii) kept cells separated and well defined, allowing an accurate optical definition of myoblasts/myotubes in arrayed and independent lanes, (iii) induced a faster differentiation of human myoblasts even in proliferative conditions.

For evaluating the extent of the differentiation process after 7 days of culture, we analyzed the presence of sarcomeric organization of myosin heavy chain II and a-actinin. The accumulation of myosin II in myofibrils is one of the final steps after premyofibril formation.[23] Fig. 4A shows that dystrophic myotubes cultured on glass for 7 days did not develop the characteristic pattern of the sarcomere: un-structured cytoplasmic staining for both proteins were observed (Fig. 4A, glass). On the contrary, dystrophic myotubes obtained on micro-patterned PAh showed a remarkable sarcomeric organization (Fig. 4A, hydrogel). The dimensions of the sarcomere are consistent with that of the sarcomere *in vivo*: contiguous Z-disks are 2.5 μm spaced.[24] On PAh, the length of myotubes ranged from 500 μm to 1 mm and the sarcomeric striations were observed on the entire length of the myotubes (as shown in the z-stack analysis of Fig. 4A). In addition, in myotubes cultured on glass, few sarcomeric striations were detected at 7 days of culture and they only partially covered the length of the myotubes (Fig. 4B). It is worth noticing how in this case the myosin striations were detected solely on myotubes formed on top of an underlying layer of fibroblasts. This is proven by the three-dimensional analysis of DAPI and myosin immunofluorescence showing that the striated staining of myosin (green) was visible only on top of a bottom layer of cells (blue) (Fig. 4C). On the other hand, as previously observed, myoblasts culture onto micropatterned hydrogel ensured their growth as a single layer of cells.

Our findings confirm on a human model what has been previously reported for murine cells:[19] myotubes cultured on glass surfaces showed visible striations only when grown on top of a cell layer and there is an optimal substrate stiffness for myoblasts differentiation.

Assuming the validity of the finding that the substrate mechanical properties can strongly affect the murine myoblasts differentiation, we investigated the effects of increasing substrate stiffness and of cell–matrix biochemical interaction in the functional differentiation of human myoblasts in terms of sarcomere formation. In particular, we evaluated the effects of: (i) hydrogels with increasing elastic modulus: E ≈ 12 kPa, 15 kPa, 18 kPa and 21 kPa; and (ii) several adhesion proteins: 100 mg ml^{-1} fibronectin, 100 mg ml^{-1} laminin and 2.5% v/v matrigels. As expected, the percentage of striated

myotubes was proportional to the time in culture, independent of both the stiffness and adhesion protein, as shown in the graphs reported in Fig. 4D. On the contrary, at 7 days of culture, the percentage of striated myotubes was strongly dependent on the substrate stiffness. At 7 days the trends were extremely repeatable, regardless of the protein used: a maximum of striated myotubes was always reached with PAh with E ≈ 15 kPa and a minimum with E ≈ 21 kPa. Such optimum was obtained on hydrogels with E ≈ 15 kPa (60.31% ± 3.78), the stiffness resembling that of physiological skeletal muscle tissue, combined with a patterning of matrigels (Fig. 4D).

For the sake of completion, we replicated the experiments using myoblasts from healthy donors, thus proving that the same methodologies used for DMD myoblasts can be extended without any modification to other cell types (Supplementary Fig. 1[†]). This result can be explained because the sarcomere formation is not directly correlated to the absence or presence of dystrophin.

These results show that the percentage of human striated myotubes is strongly dependent on substrate stiffness. At these conditions, electrically induced contractions were observed for both DMD and healthy myotubes.

The major advantage of studying myoblasts differentiation in our system (PAh and micro-patterning) is the possibility to accurately analyze the effects of cell membrane–substrate interactions by culturing a single cell monolayer. It has been largely demonstrated that myofibrillogenesis is a protracted process that begins at the membrane.[20,23] The myofibrillogenesis starts with the formation of protocostameres, early integrin adhesion sites composed of integrins themselves, a-actinin, talin and vinculin, which function as nucleation sites for a-actinin accumulation and the assembly of premyofibrilassociated Z-bodies. As differentiation proceeds, Z-bodies mature in Z-disk, the protocostameres become costamere and inter-Z-disk bridges between internal myofibril (for review see Sparrow and Schock[23]). Many lines of evidence argue strongly that the myofibril assembly starts at the integrin adhesion sites. In particular, Schwander and colleagues' data provided strong evidence that the final assembly of premyofibrils into sarcomeres is b1 integrin dependent.[25] The connection between integrins and sarcomeric structure, and thus the scaffolding of I-Z-I bands and the organization of a-actinin, actin and myosin into mature sarcomeres, seems to be directed by proteins such as N-RAP[26] and ZASP,[27] which share a LIM domain, a protein-binding domain often associated with proteins that have roles in controlling gene expression or development. The extracellular β1 integrin domain binds to an RGD (arginine-glycine-aspartate) motif, a sequence present in many ECM proteins, such as laminin and fibronectin. In this perspective, the hydrogel is a hydrophilic polymeric network that in contact with water, swells to high water content (90% w/w) and shows tissue-like elastic properties. It is worth underlining that this highly hydrated polymeric network could allow a certain degree of lateral and rotational mobility to the ECM proteins adsorbed on its surface. In contrast, proteins permanently adsorbed on glass do not have any dynamic conformational change.

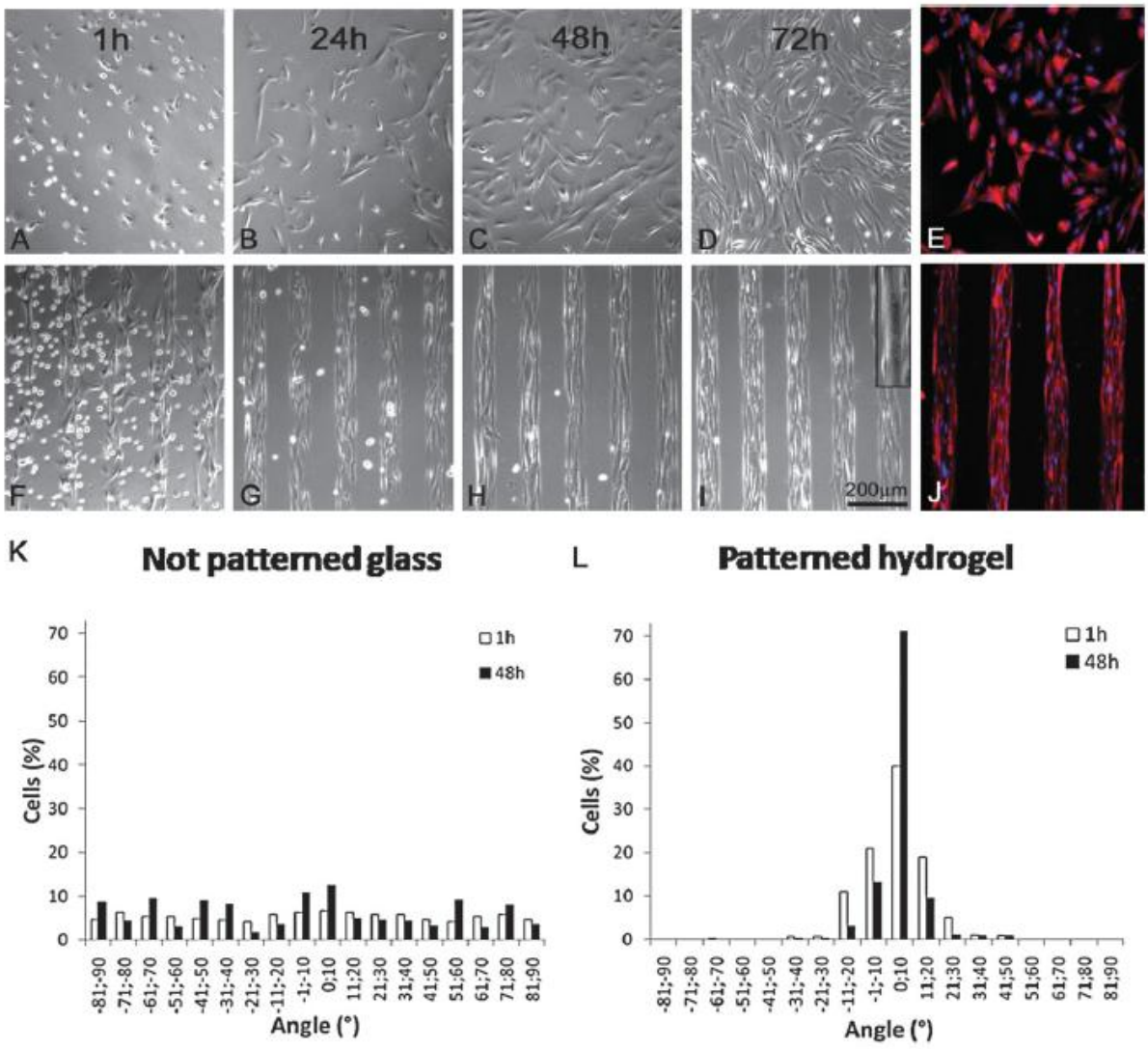

Figure 3. Time course and topology of human Duchenne primary myoblasts cultured onto glass and patterned hydrogel. (A–E) On glass, Duchenne myoblasts adhere without a preferential direction and myotubes formation start when they reach confluence. (F–J) On patterned PAh, Duchenne myoblast adhesion is guided since the first hour after seeding. After 48 h they reach confluence inside the patterned lanes and start fusing. In some cases, the topological alignment of myoblasts induced the spontaneous fusion into myotubes as soon as 72 h after (inset in I). (E, J) Desmin immunostaining and nuclear counterstaining with DAPI. (K, L) Topological control over myotubes orientation. Polar graphs representing the percentage of myotubes falling into the same tangent values onto not patterned glass (K) and patterned hydrogel (L).

Figure 4 (next page). Sarcomere organization on human dystrophic myotubes and optimum PAh elastic modulus for sarcomere formation. (A) Immunostaining of myosin heavy chain II (green) and a-actinin (red) on dystrophic myotubes formed after 7 days of culture on PAh (EE15 kPa). Myotubes on glass did not show a structured cytoplasmic staining of these sarcomeric proteins; while myotubes cultured on hydrogel showed a defined sarcomeric organization of myosin and a-actinin. Nuclei are counterstained with DAPI. Z-stack analyses of myotubes cultured on PAh highlight the myofibrillar organization of the sarcomeric proteins, the distance between contiguous z-disk and A band is 2.5 mm, consistent with literature data of physiological sarcomere length. (B) Desmin (red) and myosin heavy chain II (green) immunostaining of myotubes cultured on glass. Nuclei are counterstained with DAPI. (C) Three-dimensional analysis of DAPI and myosin staining. (D) The graphs on the left report the percentage of striated myotubes obtained on fibronectin (FN), laminin (LN) and matrigels (Mt) over the culture time. The graph on the right reports the percentage of striated myotubes as a function of the PAh stiffness after 7 days of culture. The average fusion indexes were 23%, 23%, 13% and 14% onto hydrogel with E respectively 12 kPa, 15 kPa, 18 kPa and 21 kPa. Sarcomeric striations exhibited a strong dependency on the substrate's elastic modulus. The percentage of total cells (n >10 for each sample) exhibiting actin-myosin striation showed an optimum hydrogel modulus of E ≈ 15 kPa, regardless of the adhesion protein used.

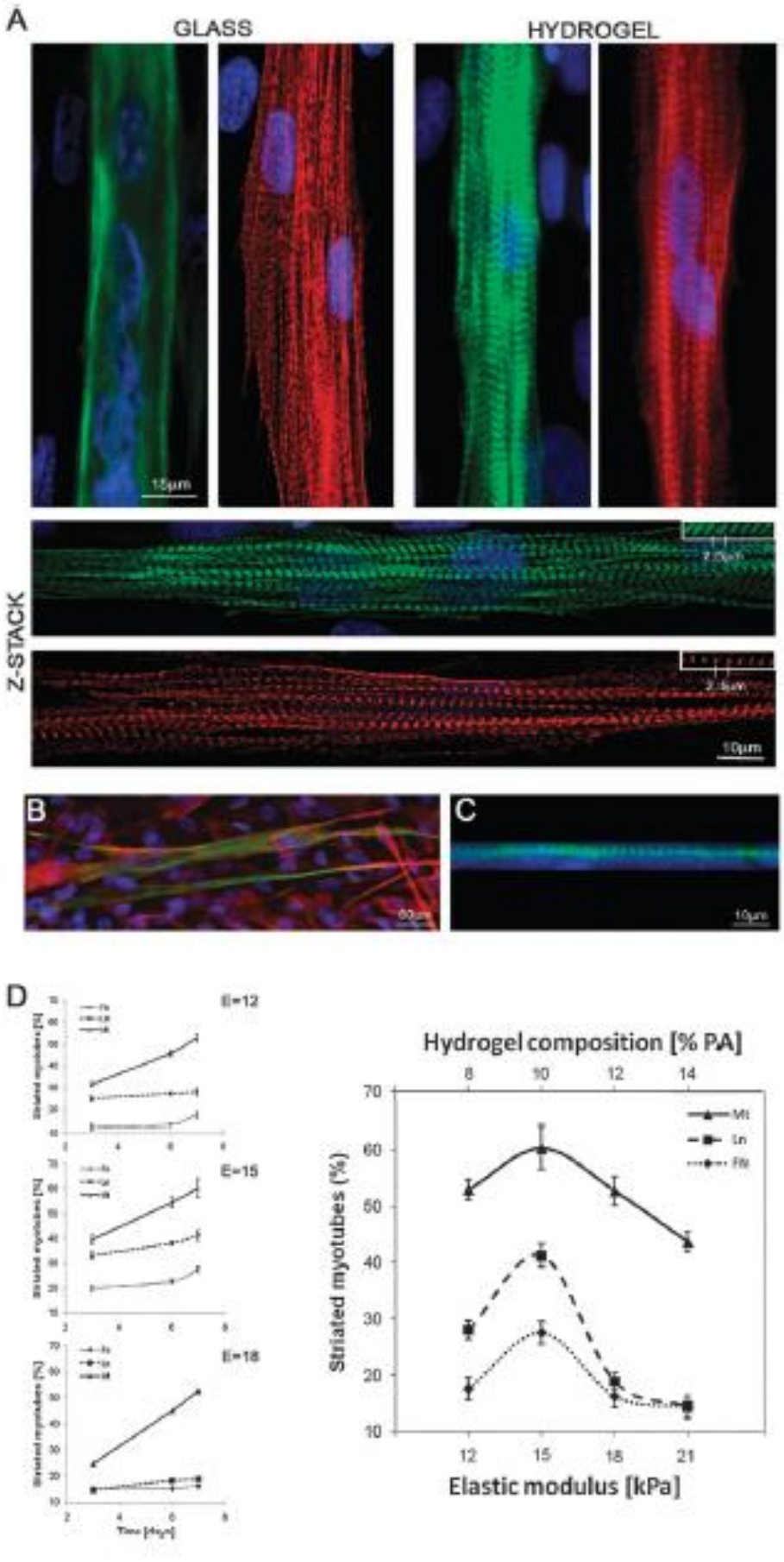
A
GLASS
HYDROGEL
15µm
Z-STACK
10µm
B
C
D
E=12
E=15
E=18
Hydrogel composition [% PA]
8
10
12
14
Striated myotubes (%)
70
60
50
40
30
20
10
Mt
Ln
Fb
12
15
18
21
Elastic modulus [kPa]

These hydrogel properties could strongly affect β1 integrin–ECM proteins interactions and consequently integrin mobility and arrangement on cell membrane. This latter aspect could strongly facilitate the integrin reorganization in the periodic and ordered structure required for the proper sarcomere assembly. In addition, it is worth underlining that our results did not show any significant difference in sarcomeric formation between dystrophic and healthy myotubes. These results were expected, since dystrophin does not seem to be involved in myofibrillogenesis, but in myotubes membrane maintenance and signaling in mature myofiber.[28] It has been recently demonstrated that dystrophin is a microtubule (MT)- associated protein that stabilizes costameric MTs and functions as a costameric cytolinker in skeletal muscle.[29]

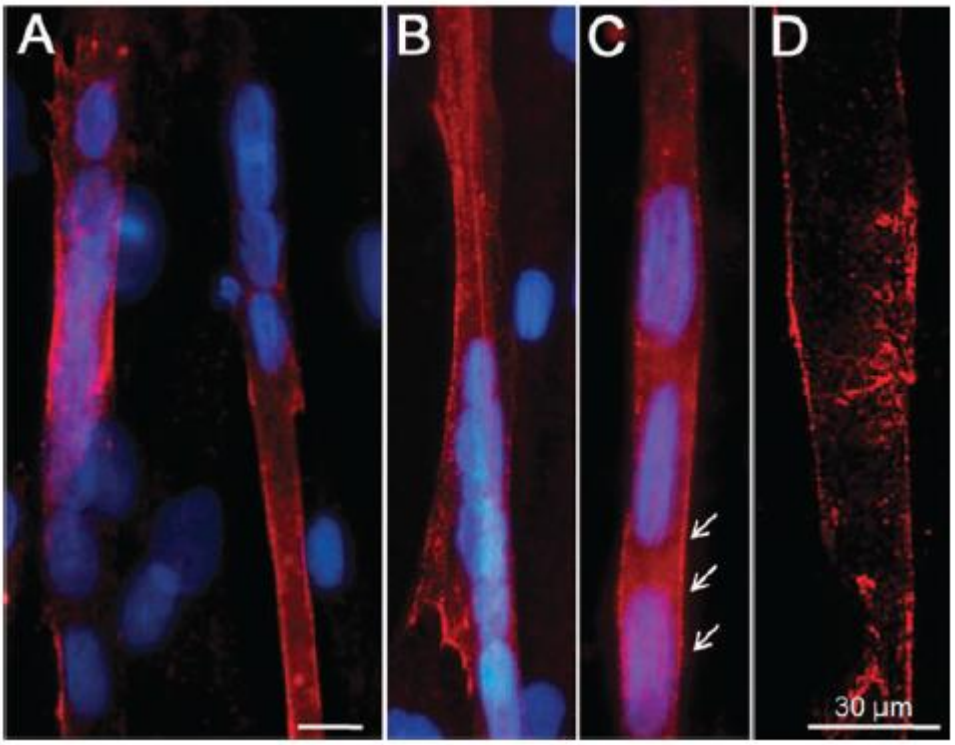

Figure 5. Dystrophin expression on myotubes from healthy donors. After 11 days of culture on PA hydrogel (E ≈ 15 kPa), dystrophin expression is observed. Nuclei are counterstained with DAPI. Dystrophin expression occurs partially (A) or along the entire myotube (B). Higher magnification (C, arrows) and confocal microscope image (D) show that dystrophin is expressed on the myotube membrane. Scale bar = 30 µm.

3.3 The engineered substrate induced high level expression of dystrophin in human healthy myotubes

In order to further investigate whether the proposed method is suitable for obtaining a valuable *in vitro* model, we verified if the differentiation process was pushed at a stage where the target of DMD pathology could be properly expressed, *i.e.*, showing a remarkable and correct dystrophin expression. Dystrophin restoration in myofibers is the objective of most experimental strategies addressed to its potential treatment, by pharmacological-, gene-, and cell-based approaches.[30] Thus, having human myotubes expressing dystrophin *in vitro* is the first and fundamental prerequisite for the fast investigation of the feasibility and efficacy of innovative therapies.[31,32]

We verified that myotubes formed from healthy donors' myoblasts on PAh (E ≈ 15 kPa) and matrigels showed a defined expression of dystrophin after 11 days of culture (Fig. 5). The analysis with a

confocal microscope revealed a specific dystrophin expression localized on the myotube membrane (Fig. 5D).

4. Conclusions

Together, our data demonstrate that human myoblasts fusion into functional myotubes can be improved by the topological organization of myoblasts in aligned and parallel lanes combined with a substrate with physiological mechanical properties and the use of an adequate adhesion protein.

The optimized substrate properties and adhesion cues allowed to obtain myotubes showing functional sarcomeric organization and encoding for a specific genetic disease. It is worth underlining that our methodology opens the perspective of testing *in vitro* the feasibility of different therapeutic strategies, such as cell- or gene-therapy, in which the dystrophin restoration is a major target. In addition, the methodology used for obtaining human myotubes fully matches the requirements of an *in vitro* model for therapeutic strategies screening: it is cheap and microscaled, rapid and easy, high-throughput, and representative of the human physiology and physiopathology.

Acknowledgements

This work was supported by TELETHON (grant n. GGP08140); Programma Operativo F.S.E. Asse ‘‘Capitale Umano’’; the Italian Ministry of University and Research (MIUR); Fondazione CARIPARO and Regione Veneto ‘‘Azione Biotech’’. We gratefully acknowledge Dr Ing. Pietro Italiano and Siltronic for gifting silicon wafers.

References

1. G. Cossu and M. Sampaolesi, Trends Mol. Med., 2007, 13, 520–526.
2. L. G. Griffith and M. A. Swartz, Nat. Rev. Mol. Cell Biol., 2006, 7, 211–224.
3. A. Dellavalle, M. Sampaolesi, R. Tonlorenzi, E. Tagliafico, B. Sacchetti, L. Perani, A. Innocenzi, B. G. Galvez, G. Messina, R. Morosetti, S. Li, M. Belicchi, G. Peretti, J. S. Chamberlain, W. E. Wright, Y. Torrente, S. Ferrari, P. Bianco and G. Cossu, Nat. Cell Biol., 2007, 9, 255–267.
4. E. P. Hoffman, R. H. Brown and L. M. Kunkel, Cell, 1987, 51, 919–928.
5. A. E. Emery, Lancet, 2002, 359, 687–695.
6. R. Bassel-Duby and E. N. Olson, Annu. Rev. Biochem., 2006, 75, 19–37.
7. X. Shi and D. J. Garry, Genes Dev., 2006, 20, 1692–1708.
8. A. Sacco, R. Doyonnas, P. Kraft, S. Vitorovic and H. M. Blau, Nature, 2008, 456, 502–506.
9. S. Kuang, M. A. Gillespie and M. A. Rudnicki, Cell Stem Cell, 2008, 2, 22–31.
10. S. Levenberg, J. Rouwkema and M. Macdonald, Nat. Biotechnol., 2005, 23, 879–884.
11. A. M. Smits, P. v. Vliet, C. H. Metz, T. Korfage, J. P. Sluijter, P. A. Doevendans and M. J. Goumans, Nat. Protoc., 2009, 4, 232–243.
12. J. Jensen, J. Hyllner and P. Bjo¨ rquist, J. Cell. Physiol., 2009, 219, 513–519.
13. C. W. Pouton and J. M. Haynes, Nat. Rev. Drug Discovery, 2007, 6, 605–616.
14. D. Eberli, S. Soker, A. Atala and J. J. Yoo, Methods, 2009, 47, 98–103.

15. J. S. Choi, S. J. Lee, G. J. Christ, A. Atala and J. J. Yoo, Biomaterials, 2008, 29, 2899–2906.

16. S. A. Riboldi, M. Sampaolesi, P. Neuenschwander, G. Cossu and S. Mantero, Biomaterials, 2005, 26, 4606–4615.

17. S. P. B. Charge` and M. A. Rudnicki, Physiol. Rev., 2004, 84, 209–238.

18. D. E. Discher, D. J. Mooney and P. W. Zandstra, Science, 2009, 324, 1673–1677.

19. A. J. Engler, S. Sen, H. L. Sweeney and D. E. Discher, Cell, 2006, 126, 677–689.

20. A. J. Engler, M. A. Griffin, S. Sen, C. G. Bonnetnann, H. L. Sweeney and D. E. Discher, J. Cell Biol., 2004, 166, 877–887.

21. M. J. Wakelam, Biochem. J., 1985, 228, 1–12.

22. E. Cimetta, S. Pizzato, S. Bollini, E. Serena, P. De Coppi and N. Elvassore, Biomed. Microdevices, 2009, 11, 389–400.

23. J. C. Sparrow and F. Schock, Nat. Rev. Mol. Cell Biol., 2009, 10, 293–298.

24. J. W. Sanger, S. Kang, C. C. Siebrands, N. Freeman, A. Du, J. Wang, A. L. Stout and J. M. Sanger, J. Muscle Res. Cell Motil.,2005, 26, 343–354.

25. M. Schwander, M. Leu, M. Stumm, O. M. Dorchies, U. T. Ruegg, J. Schittny and U. Mu¨ ller, Dev. Cell, 2003, 4, 673–685.

26. S. Carroll, S. Lu, A. H. Herrera and R. Horowits, J. Cell Sci., 2004, 117, 105–112.

27. K. Jani and F. Schock, J. Cell Biol., 2007, 179, 1583–1597.

28. D. S. Bredt, Nat. Cell Biol., 1999, 1, E89–E91.

29. K. W. Prins, J. L. Humston, A. Mehta, V. Tate, E. Ralston and J. M. Ervasti, J. Cell Biol., 2009, 186, 363–369.

30. J. V. Chakkalakal, J. Thompson, R. J. Parks and B. J. Jasmin, FASEB J., 2005, 19, 880–891.

31. N. M. Vieira, V. Brandalise, E. Zucconi, T. Jazedje, M. Secco, V. A. Nunes, B. E. Strauss, M. Vainzof and M. Zatz, Biol. Cell,2008, 100, 231–241.

32. G. McClorey, H. M. Moulton, P. L. Iversen, S. Fletcher and S. D. Wilton, Gene Ther., 2006, 13, 1373–1381.

APPENDIX C:
Micro-arrayed human embryonic stem cells-derived cardiomyocytes for *in vitro* functional assay

Elena Serena[1,2], Elisa Cimetta[1], Susi Zatti[1,2], Tania Zaglia[2], Zagallo Monica[1,2], Keller Gordon[2] and Nicola Elvassore[*,1,2]

[1]Dipartimento di Principi e Impianti di Ingegneria Chimica DIPIC, University of Padova, Padova, Italy.[2]Venetian Institute of
[2]Venetian Institute of Molecular Medicine, Padova, Italy
[*]Corresponding author Tel.: +39 049 827 5469. Fax: +39 049 827 5461. E-mail address: nicola.elvassore@unipd.it

Submitted

INTRODUCTION

The heart is one of the least regenerative organs in the body[1] and any major insult, due to ischemia, viral infection or other pathologies, can result in a significant loss of heart cells and the progression towards irreversible heart failure. The search for new therapeutic paradigms has become imperative[2] and several lines of research have been investigated[3,4,5]. In this context, the development of an *in vitro*-based cardiac tissue could be of paramount importance for many aspects of cardiology research, mainly because of the rapidity of performance, the ease of use and the lower cost of *in vitro* studies compared to *in vivo* ones.

In order to be effective, the new generation *in vitro* assays must overcome some important limitations of actual screening systems, which are mainly based on cytotoxicity measurements of cardiomyocytes randomly plated on a protein coated plastic surface[6]. In particular, new assays should: (*i*) provide information directly related to human cardiac biology and physiology; (*ii*) be highthroughput for fast and low cost screening, (*iii*) integrate a technology able to reproduce defined physio-pathological conditions or precise dosage of drugs; (iv) be user friendly.

Several *in vitro* heart models based on artificially engineered cardiac tissue have been proposed, both at the micro- and macro-scale[7,8,9,10,11,12,13,14]. Despite the originality of these works, they all test animal derived cardiomyocytes and only few *in vitro* cardiac models were developed based on human embryonic stem cell-derived cardiomyocytes (hCMs) [15,16,17,18]. However, all human models were developed at the macro-scale and they all require a high number of cardiomyocytes per construct (4×105 cells minimum). The micro-scale lab on a chip approach would be extremely useful, in addition to the well known advantages of down-scaling[19], reducing the number of hCMs needed, increasing the number of samples per batch and enhancing the high troughputness of the developed model.

While an animal cell source is very useful, for example during the troubleshooting phase in the development pipeline of a technological device or for basic science research on conserved patho-physiological cardiac mechanisms, the use of hCMs is irreplaceable in sight of a clinical application of the developed device or for specific studies on mechanisms involved in human pathologies. Human and animal cardiology can be quite different, both at the physiological and at the cellular level[20], and such differences can be the cause of withdrawal from the market of several approved drugs. Again, the development of a new therapeutic strategy for cardiac cell therapy or the analysis of a pathological environment (e.g.: inflammation developed by heart failure) on cardiomyocytes should be tested and investigated using hCMs, since these are the type of cells that would be effectively injected in the patient and used in the clinical practice.

In this scenario, the lab on a chip approach and the use of human samples emerge as the milestones to produce new generation and effective cardiac human *in vitro* models, which would be fairly representative of the human biology and physiology.

In this report, we developed, for the first time to our knowledge, an *in vitro* assay based on hCMs and micro-technologies suitable for several applications: from pharmacological analysis to physio-phatological studies on transplantable hCMs. Our model combines hCMs and micro-scale technologies, adapted to such a sensitive and variable cell source, in order to obtain a multiparametric functional assay for multipurpose testing on hCMs under well defined experimental conditions. The multiparametric functional assay was designed coupling micro-technology and stem cell engineering to achieve the following features: i) 400 parallel independent experimental replicates through hCMs micropatterning in array of circular dots (300 µm in diameter) with a consistent and repeatable number of hCMs; ii) elastic substrate with physiological stiffness, able to support hCMs contractions; iii) electrophysiological stimulation assisting the online morphometric analysis of hCMs contractions. We demonstrated that the developed human cardiac assay show functional properties responsive to cardiac drugs and physio-pathological stimuli. In addition, we gave a proof of concept that it can be used to investigate the effects of a pathological environment on hCMs potentially used in clinics, demonstrating that, besides viability and cytotoxicity, physio-toxicity tests should also be included.

RESULTS AND DISCUSSION

Micropatterned hCMs array characterization

hCMs were obtained from the human embryonic stem cell line HES2, following the protocol described by Yang and colleagues[21]. The hCMs characterization, at the end of the differentiation protocol, has been previously reported by the same group. Recently, the mechanical environment of cell culture has captured increasing interest among researchers, especially in the field of stem cell expansion and differentiation[22]. It has been demonstrated that the development of sarcomeric structures of human striated muscles[23] and the contractile functionality of chicken cardiomyocytes[24] are influenced by the substrate stiffness. For these reasons, we did not culture hCMs onto standard rigid Petri dishes or glass coverslips, but on a soft polyacrilamyde (PA) hydrogel (elastic modulus: 15kPa). The micropatterned hydrogel substrates, specifically tailored for contracting muscle cells, were designed and developed in accordance with our previous work.[23,25] (Fig. 1, A). After EB disgregation and cell seeding onto the microstructured hydrogel, the culture resulted in a 20×20 array of cellularized circular spots (Fig 1, D) defined with micrometric precision (Fig. 1, C-E). The

percentage of cardiomyocytes per spot was high, around 90% (based on the percentage of cardiac Troponin T positive cells), with a fair distribution on the entire array (Fig. 1, F-G).

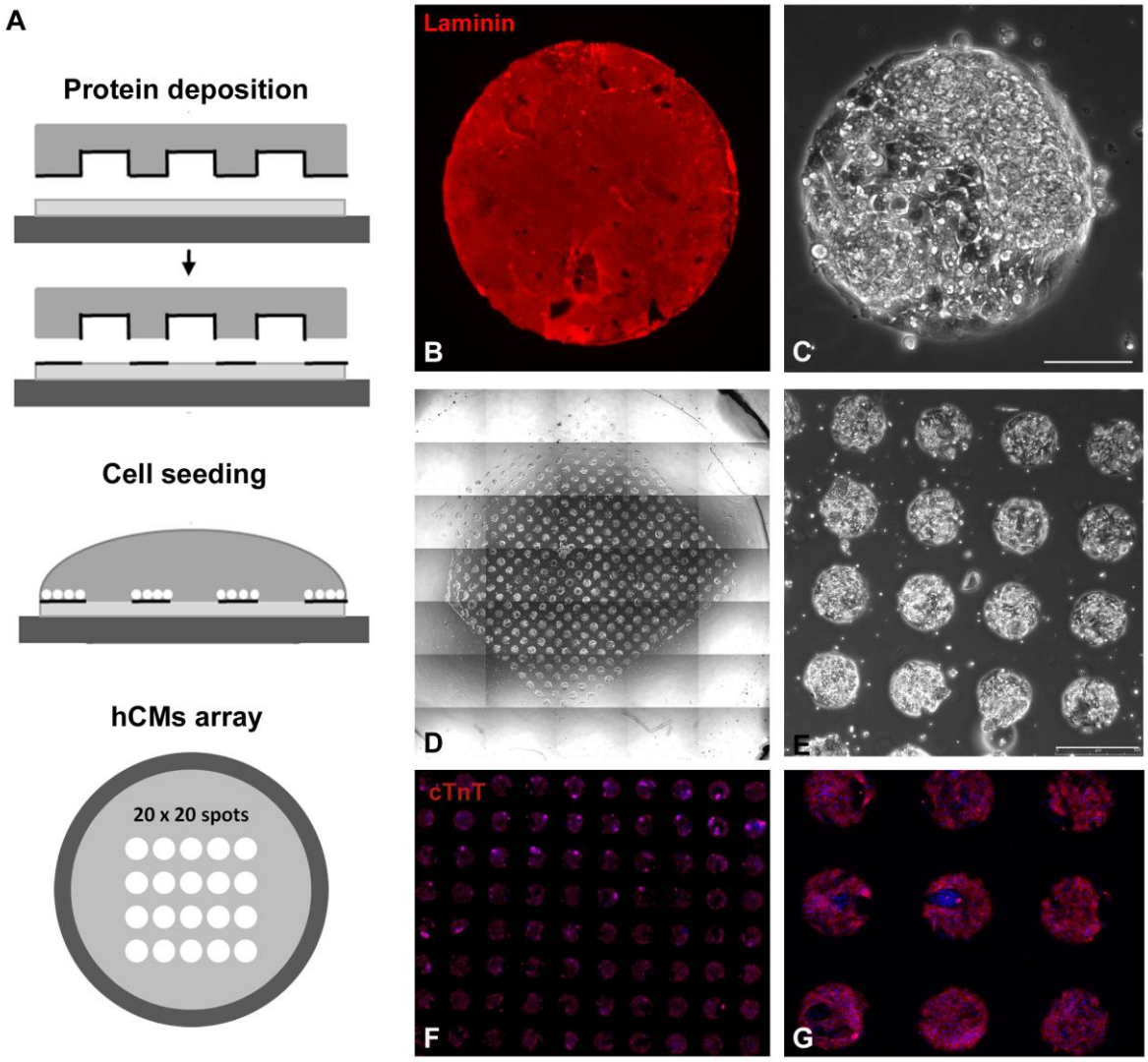

Figure 1. Microstructured hCMS culture. A: schematic representation of hydrogel micropatterning and hCMs seeding, B: laminin immunofluorescence of a micropatterned spot, C-E: microstructured hCMs culture, F-G: cTnT immunofluorescence of the hCMs culture, nuclei were counterstained with hoechst. 209x189mm (300 x 300 DPI)

The expression of cardiac Troponin T (cTnT) was maintained for several days (up to 7 days). We will thus refer to this culture as hCMs. The maintenance of cardiac markers on micropatterned cells was verified after 5-7 days of culture onto the hydrogel (Fig. 2A). cTnT, Cx43, α-actinin and Nkx2.5 were analyzed. At this time point, spontaneous and electrically induced contractions were observed (Supplementary material, Movie1).

We did not underestimate the fact that hESC-derived cardiomyocytes are not fully representative of adult cardiomyocytes: the differentiation stage of hCMs is a crucial point, with the aim of developing an *in vitro* model of human cardiac tissue. Therefore, it is worth underlining that we observed the expression of adult isoforms of cardiac Troponin I and T (Fig. 2B) in our hCMs, derived from EBs older than 25 days and cultured onto micropatterned hydrogel for at least 6 days.

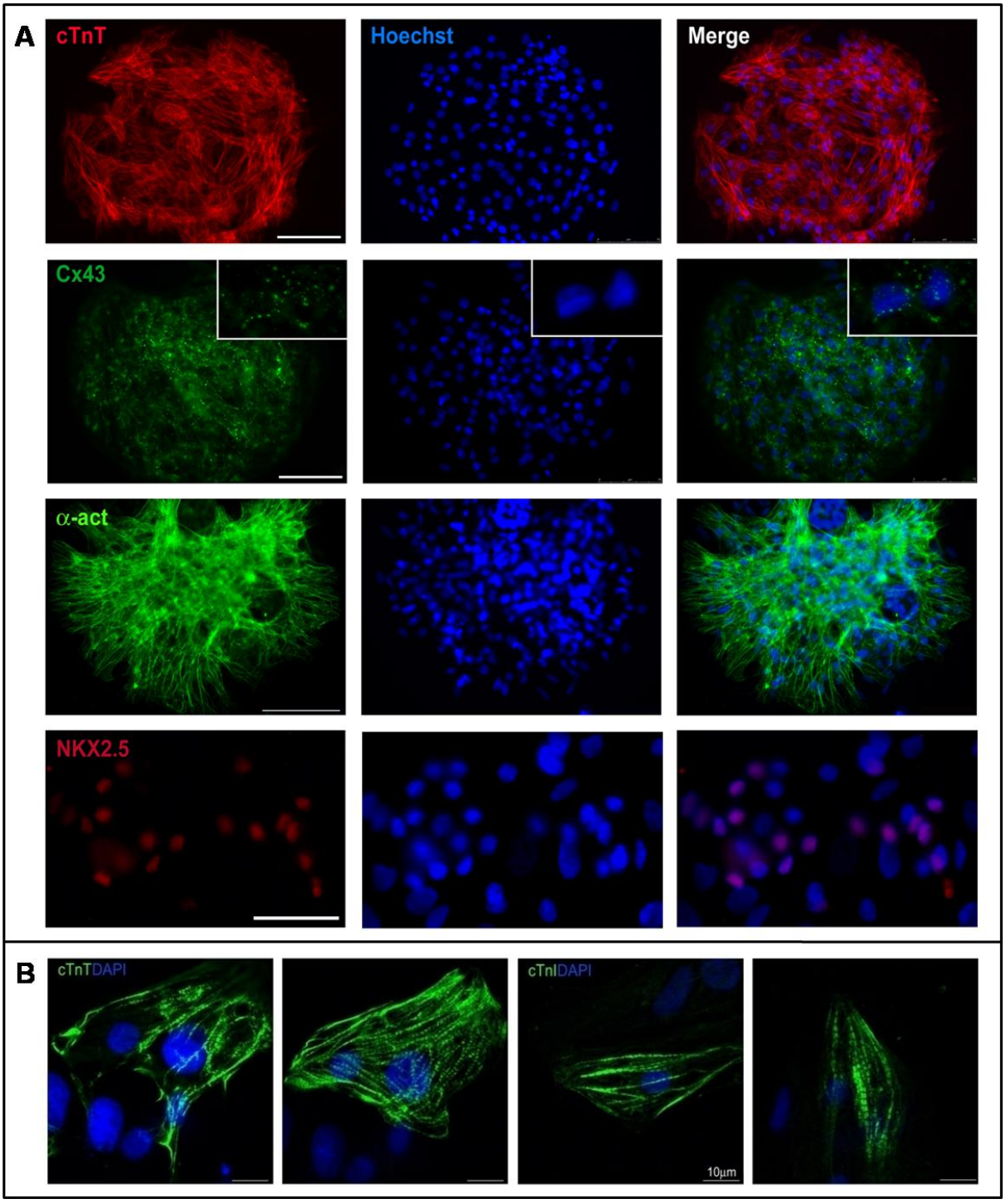

Figure 2. Characterization of microstructured hCMS culture. Cardiac markers immunofluorescence. A: cTnT, B: connexin 43, C: α-actinin, D: NKX2.5. Nuclei were counterstained with hoechst. B: Immunofluorescence against and adult isoform of cardiac Troponin I and adult/fetal isoform of cardiac Troponin T, nuclei were counterstained with hoechst. 198x235mm (150 x 150 DPI)

Although cardiac markers expression and contractions were verified and monitored in the developed array (for instance Connexin 43), we investigated the cell-cell coupling, with the goal of obtaining a higher-hierarchy functional tissue, rather than clusters of single scarcely communicating cardiac cells. Thus, gap-FRAP experiments have been performed to test the functionality of hCMs gap junctions[26] (Supplementary material, Figure 1). Confocal microscopy allowed the recording of the target cell's fluorescence recovery on a single plan before and after the photobleaching by scanning

argon laser beam (Supplementary material, Figure 1). Fluorescence recovery (Supplementary material, Figure 1 C) is related to dye transport across gap junction. Table 1 reports the fitting parameters, k and A, of the fitting recovery curves. Results of the fitting showed the presence of functional gap junctions in hCMs. The percentage of recovery for control cells was about 5 times smaller than the percentage calculated for hCMs, indicating that cultured hCMs have gap functionality and therefore proves their functional interconnection within the patterned spot.

Cell type	K [l/min]	A
hCMs	0.34 ± 0.11	24.3 ± 5.5%
control	/	5.5 ± 0.6%

In order to further optimize the developed hCMs array, we investigated the optimal substrate stiffness for hCMs culture. In particular, it has been reported that chicken cardiomyocytes contraction is inhibited when cultured onto a substrate whose stiffness ranges from 35 to 70 kPa. Such a range of substrate elasticity is representative of the non-contractile fibrotic tissue formed after a myocardial infarction, while a normal myocardium has an elastic modulus of E ≈ 10 kPa[24]. The elastic modulus of the PA hydrogel was easily tuned by varying the composition of the pre- polymer solution, as previously reported[23]. hCMs microstructured cultures were performed on a 20% PA hydrogel with E ≈ 35 kPa, in order to mimic the fibrotic tissue. After 7 days of culture we evaluated hCMs viability (live and dead assay) and contractility (Supplementary material, Figure 2). We didn't observe any significant difference between hCMs cultured on 15 kPa and 35 kPa hydrogels, in terms of viability (data not shown), functional properties (Supplementary material, Figure 2, A and C) and sarcomeric organization of cTnT (Supplementary material, Figure 2, B and D). This is likely due to the multilayer cellular growth of hCMs over the hydrogel, which hampered the substrate stiffness effects. Therefore, we proceeded by using 15 kPa hydrogels.

Usually, *in vitro* studies involving hCMs use clusters of cardiomyocyte derived by the dissection of the EB's contracting area or by co-culture with other cell types[27,28]. Our work developed a microstructured array of hCMs (20×20 spots, with a high number of hCMs per spot) because each microstructured hCMs spot could represent an independent sample deriving from the same batch of cells. Consequently, the array offers the possibility of analyzing different spots at the same time, exposed to identical conditions, with a consistent/repeatable number of hCMs per spot. The developed *in vitro* model could thus give a high number of output information per experiment and reduce the high variability usually observed when working with a primary human cell source[29].

Morphometric analysis of hCMs array

Once the cardiac phenotype of the hCMs micropatterned onto the soft substrate had been verified, we moved our investigations to the biophysical properties of these cells. We observed that the spontaneous contractile activity of arrayed hCMs was synchronous intra each spot, additional proof of functional cell-cell interactions, while the contractions become non- synchronous inter-spots. We therefore decided to couple exogenous electrical stimulation in order to verify hCMs capability to respond to external stimuli (E-C coupling) and for synchronizing the contractions of the spots (evaluating the maximum contraction frequency). The applied voltage ranged from 1 to 6.8 V/cm with a frequency ranging from 1 to 4Hz and a duration of 5 ms. We developed a "morphometric analyses" methodology based on the following steps: a) recording of hCMs contractions, b) analysis

of the hCMs displacements from the obtained movies, c) representation of the rate of displacements in a 2D graph, d) calculation of the contraction frequency (see Materials and Methods). Micropatterned hCMs showed some spontaneous beating (Fig. 3A), and they were induced to contract with exogenous electrical stimulation (Fig. 3B). We were able to monitor hCMs contractions and calculate their frequency (Fig. 3) with high accuracy. The robustness of the developed methodology is shown in figures 3B and C. Figure 3B shows the contraction traces obtained with an off-on-off sequence of electrical stimulation: 0V/cm; 6 V/cm at 2Hz for 4.5 s; 0 V/cm (dashed line). Spontaneous contractions are not present in the absence of the electrical field, while during electrical stimulation hCMs are induced to contract and paced to a frequency of 2 Hz. Similarly, figure 3C shows a contraction-graph of spontaneously contracting hCMs. The applied stimulation, 6 V/cm and 1 Hz frequency, stops after 5 s. The obtained graph (Fig. 3C) clearly shows that hCMs are paced during the application of an exogenous electrical stimulation (from 1 to 5 s their contraction frequency is 1 Hz), while after the stimulation they return to a spontaneous contraction frequency of 0.6 Hz.

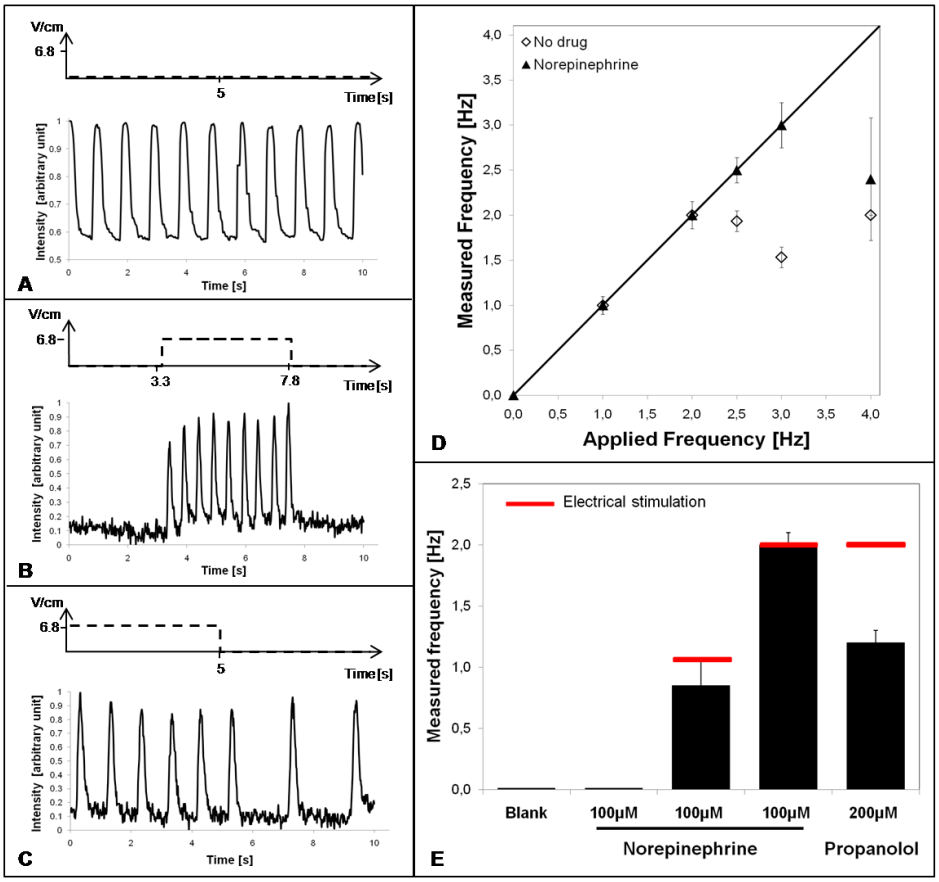

Figure 3. Experimental validation of morphometric analysis. In graphs A-C, the dashed line represents the applied exogenous electrical stimulation, the solid line shows the contractions/displacement of hCMs. A: morphometric analysis of spontaneous contractions, B: morphometric analysis of hCMs induced to contract with electrical stimulation, C: morphometric analysis of spontaneously contracting hCMs captured by exogenous electrical stimulation. Graphs D-E validate the experimental procedure with norepinephrine and propranolol. D: morphometric analysis of microstructured hCMs culture treated with culture medium (No drug) and 100 ,M norepinephrine. E: contraction frequency of control hCMs (blank) and hCMs exposed to norepinephrine and propranolol. Red squares represent the frequency of the applied electrical stimulation. 211x191mm (150 x 150 DPI)

The morphometric analysis has been developed based on a methodology widely accepted by researchers in this field: imaging analyses of contracting areas. For instance, studying contracting cells or tissues by video recording and digitalizing of the captured images has been applied for contractions of both three-dimensional tissue constructs[11,30,31,32,33] and two-dimensional cell culture[34,35,36]. We improved the analysis through the use of micropatterning: each hCMs spot has clear and defined edges, and so contracting cardiomyocytes are detected and analyzed with higher accuracy.

Application of the in vitro assay: pharmacological assay

To further support the robustness of our methodology and to give evidence of its applicability, we investigated the capability of detecting the chronotropic effects of the β-adrenergic agonist norepinephrine (Fig. 3D) and the β-AR antagonist propranolol (Fig. 3D, E). hCMs stimulation with norepinephrine led to an increase in the frequency of hCMs capturing with electrical stimulation. The maximum capturing frequency for hCMs with control medium was 2 Hz, while the addition of 100 µM norepinephrine increased the capturing frequency to 3 Hz (Fig. 3D). On the contrary, treatment with 200 µM propranolol inhibited the norepinephrine action and lowered the contraction frequency to 1 Hz, even during a 2 Hz electrical stimulation (Fig. 3E).

These results are an experimental validation of the methodology used, but at the same time they indicate that the cultured hCMs express β-receptors and they are a proof of concept of one of the possible applications of our model, pharmacological studies.

Application of the in vitro model: pathological conditions assay

In view of giving a proof of concept that our system could be used as an *in vitro* model for testing the effects of a pathological environment on the functional properties of transplantable human cardiomyocytes, we exposed hCMs to hydrogen peroxide (H_2O_2) to mimic the oxidative stress implicated in various disease states. In fact, reactive oxygen species are generated during both ischemia and reperfusion phases[37] and the inflammatory environment of a healing infarct could present high levels of oxygen-free radicals[38]. We thus exposed micropatterned hCMs to increasing levels of H2O2 (0, 0.01 and 0.1 mM) for 1 and 16 hours, in accordance with other studies[39]. hCMs viability and functional properties were analyzed. We observed that hCMs viability after 1 and 16 hours was not affected by any of the H_2O_2 concentrations tested (Fig. 4A). The percentage of dead cells (Live and Dead test) were (4.5 ± 1) % in control, (3 ± 1) % in samples treated with 0,01 mM H_2O_2 and (3.5 ± 1) % in hCMs treated with 0.1 mM H2O2. Positive control of hydrogen peroxide citotoxicity was performed using 0.5 mM H_2O_2 solution, showing 100% of dead hCMs (data not shown). Interestingly the contractility and E-C coupling capability were maintained for all conditions, after short time exposition (1 hour). On the other hand, the highest concentration of H_2O_2 (0.1 mM) applied for 16 hours (Fig. 4B) suppressed the functional properties of hCMs (contractility). This result suggests that a low level of oxidative stress is ineffective for hCMs viability, while it could indeed compromise their functionality. This experimental observation was confirmed with an average of 50 individual spots and 3 independent analyses. The results obtained with hCMs are in accordance with recent data reported for murine skeletal muscles and rat cardiomyocytes. In particular, rat cardiomyocytes exposed to 0.2 mM H_2O_2 start showing modifications in the calcium handling as soon as 90s after treatment.

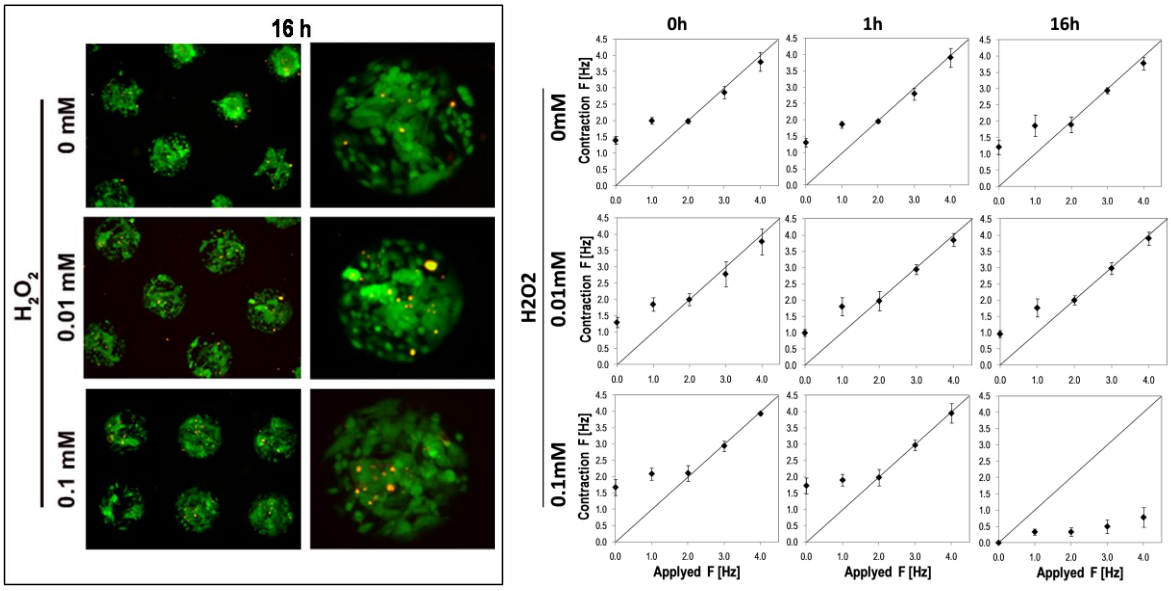

Figure 4 (A) Effects of oxidative stress on hCMs. A: live and dead analysis after 16 hours of exposure to 0 mM, 0.01 mM and 0.1 mM H_2O_2. 111x129mm (150 x 150 DPI). (B) **(B)** Effects of oxidative stress on hCMs. B: mophometric analisis of hCMs exposed to 0 mM, 0.01 mM and 0.1 mM H_2O_2 for 0, 1 and 16 hours. 1214x1050mm (96 x 96 DPI).

As recently suggested[40,41], the suppression of hCMs contractility after H_2O_2 treatment, observed in this work, could derive from the interaction between reactive oxygen species (ROS) and Ca^{2+} handling machinery and myofibrils. Indentifying the targets of ROS is not straightforward, although the *in vitro* arrayed hCMs and morphometric analysis developed in this study could be a good complementary tool. In fact, it is well know that the *in vivo* environment encountered after injection is a hostile niche that compromise cell viability and functional engraftment. What is still unclear is why the surviving injected cells do not integrate or have a poor functional integration with the host tissue. Several hypotheses have been formulated such as anoikis, mitochondrial death and also induction of apoptotic pathways[1]. In this scenario, our assay could potentially be used to investigate *in vitro* the best preconditioning strategy or pro-survival factors, which can increase the number of surviving and integrating hCMs after transplantation1 into a diseased heart.

Taken together, the results clearly indicate that an *in vitro* test merely based on cell toxicity could give misleading outcomes, especially in the case of cardiac drug or therapy development. Such a physiotoxicity test, analyzing physiology in parallel to cytotoxicity, is thus required in order to have a complete and reliable set of data.

EXPERIMENTAL METHODS

Human cardiomyocytes derivation and culture

Human cardiomyocytes (hCMs) were derived from HES2 cell line as previously described by Yang et al[21]. Briefly, HES2 colonies were detached from a matrigel coated dish with collagenase IV (Invitrogen) and trypsin (Invitrogen) and transferred to low adhesive dishes for the EB formation in aggregation medium: basal medium additioned with 10ng/mL BMP4 (R&D system). From day 1 to day 4 EB were cultured in stage I medium: basal medium (see supplementary materials) with 10ng/mL BMP4, 5ng/mL βFGF (R&D system) and 6ng/mL Activin A (R&D system). EB were then cultured in stage II medium, day 4 to day 8, consisting of basal medium and 10ng/mL VEGF (R&D

system) and 150ng/mL DKK (R&D system). Finally, from day 8 to day 14, the culture medium consisted of basal medium and 10ng/mL VEGF and 5ng/mL βFGF. Cultures were maintained in a 5% CO_2, 5% O_2, 90% N2 environment for the first 14 days and then transferred into a 5% CO_2 air environment.

Hydrogel production and protein micropatterning

Polyacrilammide hydrogel and the micropatterning of adhesion proteins were prepared as previously described[23,25]. See supplementary materials for details.

hCMs microstructured culture

Fully differentiated EBs, ranging from 27 to 39 days old, were dissociated to single cells in order to obtain the microstructured hCMs array. EBs were treated with 0.2% Collagenase Type I (Invitrogen) for 45 minutes at 37°C and with trypsin for 5 minutes at 37°C. Trypsin was quenched with Stop solution (50% FCS, 50% IMDM (Invitrogen)). Gentle resuspension of the loosened EBs ensured the obtainment of a single cell suspension. 300 µL of cell suspension (2.7×105 cells/mL) was dropped over the hydrogel, previously micropatterned (Fig. 1A), and the hCMs were allowed to adhere for 5-8 hours. Cell cultures were kept at 37°C, 5% CO_2.

Immunohystochemistry

Primary antibodies were against cardiac troponin T (cTnT, clone 13-11, NeoMarkers) , α-actinin (clone 1A4, Sigma Aldrich), connexin 43 (Cx43, clone 4E6.2, Chemicon), Nkx2.5 (clone A-16, Santa Cruz Biotechnology), adult isoforms of cardiac troponin I[42] and adult/fetal isoform of cardiac Troponin T[43] (Ti1 and RVC2 respectively, kindly given by Professor Schiaffino, Padova University).

Live and Dead assay

Cell viability was evaluated with the LIVE/DEAD assay (Invitrogen). Briefly, hCMs were incubated with 150 µl of 3µM calcein and 3µM ethidium bromide in D-PBS (Gibco) for 45 minutes at room temperature. Following incubation, the cells were washed with PBS and labeled cells were observed under a fluorescence microscope.

Gap-FRAP analysis

In order to evaluate the functional interconnection between hCM, gap junction functionality was quantitatively determined in living cells by gap-FRAP assay. hMCs were loaded with calcein AM (3µM, 45min, Invitrogen), which permeates gap junction channels. FRAP was performed using a confocal laser scanning microscope (Leica), with an argon laser source at 496nm. See supplementary materials for details.

Morphometric analysis

The morphometric analysis of hCMs contractions were performed coupling the acquisition of contraction displacement by a fast acquisition camera (blue fox, Matrix Vision Gmbh) with a system for electrical stimulation of the culture[30,44,32].

The contraction frames were acquired for 5 or 10 seconds every 50ms. hCMs displacement was analyzed by fixing circular regions of interest (ROIs, 2µm diameter) and analyzing their intensity with the Image. The intensity values were then plotted in a graph showing the intensity, in arbitrary unit, versus time, seconds (Figure 4). 6 to 10 ROIs of 6-8 independent hCMs spots were analyzed for each acquired series of frames.

The electrical stimulation was applied to the hCMs array using two carbon electrodes (Ladd Research, 3 mm in diameter and 20 mm in length) placed at 10mm distance and held by a PDMS holder designed to fit a 35mm Petri dish and to keep electrodes immersed in the culture medium during the analysis. The electrodes were connected via platinum wires to a function generator (Amel, model 568) programmed to produce a square wave with a 0 V baseline and impulses ranging from 1V/cm to 6.8V/cm for 5ms with frequency ranging from 1 to 4Hz. A third platinum electrode was inserted to monitor the electrical stimulation by an oscilloscope (LeCroy, LT322). The chronotropic agents noreinephrine and propanolol (Sigma Aldrich) were added to the medium to the final concentrations of 100 and 200µM.

CONCLUSIONS

To our knowledge, we developed for the first time an *in vitro* model based on human cardiomyocytes and *ad hoc* micro-technologies for pharmacological or physio-pathological studies. The developed array of micropatterned hCMs lead us to gain repeatability and robustness, and allowed multiple analyses per batch of cells. This study demonstrates the feasibility of developing an *in vitro* based test for hCMs, able to give insight on both viability and functionality of hCMs. Secondly, we demonstrated that collecting information about the functional properties of hCMs could give a clearer scenario about possible secondary physiological effects of a pathological environment (e.g.: oxidative stress).

Importantly, this study emphasizes the importance of multiple readouts from an *in vitro* model, both in terms of the number of data acquired in parallel (array of 20×20 spots) and in terms of the type of analysis (citotoxicity and functional contractions).

ACKNOWLEDGMENTS

We thank Riello Massimo (Padova University), Giulitti Stefano (Padova University), for help with the experimental work. This work was supported by Progetti Di Eccellenza Cariparo and Fondo Sociale Europeo (grant code 2105/1/10/1268/2008).

SUPPLEMENTARY MATERIALS

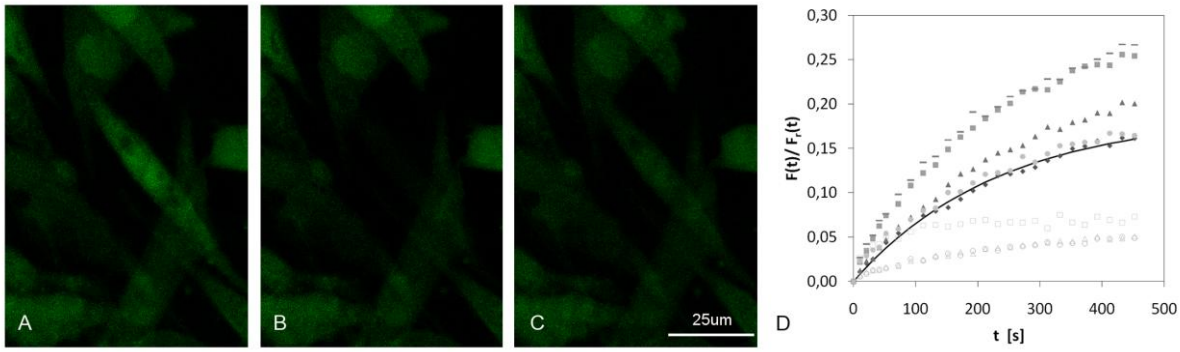

Figure S1. Gap FRAP analysis. A-C: Gap FRAP, representative images of fluorescence restoration in hCMs, target cell is indicated by an arrow, scale bar: 50 mm. A: intensity of calceine AM fluorescence before photobleaching, B: fluorescence right after photobleaching, C: fluorescence recovery after 7.5 minutes. D: graph representing the kinetic profiles of raw and fitted recovery data. 201x74mm (150 x 150 DPI)

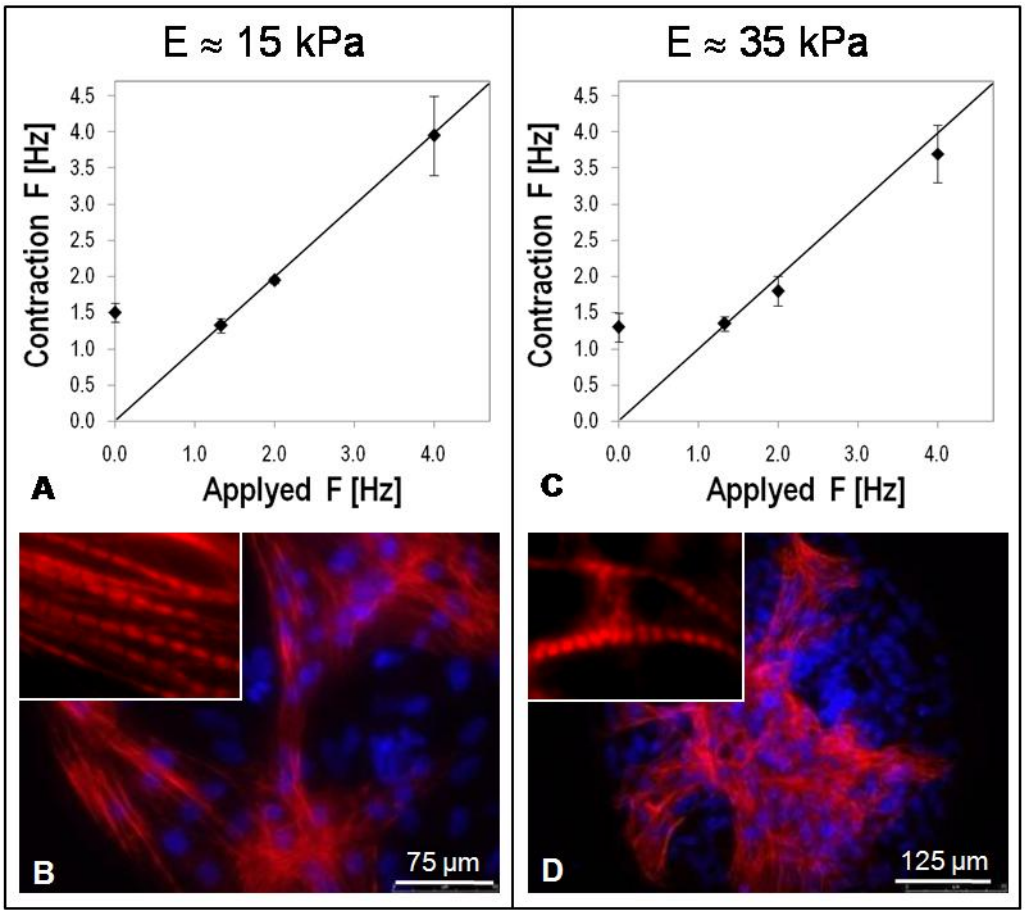

Figure S2. Effects of susbtrate stiffness on hCMs. A, B: mophometric analisis and cTnT immunofluorescence of hCMs cultured onto 15 kPa, B, D: mophometric analisis and of cTnT immunofluorescence of hCMs cultured onto a 35 kPa hydrogel. Nuclei were counterstained with hoechst. 141x138mm (150 x 150 DPI)

REFERENCES

1. Laflamme, M.A. *et al.* Cardiomyocytes derived from human embryonic stem cells in pro- survival factors enhance function of infarcted rat hearts. *Nat Biotech* 25, 1015-1024 (2007).

2. Habib, M., Caspi, O. & Gepstein, L. Human embryonic stem cells for cardiomyogenesis. *J. Mol. Cell. Cardiol.* 45, 462-474 (2008).

3. Freund, C. & Mummery, C.L. Prospects for pluripotent stem cell-derived cardiomyocytes in cardiac cell therapy and as disease models. *J. Cell. Biochem.* 107, 592-599 (2009).

4. Shin, D.D. *et al.* Review of current and investigational pharmacologic agents for acute heart failure syndromes. *Am. J. Cardiol.* 99, 4A-23A (2007).

5. Wang, F. & Guan, J. Cellular cardiomyoplasty and cardiac tissue engineering for myocardial therapy. *Adv. Drug Deliv. Rev.* 62, 784-797 (2010).

6. Möller, C. & Slack, M. Impact of new technologies for cellular screening along the drug value chain. *Drug Discov. Today* 15, 384-390 (2010).

7. Katare, R.G., Ando, M., Kakinuma, Y. & Sato, T. Engineered heart tissue: a novel tool to study the ischemic changes of the heart in vitro. *PLoS ONE* 5, e9275 (2010).

8. Hansen, A. *et al.* Development of a drug screening platform based on engineered heart tissue. *Circ. Res.* 107, 35-44 (2010).

9. Engelmayr, G.C., Jr *et al.* Accordion-like honeycombs for tissue engineering of cardiac anisotropy. *Nat Mater* 7, 1003-1010 (2008).

10. Masuda, S., Shimizu, T., Yamato, M. & Okano, T. Cell sheet engineering for heart tissue repair. *Adv. Drug Deliv. Rev.* 60, 277-285 (2008).

11. Radisic, M. *et al.* Functional assembly of engineered myocardium by electrical stimulation of cardiac myocytes cultured on scaffolds. *Proc. Natl. Acad. Sci. U.S.A.* 101, 18129-18134 (2004).

12. Song, H. *et al.* Interrogating functional integration between injected pluripotent stem cell- derived cells and surrogate cardiac tissue. *Proc. Natl. Acad. Sci. U.S.A.* 107, 3329-3334 (2010).

13. Grosberg, A., Alford, P.W., McCain, M.L. & Parker, K.K. Ensembles of engineered cardiac tissues for physiological and pharmacological study: Heart on a chip. *Lab on a Chip* (2011).doi:10.1039/c1lc20557a

14. Kim, S.B. *et al.* A cell-based biosensor for real-time detection of cardiotoxicity using lensfree imaging. *Lab Chip* 11, 1801-1807 (2011).

15. Shapira-Schweitzer, K., Habib, M., Gepstein, L. & Seliktar, D. A photopolymerizable hydrogel for 3-D culture of human embryonic stem cell-derived cardiomyocytes and rat neonatal cardiac cells. *J. Mol. Cell. Cardiol.* 46, 213-224 (2009).

16. Caspi, O. *et al.* Tissue engineering of vascularized cardiac muscle from human embryonic stem cells. *Circ. Res.* 100, 263-272 (2007).

17. Tulloch, N.L. *et al.* Growth of engineered human myocardium with mechanical loading and vascular coculture. *Circ. Res.* 109, 47-59 (2011).

18. Schaaf, S. *et al.* Human engineered heart tissue as a versatile tool in basic research and preclinical toxicology. *PLoS ONE* 6, e26397 (2011).

19. Hong, J., Edel, J.B. & deMello, A.J. Micro- and nanofluidic systems for high-throughput biological screening. *Drug Discovery Today* 14, 134-146 (2009).

20. Bers, D.M. Cardiac excitation-contraction coupling. *Nature* 415, 198-205 (2002).

21. Yang, L. *et al.* Human cardiovascular progenitor cells develop from a KDR+ embryonic-stem- cell-derived population. *Nature* 453, 524-528 (2008).

22. Engler, A.J., Sen, S., Sweeney, H.L. & Discher, D.E. Matrix elasticity directs stem cell lineage specification. *Cell* 126, 677-689 (2006).

23. Serena, E. *et al.* Soft substrates drive optimal differentiation of human healthy and dystrophic myotubes. *Integr Biol (Camb)* 2, 193-201 (2010).

24. Engler, A.J. *et al.* Embryonic cardiomyocytes beat best on a matrix with heart-like elasticity: scar-like rigidity inhibits beating. *J. Cell. Sci.* 121, 3794-3802 (2008).

25. Cimetta, E. *et al.* Production of arrays of cardiac and skeletal muscle myofibers by micropatterning techniques on a soft substrate. *Biomed Microdevices* 11, 389-400 (2009).

26. Giaume, C. *Connexin methods and protocols*. (Humana Press: 2001).

27. Braam, S.R. *et al.* Prediction of drug-induced cardiotoxicity using human embryonic stem cell- derived cardiomyocytes. *Stem Cell Res* 4, 107-116 (2010).

28. Jonsson, M.K.B. *et al.* Quantified proarrhythmic potential of selected human embryonic stem cell-derived cardiomyocytes. *Stem Cell Res* 4, 189-200 (2010).

29. Pera, M.F. & Tam, P.P.L. Extrinsic regulation of pluripotent stem cells. *Nature* 465, 713-720 (2010).

30. Tandon, N. *et al.* Electrical stimulation systems for cardiac tissue engineering. *Nat Protoc* 4, 155-173 (2009).

31. Radisic, M. *et al.* Optical mapping of impulse propagation in engineered cardiac tissue. *Tissue Eng Part A* 15, 851-860 (2009).

32. Cannizzaro, C. *et al.* Practical aspects of cardiac tissue engineering with electrical stimulation. *Methods Mol. Med.* 140, 291-307 (2007).

33. Radisic, M. *et al.* Medium perfusion enables engineering of compact and contractile cardiac tissue. *Am. J. Physiol. Heart Circ. Physiol.* 286, H507-516 (2004).

34. Dolnikov, K.*et al.* Functional properties of human embryonic stem cell-derived cardiomyocytes: intracellular Ca2+ handling and the role of sarcoplasmic reticulum in the contraction. *Stem Cells* 24, 236-245 (2006).

35. Au, H.T.H., Cheng, I., Chowdhury, M.F. & Radisic, M. Interactive effects of surface topography and pulsatile electrical field stimulation on orientation and elongation of fibroblasts and cardiomyocytes. *Biomaterials* 28, 4277-4293 (2007).

36. Heidi Au, H.T., Cui, B., Chu, Z.E., Veres, T. & Radisic, M. Cell culture chips for simultaneous application of topographical and electrical cues enhance phenotype of cardiomyocytes. *Lab Chip* 9, 564-575 (2009).

37. Vanden Hoek, T.L., Li, C., Shao, Z., Schumacker, P.T. & Becker, L.B. Significant levels of oxidants are generated by isolated cardiomyocytes during ischemia prior to reperfusion. *J. Mol. Cell. Cardiol.* 29, 2571-2583 (1997).

38. Robey, T.E., Saiget, M.K., Reinecke, H. & Murry, C.E. Systems approaches to preventing transplanted cell death in cardiac repair. *J. Mol. Cell. Cardiol.* 45, 567-581 (2008).

39. Cook, S.A., Sugden, P.H. & Clerk, A. Regulation of bcl-2 family proteins during development and in response to oxidative stress in cardiac myocytes: association with changes in mitochondrial membrane potential. *Circ. Res.* 85, 940-949 (1999).

40. Lamb, G.D. & Westerblad, H. Acute effects of reactive oxygen and nitrogen species on the contractile function of skeletal muscle. *J. Physiol. (Lond.)* 589, 2119-2127 (2011).

41. Greensmith, D.J., Eisner, D.A. & Nirmalan, M. The effects of hydrogen peroxide on intracellular calcium handling and contractility in the rat ventricular myocyte. *Cell Calcium* 48, 341-351 (2010).

42 Saggin, L., Gorza, L., Ausoni, S. & Schiaffino, S. Troponin I switching in the developing heart. *J.Biol. Chem.* 264, 16299-16302 (1989).

43. Saggin, L., Ausoni, S., Gorza, L., Sartore, S. & Schiaffino, S. Troponin T switching in the developing rat heart. *J. Biol. Chem.* 263, 18488-18492 (1988).

44. Serena, E. *et al.* Electrophysiologic stimulation improves myogenic potential of muscle precursor cells grown in a 3D collagen scaffold. *Neurol. Res.* 30, 207-214 (2008).

APPENDIX D:
Supplementary methods of chapter 3

Human primary myoblast culturing

Human primary myoblasts (both wild type and DMD) were provided by the ‘‘Telethon BioBank’’ (Telethon Research Service, Istituto Nazionale Neurologico ‘‘Carlo Besta’’, Milano, Italy). Myoblasts were expanded in proliferation medium: 60% highglucose Dulbecco’s Modified Eagle’s Medium (Glutamax, Invitrogen), 20% MediumM199 (Sigma), 20% FBS (Invitrogen), 10 ng ml/1 EGF (PeproTech), 2 ng ml/1 b-FGF (PeproTech), 10 mg ml/1 insulin (insulin from bovine pancreas, Sigma), Penicillin-Streptomycin-Glutamine (Invitrogen). Myoblasts were induced to form myotubes in differentiating medium: 98% High-Glucose DMEM, 2% horse serum (Invitrogen), 30 mg mL/1 insulin, penicillin, streptomycin and glutamine.

Murine satellite cells culturing

Four-month-old wild-type mice (strain C57BL/6J; Jackson Laboratories) mice were used. Animals were housed and surgically treated at the Animal Colony of the Centro Interdipartimentale Vallisneri, University of Padova, under the conditions specified by the relevant Italian bylaws.

Single muscle fibers were isolated from flexor digitorum brevis (FDB) and extensor digitorum longus (EDL) from 2-mo-old male wild type mice. Freshly isolated SCs were stripped off the fibers by repeated passage through a 18-gauge needle.

Human Mesoangioblasts culturing

Human mesoangioblasts derived from healthy donors were expanded in gelatin-coated dish with proliferation medium composed of MegaCell™ DMEM (Sigma-Aldrich) supplemented with 5% heat inactivated fetal bovine serum (Invitrogen), 2 mM L-Glutamine (Invitrogen), 1% non-essential aminoacids (Invitrogen), 0,1 mM β-mercaptoethanol (Invitrogen), 5 ng/ml β-FGF (PeproTech), 1% penicilin-streptomicin (Invitrogen). Mesoangioblasts were induced to differentiate into myotubes by changing proliferation medium with the same differentiating medium used for human primary myoblasts.

Lipophilic tracers

Myoblasts were resuspended in proliferation medium at a concentration of 1 x 106 cells/mL. 5µL of the tracer (Invitrogen) solution (2.5 mg/mL in dimethylsulfoxide) were added every 1 mL of cell suspension. The suspension was gently resuspended and incubated at 37°C for 10 minutes. The cells were then centrifuged at 350 g for 5 minutes and washed twice with proliferation medium in order to eliminate the traces in excess.

Co-colture experiments

The co-culture experiments were set up by mixing the two cell populations, dystrophic cells and wild type (dystrophin-positive: human primary myoblasts, murine satellite cells and human mesangioblasts) cells, in defined ratios: 1:9, 1:29, 1:89, respectively. 300 µL of cell suspension (1×10^5 cells/mL) was dropped over the micropatterned hydrogel and the myoblasts allowed to adhere to the patterned surface. Cell cultures were kept at 37 °C, 5% CO2. During proliferation, co-culture cells were maintained in a 1:2 mix of each specific cell medium (50% medium of cell type A + 50% medium of cell type B). Once confluent, generally after 2 or 3 days from seeding, the medium was switched to the differentiating medium. The cultures were stopped after 8 days of differentiation.

Immunofluorescence analyses

Primary antibodies used in this study were against myosin heavy chain II (mouse monoclonal, Sigma-Aldrich), α-actinin (mouse monoclonal, Sigma-Aldrich) and dystrophin (rabbit polyclonal, Abcam). A standard immunohistochemistry protocol was used. Nuclei were counterstained with DAPI (Sigma Aldrich) and samples were mounted with Elvanols, and viewed under a fluorescence microscope.

Western blot analyses

Myotubes were treated ice-cold with 50 µl of lysis buffer: 50mM Tris-HCl pH 7.5, 150mM NaCl, 0.5mM DTT, 10% Glycerol, 1mM EDTA, 10mM MgCl2, 2% SDS, 1% Triton X-100 1 mM PMSF (Sigma), 1 mM NaV (Sigma), 5 mM NaF (Sigma), 3 mM β-glycerol (Sigma), and Complete EDTA-free protease inhibitor cocktail (Roche). Lysis buffer were dropped directly onto the hydrogel surfaces and incubated at 4°C for 1 h. After 1 h treatment, lysis buffer was resuspended on the hydrogel in order to collect all the cellular contents. Cell fractions were sedimented by centrifugation at 13000 g for 20 min at 4°C, and supernatant collected. 10 µg per lane of protein extract were solubilized in loading buffer (Invitrogen), 10% DTT (Invitrogen) and heated for 10 minutes at 70°C. Proteins were resolved in 3-8% precast gels (Tris-Acetate NuPAGE, Invitrogen) and then transferred on PVDF membranes (Invitrogen) under a potential difference of 45V, 400mA for 6 h. Membranes were blocked with 5% nonfat dry milk in TBST (TBS, 0.05% Tween 20) and then probed with primary antibodies for dystrophin (Abcam), myosin heavy chain II (Sigma-Aldrich) and β-actin (Sigma-Aldrich), and then with the proper HRP–conjugated secondary antibodies: goat anti-rabbit antibody (Invitrogen) and goat anti-mouse antibody (BioRad). Proteins were visualized by enhanced chemiluminescence (GE Healthcare) and dystrophin content was quantified by densitometry using ImageJ software (US National Institutes of Health). For each culture condition, we quantified the intensity of dystrophin bands and normalized by the housekeeping protein, β-actin. Afterwards, we normalized the result obtained from the 1:9 ratio by the one of the wild type culture.

APPENDIX E:
Supplementary methods of chapter 4

Human induced pluripotent stem (hiPS) cells culturing

hiPS cells will be expanded in colonies according to the protocol described by Kazuki and colleagues[1] and hiPS cells-derived EBs were differentiated towards the cardiac lineage according to the protocol described by Kattman and colleagues[2].

Briefly, hiPS colonies were cultured on a feeder layer of mitomycin-C inactivated murine embryonic fibroblasts (MEF). The culture medium composition was: DMEM/F12 containing 20% KSR, 2 mM L-glutamine, 0.1 mM non essential amino acids, 0.1 mM 2-mercaptoethanol, 50 units and 50 mg/ml penicillin and streptomycin and 4 ng/mL basic fibroblast growth factor (bFGF).

To maintain the pluripotent state for a high number of passages and avoid chromosomal aberrations, the colonies were splitted with the mechanical method, usually once a week. hiPS were washed with PBS and treated with 1 mL of CTK solution for 30 seconds. CTK solution was prepared as follows: add 5 mL of 2.5% trypsin, 5 mL of 1 mg/mL collagenase IV, 0.5 mL of 0.1 M CaCl2 and 10 mL of KSR into 30 mL of distilled water. The mechanical separation of colonies was done with the use of a stereomicroscope to dissect the undifferentiated colonies into several pieces using a cutting pipette. These selected pieces then are replated, with ratios usually ranging between 1:2 to 1:4, onto dishes containing fresh MEF feeders. The medium was changed daily.

Before freezing the colonies, iPS were treated for 1 hour at 37°C with 10 µM of Y-27632, which is a specific inhibitor of p160-Rho-associated coiled-coil kinase and increases the survival after thawing. iPS colonies were then mechanically detached from MEF, as described, centrifuged at 160 g for 5 minutes to remove the culture medium, resuspended in 200 µL of DAP213 solution and snap frozen in liquid nitrogen. The DAP123 solution was prepared adding 1.43 mL of DMSO, 1 mL of 10 M of acetamide and 2.2 mL of propylene glycol into 5.37 mL of culture medium.

Immunofluorescence analyses

A standard immunohistochemistry protocol was used. Primary antibodies used were: mouse monoclonal anti Oct4 (Santa Cruz #SC5279) diluted 1:200, rabbit polyclonal anti Sox2 (Millipore #AB5603) diluted 1:300, rabbit polyclonal anti c-myc (Santa Cruz #SC 764) diluted 1:100, mouse monoclonal anti Tra-1-60 (Millipore #MAB4360) diluted 1:250, mouse monoclonal anti Tra-1-81 (Millipore #MAB4381) diluted 1:200, rabbit polyclonal anti GFP conjugated with Alexa-594 (Invitrogen #A21312) diluted 1:100, mouse monoclonal anti cardiac Troponin T (Thermoscientific #MS-295-P) diluted 1:100, mouse monoclonal anti α-actinin (Sigma-Aldrich #A7811) diluted 1:100, rabbit polyclonal anti Dystrophin (Sigma #D8281) diluted 1:200, mouse monoclonal anti Cx43 (Millipore #MAB3067) diluted 1:100, goat polyclonal anti SERCA2a (SantaCruz #CS 8094) diluted 1:200 and goat polyclonal anti GATA4 (Santa Cruz #SC 1237) diluted 1:200. Secondary antibodies were: goat anti mouse (Invitrogen #A11005 and #A11001) diluted 1:200, goat anti rabbit (Invitrogen #A11012 and A1108) diluted 1:200, donkey anti goat (Jackson ImmunoLab #705-165-003) diluted 1:300.

Nuclei were counterstained with DAPI (Sigma Aldrich) and samples were mounted with Elvanols, and viewed under a fluorescence microscope.

Cytospin analyses

5-6 × 104 cells were resuspended in 300 µL of medium. The cell suspension was placed in the appropriate slots in the cytospin and centrifuged at 160g for 5 minutes. The slides were immediately fixed in PFA 2% and maintained in PBS 1X until immunofluorescence was performed.

RT-PCR analyses

Total RNA from hiPSc colonies and differentiated EBs was purified RNeasy Mini Kit (Qiagen), in accordance with the manufacturer's instructions, or with TRIzol reagent (Invitrogen) and treated with a Turbo DNAfree kit (Applied Biosystems) to remove genomic DNA contamination. First-strand complementary DNA (cDNA) synthesis was performed using using an oligo-(dT)20 primer and the cDNA Reverse Transcription Kit (Applied Biosystems). PCR was performed with cDNA using AmpliTaq Gold (Applied Biosystems). Amplifications were performed with an annealing temperature of 55 or 58 °C for 30–35 cycles, then amplified fragments were resolved by electrophoresis on a 2% agarose gel, followed by staining with ethidium bromide. Primer sequences are reported in the following table.

	FORWARD PRIMER	**REVERSE PRIMER**
dystrophin isoform Dp427m	TTCCCCCTACAGGACTCAGA	TCTTCCCACCAAAGCATTTT
dystrophin isoform Dp427l	CTCATGATGAAAGAGAAGATGTTCAA	CTGTCAGGCCTTCGAGGA
dystrophin isoform Dp140	TGCTGGCTGCTCTGAACTAA	GGCTTCCCAATTTTTCCTGT
dystrophin isoform Dp71	CTGGGAAGCTCACTCCTCCA	AGAGAGGGACGTTGACCAAAT
dystrophin exon junction 5-6	CCTGACAGGGCAAAAACTGCCAA	TGTGTGGCTGACTGCTGGCAA
dystrophin exon junction 11-12	CGGAGCCCATTTCCTTCACAGCATT	CCGGCCCTGATGGGCTGTCA
dystrophin exon junction 24-25	GACTCGGGGAATTGCAGGCTT	GGGCAGGCCATTCCTCCTTCA
dystrophin exon junction 27-28	GGCCTGCCCTTGGGGATTCA	TCTGGCATAGACCTGTTGGCACA
dystrophin exon junction 37-38	TGCCTGGGGAAAGGCTACTCA	GCAGTGGTCACCGCGGTTTG
NKX2.5	GCGATTATGCAGCGTGCAATGAGT	AACATAAATACGGGTGGGTGCGTG
cTnT	TTCACCAAAGATCTGCTCCTCGCT	TTATTACTGGTGTGGAGTGGGTGTGG
MLC2A	ACATCATCACCCACGGAGAAGAGA	ATTGGAACATGGCCTCTGGATGGA

Genomic PCR analyses

Genomic DNA was extracted from CHO cell clones using a genomic extraction kit (Gentra Systems, Minneapolis, MN), and PCR were performed using primers reported in the following table.

	FORWARD PRIMER	**REVERSE PRIMER**
HPRT junction	TGGAGGCCATAAACAAGAAGA	CCTTGACCCAGAAATTCCAC
EGFP	ATGGTGAGCAAGGGCGAGG	TTACTTGTACAGCTCGTCCATGCC
NKX2.5 promoter	TCATGATCACCCCACTTGCC	GAGCGATGAGCAGTTTCGTGTC
NKX2.5 upstream enhancer 1	TCTGGAGCTGCTCTGGGAAC	TCCTACCAGCCTCGGGTTCT
NKX2.5 upstream enhancer 2	GCAGGACAAACAAACAGCCTTC	GTCCCGAGGCAGGAAAAATC

FISH analyses

FISH analyses were performed using either fixed metaphase or interphase spreads using digoxigenin-labeled (Roche, Basel, Switzerland) human COT-1 DNA (Invitrogen) and biotinlabeled BAC DNA (RP11-466H21), essentially as described by Tomizuka and colleagues[3]. Chromosomal DNA was counterstained with DAPI (Sigma). Images were captured using the NIS Elements system (Nikon, Tokyo, Japan).

References

1. Kazuki, Y. et al. Complete genetic correction of ips cells from Duchenne muscular dystrophy. Mol. Ther. 18, 386-393 (2010).

2. Kattman, S.J. et al. Stage-specific optimization of activin/nodal and BMP signaling promotes cardiac differentiation of mouse and human pluripotent stem cell lines. Cell Stem Cell 8, 228-240 (2011).

3. Tomizuka, K. et al. Functional expression and germline transmission of a human chromosome fragment in chimaeric mice. Nat. Genet. 16, 133-143 (1997).

Acknowledgements

This work was supported by FONDAZIONE TELETHON (grant n. GGP08140), FONDAZIONE CITTÀ DELLA SPERANZA (Padova) and FONDAZIONE “ING. ALDO GINI”.

PhD Activities

SCIENTIFIC PUBLICATIONS:

Susi Zatti, Alice Zoso, Elena Serena, Camilla Luni, Elisa Cimetta and Nicola Elvassore *"Micropatterning topology on soft substrates affects myoblast proliferation and differentiation"* Langmuir, 2012. (Reported in Appendix A).

Elena Serena, Susi Zatti, Elena Reghelin, Alessandra Pasut, Elisa Cimetta and Nicola Elvassore *"Soft substrates drive optimal differentiation of human healthy and dystrophic myotubes"* Integrative Biology, 2010. (Reported in Appendix B).

Elena Serena, Elisa Cimetta, Susi Zatti, Tania Zaglia, Zagallo Monica, Keller Gordon and Nicola Elvassore *"Micro-arrayed human embryonic stem cells-derived cardiomyocytes for in vitro functional assay"* Submitted. (Reported in Appendix C).

SELECTED CONGRESSED (chronologic order):

Elena Serena, Elisa Cimetta, Susi Zatti, Elena Reghelin, Alessandra Pasut, Nicola Elvassore *"Engineering an in vitro model of human muscle dystrophy for high-throughput screenings and development of therapeutic strategies"* XV Telethon Scientific Convention, Riva del Garda (Trento - Italy), March 9-11 2009.

Elena Serena, Elisa Cimetta, Susi Zatti, Giulitti Stefano, Gordon Keller, Nicola Elvassore *"Microscale in vitro technologies for screening pathological conditions on human embryonic stem cells-derived cardiomyocytes: an in vitro model for cardiac cell therapy"* ISSCR - International Society of Stem Cell Research, 7th Annual Meeting, Barcellona (Spain), July 8-11 2009.

Susi Zatti, Elena Serena, Alice Zoso, Elisa Cimetta, Nicola Elvassore *"Engineering an in vitro 3D model of human skeletal muscle myogenesis"* VIMM - Venetian Institute of Molecular Medicine, 8th Annual Meeting, Marostica (Vicenza - Italy), October 23-24 2009.

Elisa Cimetta, Elena Serena, Tania Zaglia, Susi Zatti, Alessandro Zambon, Gordon Keller, Nicola Elvassore *"A Microfluidic Platform for the Spatial-Temporal Generation of Infarcted Heart Conditions: Highthroughput Screening On Human Embryonic Stem Cells-Derived Cardiomyocytes"* SBE's Second International Conference on Stem Cell Engineereing, Boston (MA) USA, May 2-5, 2010.

Elena Serena, Elisa Cimetta, Tania Zaglia, Susi Zatti, Monica Zagallo, Senastian Martewicz, Massimo Riello, Gordon Keller, Nicola Elvassore *"Microscale in vitro model for screening pathological conditions on hESC-derived cardiomyocytes"* International Society for Heart Research, XXth World Congress, Kyoto (Japan), May 13-16 2010.

Elena Serena, Elisa Cimetta, Tania Zaglia, Susi Zatti, Monica Zagallo, Alessandro Zambon, Sebastian Martewicz, Massimo Riello, Gordon Keller, Nicola Elvassore *"An in vitro model for cardiac cell therapy: coupling a microfluidic platform with arrayed human embryonic stem cells-derived cardiomyocytes for screening pathological conditions"* European Society of Cardiology - Frontiers in Cardiovascular Biology Congress" Berlin (German), July 16-19 2010.

Susi Zatti, Alice Zoso, Francesca Lo Verso, Elena Serena, Nicola Elvassore "Engineering an in vitro model of human muscle dystrophy for pre-clinical trials of cell therapy approaches" VIMM - Venetian Institute of Molecular Medicine, 9th Annual Meeting", Marostica (Vicenza - Italy), November 12-13, 2010.

Elena Serena, Susi Zatti, Elisa Cimetta, Alice Zoso, Francesca Lo Verso, Alessandro Zambon, Stefano Giulitti, Federica Michielin, Nicola Elvassore, *"Engineering an in vitro model of human muscle dystrophy for high-throughput screenings and development of therapeutic strategies"* XVI Telethon Scientific Convention, Riva del Garda (Trento - Italy), March 7-9 2011.

CO-SUPERVISION OF UNDERGRADUATE STUDENTS MASTER DEGREE THESIS

Alice Zoso "Sviluppo tecnologico su microscala di un modello *in vitro* di muscolo scheletrico umano" Supervisor: Nicola Elvassore. AA: 2009/2010.

Francesca Lo Verso "Sviluppo e validazione di un modello in vitro di terapia cellulare per la Distrofia Muscolare di Duchenne: analisi del ripristino dell'espressione di distrofina in muscolo scheletrico distrofico umano." Supervisor: Nicola Elvassore. AA: 2009/2010.

PERIODS OF TRAINING ABROAD

24 May 2011 - 28 May 2011, at the Chromosome Engineering Research Center, Tottori University - Faculty of Medicine, Yonago, Japan, under the supervision of Prof. Mitsuo Oshimura.